PONTIFICIA UNIVERSIDAD CATOLICA DE CHILE
ESCUELA DE INGENIERIA

HARNESSING THE SYSTEMIC RESPONSE OF *OENOCOCCUS OENI* TO PH AND ETHANOL BY EXPERIMENTAL DATA INTEGRATION INTO A GENOME-SCALE METABOLIC MODEL

MAGDALENA S. RIBBECK

Thesis submitted to the Office of Research and Graduate Studies in partial fulfillment of the requirements for the Degree of Master of Science in Engineering

Advisor:
EDUARDO AGOSIN

Santiago de Chile, November, 2017

PONTIFICIA UNIVERSIDAD CATOLICA DE CHILE
ESCUELA DE INGENIERIA

HARNESSING THE SYSTEMIC RESPONSE OF *OENOCOCCUS OENI* TO PH AND ETHANOL BY EXPERIMENTAL DATA INTEGRATION INTO A GENOME-SCALE METABOLIC MODEL

MAGDALENA S. RIBBECK

Members of the Committee:

EDUARDO AGOSIN

DANIEL GARRIDO

PEDRO SAA

ENZO SAUMA

Thesis submitted to the Office of Research and Graduate Studies in partial fulfillment of the requirements for the Degree of Master of Science in Engineering

Santiago de Chile, November, 2017

AGRADECIMIENTOS

Quisiera agradecer al laboratorio de biotecnología por su ayuda y apoyo durante el desarrollo de esta tesis, en especial al equipo *Oenococcus*: Sebastián Mendoza, Ángela Contreras y Pablo Cañón, quienes fueron parte importante en el proceso de generación del conocimiento, además de ser quienes me enseñaron y compartieron conmigo cada una de las victorias y pormenores del trabajo. De igual forma, quiero agradecer a Cindy, Jonathan, Catalina y Gabriela por su apoyo en la realización de los experimentos y procesamiento de datos, y a Fabián por su apoyo en el análisis de las capacidades del modelo generado en esta tesis. También al profesor Eduardo Agosín, mi tutor, cuya guía me ayudó a definir el trabajo y a enfrentar los problemas más complicados. Y por último, un agradecimiento especial a mi familia y mi pololo Augusto, y a mis amigos Francisco, Min, Kritsye y Valentina, quienes me acompañaron a lo largo del trabajo, y me animaron y apoyaron hasta el final.

CONTENTS

Page

INDEX OF TABLES

Page

INDEX OF FIGURES

Page

RESUMEN

La fermentación maloláctica es un proceso clave para determinar la calidad de vinos tintos y de algunos vinos blancos y espumantes, dado que mejora sus cualidades organolépticas. Sin embargo, este proceso todavía es escasamente comprendido y por ello el crecimiento de la principal bacteria que lleva a cabo este proceso, *Oenococcus oeni*, no siempre se logra. En este trabajo, se buscó una mejor comprensión del impacto del pH y el etanol sobre la fisiología de *O. oeni* en condiciones enológicas. Para ello, *O. oeni* PSU-1 fue cultivado en el medio definido MaxOeno basado en los componentes del vino, conteniendo 0, 3, 6, 9 and 12% v/v de concentración de etanol; y separadamente, en medio MaxOeno a pH 4,0, 3,5 and 3,2; en cada uno de los casos, cuatro fases de crecimiento fueron identificadas. Esta información experimental fue analizada por medio de dos modelos a escala genómica (MEG) por medio de un enfoque sistémico: iSM454, el primer MEG desarrollado para *O. oeni* PSU-1; e iMR453, la segunda versión de este modelo desarrollada durante esta tesis y que se encuentra balanceada por masa y carga. Para este análisis, dos novedosas metodologías fueron aplicadas: simulación simultánea de las fases de crecimiento, y el uso del algoritmo AUTOPAD, desarrollado en esta tesis, que permite ajuste del pH interno y externo de un MEG en base a la modificación del estado de protonación de sus metabolitos.

Los resultados muestran que los ácidos málico y cítrico son vitales en condiciones de stress, dado que fueron capaces de contrarrestar más del 50% de la entrada de protones provocada por la F_0F_1-ATPasa, y con ello permitir mayor generación de energía; y que la síntesis de manitol y eritritol es una fuente importante de $NAD(P)^+$, especialmente a alta concentración de etanol, donde puede regenerar el 51-57% de los cofactores usados por el catabolismo de azúcares. También, que el pH interno es una variable importante que debe ser considerada al estudiar bacterias acidofílicas como *O. oeni*, dado que el pH afecta los estados de protonación y con ello afecta las ventajas de utilizar una vía específica u otra para el consumo de protones.

Palabras clave: *Oenococcus oeni*, modelo metabólico a escala genómica, stress por etanol, stress por pH, ajuste de pH automático, regeneración de $NAD(P)^+$, síntesis de ATP, fermentación maloláctica

ABSTRACT

Malolactic fermentation is a key process that determines the quality of red wines and some white and sparkling wines, as it improves its organoleptic properties. However, it is still scarcely understood, and growth of the main bacteria that carries out this process, *Oenococcus oeni*, is not always achieved. In this work, a better understanding of the impact of pH and ethanol content in the physiology of *O. oeni* under oenological conditions was searched. To do this, *O. oeni* PSU-1 was cultivated in the wine-like defined medium MaxOeno containing 0, 3, 6, 9 and 12% v/v ethanol concentration; and separately, in MaxOeno at pH 4.0, 3.5 and 3.2; in each case, four growth phases were identified. This experimental data was analyzed with two genome-scale metabolic models (GSMM) by a system-based approach: iSM454, the first GSMM developed for *O. oeni* PSU-1; and iMR453, the second version of this model that was developed in this thesis and is mass and charge balanced. For this analysis, two novel modeling approaches were used: simultaneous simulation of the growth phases; and the use of the AUTOPAD algorithm, developed in this thesis, that allows internal and external pH adjustment of a GSMM based on the modification of the protonation state of the metabolites.

Results showed that malic and citric acid are vital for ATP generation at stress conditions, as they are used to countervail over 50% of the proton influx caused by F_0F_1-ATPase; and that mannitol and erythritol synthesis is an important source of $NAD(P)^+$, especially at increasing ethanol concentrations, where it can countervail for 51-57% of its usage for sugar catabolism. Also, our results showed that internal pH is an important variable that should be taken into account when studying acidophilic bacteria like *O. oeni*, as pH affects the protonation state and thus can activate or deactivate the advantages of using a specific route for proton consumption.

Keywords: *Oenococcus oeni*, genome-scale metabolic model, ethanol stress, pH stress, automatic pH adjustment, AutoPAD, $NAD(P)^+$ regeneration, ATP synthesis, malolactic fermentation

1. INTRODUCTION

1.1 Processes involved in wine elaboration

Wine is a highly complex ecological niche where a series of yeast, bacteria, fungi and viruses could interplay, impacting the quality of the final product (Toit & Pretorius, 2000). Wine elaboration includes two processes in which microorganisms play a fundamental role: alcoholic and malolactic fermentation. Alcoholic fermentation (AF) is the first step and the basis of winemaking. It is at this stage where most ethanol is generated, and where grape must is transformed into wine. This process is conducted by different genera of yeasts and some bacteria, but the most abundant microorganism at the end of the fermentation - and the representative of this step - is the budding yeast *Saccharomyces cerevisiae* (Zamora, 2008).

AF is sometimes followed by a second fermentation, the malolactic fermentation (MLF). This process is essential for the production of most red wines and is also desirable for some white and sparkling wines, as it contributes to microbial stability through the removal of remaining carbon sources after the alcoholic fermentation (Bartowsky, 2005; Bartowsky, Costello, & Chambers, 2015; Bauer & Dicks, 2004); and further improves the whole quality of wine through pH increase - transforming malic into lactic acid - and generation of unique, aromatic compounds (Bartowsky, 2005; Bartowsky et al., 2015; Bauer & Dicks, 2004). This second stage is carried out by lactic acid bacteria (LAB), among which the most important representative is the bacterium *Oenococcus oeni*.

Both AF and MLF can be carried out by native microorganisms, which are present in grapes, roots, leaves, as well as in winery machinery (Ralph E. Kunkee, 1968; Lafon-Lafourcade, Carre, & Ribéreau-Gayon, 1983); or by inoculation with commercial dry microorganisms. Native microorganisms have the advantage of producing wine with a higher complexity in flavor (Fleet, 1993). However, this process is usually longer, and more prone to spoilage (Bauer & Dicks, 2004). It also requires major control in

order to achieve the quality desired. Inoculation, on the other hand, allows to minimize the eventual delay of this step, as it favors the growth of the microorganism(s) of election to carry out the MLF; however, the palette of expected flavors might not reach the complexity of native microorganisms (Fleet, 1993).

MLF can occur sequentially or simultaneously with AF. Traditionally, MLF is a process that occurs after AF and is rare that it develops simultaneously without intervention, as bacteria that carry out MLF are present in low numbers during AF and, therefore, need to be inoculated (Fleet, 1993). Simultaneous fermentation reduces overall fermentation time, allowing rapid stabilization, leaving less time for potential spoilage (Bartowsky et al., 2015). However, there is a constant risk of high bacterial growth, which could inhibit yeast growth and, thus, results in sluggish or stuck fermentations (Fleet, 1993). This is why industry has mainly opted for the sequential process (Bartowsky et al., 2015).

In this chapter, a brief introduction to alcoholic fermentation and the microorganisms that carry out this fermentation are described. A more detailed description of malolactic fermentation is then presented, as well as to the microorganisms responsible of this process, the focus of this thesis.

1.1.1 Alcoholic fermentation

Alcoholic fermentation (AF) is the first step in winemaking, as well as its most characteristic step. During this stage, sugars - mainly glucose and fructose - are fermented into ethanol and carbon dioxide. Alcoholic fermentation is considered successful when all fermentable sugars are consumed (Zamora, 2008). Simultaneously to the synthesis of ethanol, other biochemical and physicochemical reactions occur. Among the latter, a series of compounds critical for the organoleptic properties of wine, i.e. fusel alcohols, ethyl esters, acetate esters, carbonyls and volatile fatty acids (Cordente, Curtin, Varela, & Pretorius, 2012) , are also

synthesized. Most fermentative aromas that contribute to wine flavor are formed during this step (Mateo, Jiménez, Pastor, & Huerta, 2001).

The alcoholic fermentation is carried out by yeasts. At the end of the fermentation, the yeast *Saccharomyces cerevisiae* is the most abundant species, as it has higher tolerance to ethanol (Zamora, 2008). This is why *S. cerevisiae* is usually known as the responsible for AF. However, there are other yeasts that can perform this process. Within the genus *Saccharomyces*, those which can also perform a complete AF without the production of off-flavors are usually called wine yeasts (Toit & Pretorius, 2000). There are other genera of yeasts that sometimes are present in wine that are able to partially carry out AF. These are known as non-*Saccharomyces* yeasts, and are often associated to the generation of esters and off-flavors. Some of the genera involved correspond to *Brettanomyces*, *Dekkera*, *Schizosaccharomyces* and *Zygosaccharomyces* (Toit & Pretorius, 2000). Spontaneous fermentations usually involved both wine and non-*Saccharomyces* yeasts, whose predominance varies depending on the time of the fermentation: at the beginning, microorganisms of the genera *Kloeckera*, *Hanseniaspora* and *Candida* mainly develop; in the mid-fermentation, *Pichia* and *Metschnikowia spp* prevail; and at the end of the fermentation, when alcoholic levels are higher, *Saccharomyces cerevisiae* is the predominant microorganism. Inoculation allows to increase the initial population of *S. cerevisiae* strains selected for certain desirable characteristics (Zamora, 2008), such as tolerance to high initial sugar concentration (Mateo et al., 2001); and insurance of completion of AF. Consequently, inoculation is usually preferred in industry, and spontaneous fermentation is employed mainly in traditional wineries (Zamora, 2008).

1.1.2 Malolactic fermentation

Malolactic fermentation (MLF) is a key operation for the quality of red wines, as well as for some white and sparkling wines. During this stage, microbial stability in wines increases by reducing the carbon available for spoilage bacteria (Bartowsky,

2005; Ralph E. Kunkee, 1968); a number of unique compounds are produced as well, which improves the organoleptic properties of a wine (Bartowsky, 2005; S.-Q. Liu, 2002) and adds complexity to wine flavor (S.-Q. Liu, 2002). This stage receives its name as it is marked the conversion of the dicarboxylic L-malic acid into the monocarboxylic L-lactic acid, a malic decarboxylation that is known as malolactic fermentation. A direct consequence of this reaction due to the conversion of L-malic acid into L-lactic acid is an increase in pH (Bauer & Dicks, 2004; R E Kunkee, 1991; Versari, Parpinello, & Cattaneo, 1999) from 0.1 to 0.2 units (Bartowsky et al., 2015); and a decrease in titratable acidity (Bartowsky et al., 2015; Ralph E. Kunkee, 1968; Versari et al., 1999), resulting in a wine with a softer mouth feel (Nielsen, Richelieu, Nielsen, S, & Hørsholm, 1999).

MLF is desirable for some wines, although it can also be detrimental to others. Grapes originating from warmer areas, tend to be less acid; hence, a further decrease in acidity may be deleterious for its sensory properties and may impact biological stability (Bauer & Dicks, 2004; Versari et al., 1999). In contrast, in cold wine regions, MLF is essential in order to decrease the acidity produced due to excess of malic acid (R E Kunkee, 1991; S.-Q. Liu, 2002) and could also be encouraged in order to gain a specific organoleptic profile (Bauer & Dicks, 2004).

MLF is mainly carried out by LAB, which are Gram-positive, catalase-negative, non-motile, non-spore forming bacteria (Toit & Pretorius, 2000). It is worthy to notice that after alcoholic fermentation, wine is a harsh medium due to its low pH (less than 3.5), high concentration of SO_2 (above 50 ppm) and high levels of ethanol (over 12%) (Bauer & Dicks, 2004); in addition to a low availability of nutritional compounds. All of these characteristics prevent the development of most microorganisms in this medium. LAB that are able to survive in wine and, thus, are associated with grape must and wine, belong to four genera: *Lactobacillus*, *Leuconostoc*, *Oenococcus* and *Pediococcus* (Bauer & Dicks, 2004; S.-Q. Liu, 2002; Toit & Pretorius, 2000). They usually do not grow during alcoholic fermentation, but proliferate during malolactic fermentation, reaching populations of 10^5-10^8 cfu/ml

(Toit & Pretorius, 2000). Among these LAB, *Oenococcus oeni* dominates in wines with low pH (3.0-3.5), confirming that this species is the most suited to survive in wine conditions (Versari et al., 1999). Also, as this bacterial species shows high adaptability to wine conditions, towards the end of alcoholic fermentation MLF is mainly driven by *Oenococcus oeni* (Bauer & Dicks, 2004). *Lactococcus* and *Pediococcus spp* can be found in wines with pH around 3.5 to 4.0 (Davis, Wibowo, Lee, & Fleet, 1986; Toit & Pretorius, 2000), yet their contribution to malolactic fermentation is usually not as critical (Davis et al., 1986), and are more related to undesirable characteristics in wine (Bartowsky, 2005). It is noteworthy that *S. cerevisiae* is also able to consume limited amounts of malic acid; and other, wine-related, undesirable yeasts like *S. pombe, Schizosaccharomyces malidevorans* and *Z. bailii* can strongly degrade it, damaging wine quality (Toit & Pretorius, 2000).

MLF is a delicate process that is still only partially understood and difficult to predict (Guzzo et al., 2000; Versari et al., 1999). On one hand, starting MLF is, sometimes, a challenge. Spontaneous MLF usually occurs a few days after the completion of alcoholic fermentation (Lonvaud-Funel, 1999), when bacterial population has reached about 10^6 CFU ml^{-1} (Versari et al., 1999); and its completion is expected within a few weeks after the harvest date (Kunkee, 1991). However, spontaneous MLF is unpredictable, and it may be triggered even months after the completion of alcoholic fermentation, a period during which wine is susceptible to spoilage due to other LAB (Bauer & Dicks, 2004; Davis et al., 1986). To cope with these uncertainties, some commercial starter cultures have been developed and are available in the market; the latter can be inoculated into wine, reducing the probability of spoilage (Bauer & Dicks, 2004) and ensuring better control of the MLF onset (Nielsen et al., 1999). Unfortunately, several of these starters are often unsuccessful because of the rapid decrease of cell viability after inoculation (Bauer & Dicks, 2004), and the requirement of a fastidious adaptation process before wine inoculation (Tourdot-Maréchal, Gaboriau, Beney, & Divies, 2000). On the other hand, a long MLF is not desired either. Excessive deacidification is characterized by

a loss in red color due to the increase in pH (Bauer & Dicks, 2004; Toit & Pretorius, 2000), and may indirectly encourage microbial spoilage resulting from more desirable growth conditions for other LAB, which are less acid tolerant than *O. oeni* (Toit & Pretorius, 2000). Also, misplaced growth of *O. oeni* (i.e, misplaced MLF) - and the subsequent biosynthesis of acetic acid - has been associated with sluggish and stuck fermentations, as acetic acid is known to inhibit growth and fermentation of *Saccharomyces spp.* (Toit & Pretorius, 2000). These are some of the reasons why MLF is one of the most difficult steps to control in winemaking (Nielsen et al., 1999), and why a better understanding of MLF is a necessity in order to obtain better and more predictable fermentations (Kunkee, 1968; Lonvaud-Funel, 1999; Versari et al., 1999).

1.2 *Oenococcus oeni*

Oenococcus oeni is the preferred bacterium to carry out MLF. It is acid-tolerant (Chu-Ky, Tourdot-Marechal, Marechal, & Guzzo, 2005; S.-Q. Liu, 2002), displaying survival at pH 3.0-3.5 (Bauer & Dicks, 2004; Versari et al., 1999); resistant to high ethanol content (>10% v/v) and SO_2 concentrations (<50 ppm) (Bartowsky et al., 2015; Bauer & Dicks, 2004); and develops a unique flavor profile (Liu, 2002). *O. oeni* is a Gram-positive, catalase negative, microaerophilic LAB (Maicas, Ferrer & Pardo, 2002; Bartowsky, 2005). Considering evolutionary aspects, and in common with other LAB, *O. oeni* has reduced their genome size to achieve niche adaptation, abandoning versatility and metabolic efficiency in the process (Gänzle, 2015). A unique feature of this specie is that it does not require iron for growth, as it does not possess aerobic, neither anaerobic, electron transfer chains (Gänzle, 2015; Salema, Lolkema, & Roma, 1996). As a consequence, it needs alternative mechanisms to generate the proton motive force required to generate ATP. Malolactic fermentation is one of these mechanisms. Considering the different pKa of malic and lactic acid, this reactions result in the consumption of one proton for each lactic acid generated,

which is then exported outside of the cell in an electroneutral process (Salema et al., 1996).

O. oeni metabolizes sugars via the phosphoketolase pathway, also known as heterolactic fermentation (HLF) (Bartowsky, 2005; Maicas, Ferrer, & Pardo, 2002). This pathway generates ATP and NAD(P)H through the heterofermentative catabolism of sugars, generating a mixture of products, i.e. carbon dioxide, ethanol, acetic acid or acetaldehyde, and lactic acid (Bartowsky, 2005). In the first part of this pathway, HLF consumes two moles of $NAD(P)^+$, one of ATP and one of phosphate per mole of fermented hexose, yielding one mole of pyruvate, one of acetyl-P and one of carbon dioxide (Figure 1-1). Then, these intermediary metabolites are oxidized to generate a mixture of products, whose final concentration depends on the availability of $NAD(P)^+$ in the cell. Thus, acetyl-P can be converted into acetate, yielding one mole of ATP per mole of acetyl-P; or to ethanol, yielding two moles of NAD^+ (Maicas, Ferrer & Pardo, 2002). Glyceraldehyde-3P is used to generate pyruvate, yielding one mole of NADH and two of ATP per mole of glyceraldehyde-3P. The resulting pyruvate can be either transformed into D-lactate by lactate dehydrogenase, consuming NADH (Zaunmüller, Eichert, Richter, & Unden, 2006); generate acetyl-P by pyruvate oxidase (Wagner et al., 2005), which is subsequently transformed into acetate or ethanol; or produce acetyl-CoA by pyruvate dehydrogenase, generating NAD(P)H (Wagner et al., 2005). As illustrated in Figure 1-1, all fluxes converge to acetyl-phosphate, which can be considered the central branching point of the metabolism in this microorganism (Gänzle, 2015).

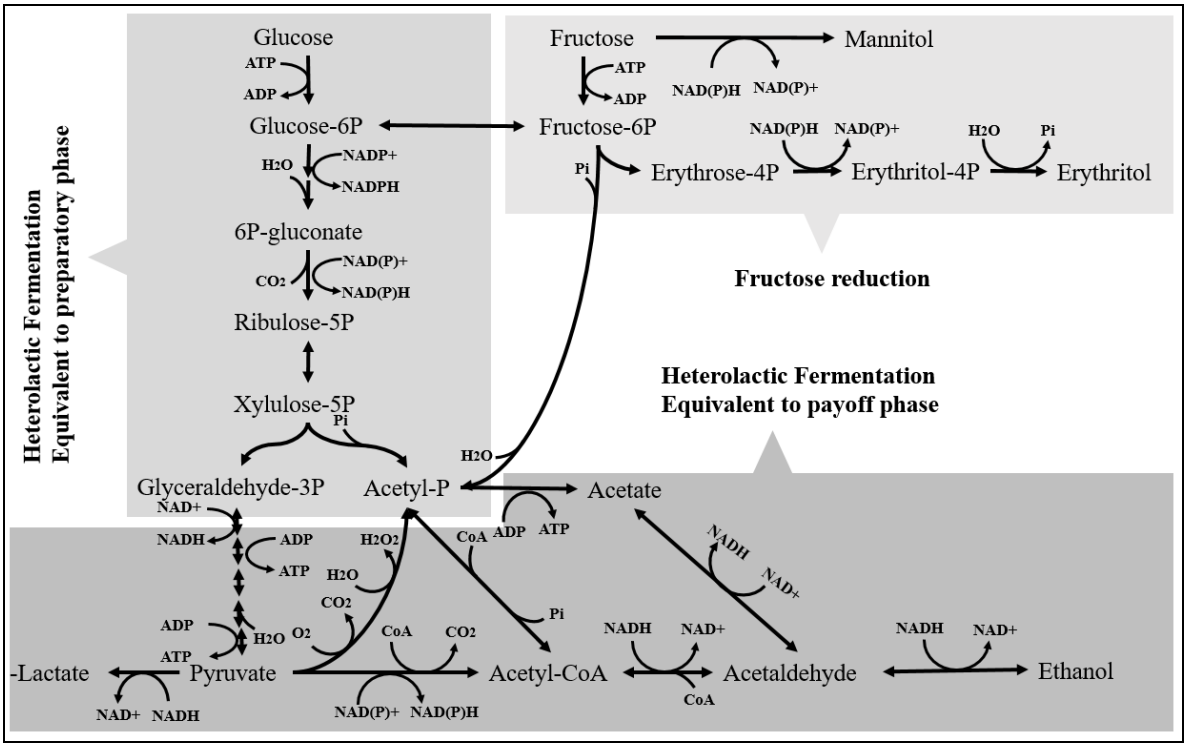

Figure 1-1: Heterolactic fermentation and fructose reduction

The synthesis of lactic and acetic acids by *O. oeni*, as well as by other LAB, provides them with an important advantage over other microorganisms, as these weak acids have a potent antimicrobial activity. The latter is due to the fact that undissociated form - more abundant at low pH than the corresponding dissociated one - can freely move across the cell membrane. Since cytoplasmic pH is generally higher than that of the growth medium, weak acids dissociate, releasing a proton in the cytoplasm and causing acidification (Cotter & Hill, 2003); this disrupts the cytoplasmic anion pool, affecting the integrity of purine bases and results in denaturation of essential enzymes inside the cells (Wu, Huang, & Zhou, 2014). As a result, cell growth arrests and cells eventually die. This effect is further enhanced by the acidification that *O. oeni* produces in the culture medium during growth, through the production of the aforementioned weak acids and other secondary products (Cotter & Hill, 2003). For

example, lactic acid can also permeabilize the outer membrane of Gram-negative bacteria, enhancing other antimicrobial substances (Alakomi, Skyttä, Saarela, & Helander, 2005).

Several studies have shown that *O. oeni* can reach higher specific growth rates when the medium includes, besides a carbon source, an alternative electron acceptor. This compound is then employed to oxidize NAD(P)H, allowing acetyl-P to be metabolized into acetate instead of ethanol, thus generating a higher yield of ATP (Gänzle, 2015). Electron acceptors that have been shown to increase specific growth rate includes fructose (Maicas, González-Cabo, Ferrer, & Pardo, 1999), and pyruvate (Maicas et al., 2002). Fructose can be either metabolized through HLF or transformed into mannitol (Gänzle, 2015) or erythritol (Maicas et al., 2002; Wagner et al., 2005) (Figure 1-1). Pyruvate can be reduced into lactate (Maicas et al., 2002). In these processes $NAD(P)^+$ is regenerated.

1.3 Strategies used by LAB for survival under acidic conditions

Inhabiting an acidic medium is a challenge for any microorganism. Due to the difference between cytoplasmic or internal pH (pH_{in}), and the culture medium or external pH (pH_{out}), and due to the difference of electrochemical potential between the cytoplasm and the medium, a proton influx is generated to the inside of the cell. If not harnessed, this proton influx will cause a decrease in pH_{in} that will be detrimental for the cells. When this happens, the same strategy that LAB employ to deal with other bacteria, i.e. production of lactic and acetic acids, can be detrimental, as undissociated lactic and acetic acids are predominant at acidic conditions. Therefore, they can permeate the cytoplasmatic membrane of LAB and dissociate inside the cell, which has a higher pH, decreasing pH_{in} (Wu et al., 2014).

To a certain level, and depending on its own acid tolerance, LAB can adjust to an acidic medium by either maintaining its pH_{in} or maintaining the gradient of pH (ΔpH) between the inside and the outside. This response is specie-specific: for example,

Lactococcus lactis (Breeuwer, Drocourt, Rombouts, & Abee, 1996) and *O. oeni* (Bouix & Ghorbal, 2015) relay on maintaining constant pH_{in} . On the other side, *Lactobacillus delbrueckii* and *Streptococcus thermophilus* maintains its ΔpH (Siegumfeldt, Björn Rechinger, & Jakobsen, 2000). When the bacterial cells are no longer able to maintain the pH_{in} or ΔpH, cell growth is affected (Bouix & Ghorbal, 2015; Nannen & Hutkins, 1991).

LAB possesses a combination of constitutive and inducible strategies whose expression enables acidurance. These include proton removal, alkalization of external environment, expression of transcriptional regulators, production of general shock proteins and chaperones, and changes in the composition of the cell envelope (Cotter & Hill, 2003). Studies on the physiology of LAB have mainly focused on lactose fermentation, citrate metabolism and protein degradation, which have led to the conclusion that translocation processes across the cytoplasmic membrane are crucial for survival under energy-limited conditions, and often are the rate controlling steps in the metabolism (Konings, 2006; Konings et al., 1997).

Translocation processes can be classified in two types: primary transport systems, which couples light or chemical reactions to vectorial translocation of ions across the membrane (Konings et al., 1997; Poolman, 1993); and secondary transport systems, which convert the (electro)-chemical energy of one solute into the (electro)-chemical energy of another solute (Konings et al., 1997; Poolman, 1993). Below, I describe primary and secondary transport systems used by LAB for acidurance, highlighting the strategies that have been found in *O. oeni*.

1.3.1 Primary transport systems

In the field of primary transport processes, ABC transporters and ATPases have been described for LAB. Among these transporters, only ATPases have been related to pH adaptation. F_0F_1-ATPase links the production of ATP to proton translocation, in a reversible process that can either consume ATP to extrude protons or synthesize ATP

by generating a proton influx. **T**here is evidence from both chemostat and batch cultures that this enzyme plays a key role in regulating pH_{in}, and that it may even be the most important mechanism involved in internal pH regulation (Sullivan & Condon, 1999). K^+-ATPase has also been associated with acidurance (Cotter & Hill, 2003; van de Guchte et al., 2002).

As discussed above, the respiratory chain, a classic member of this type of transporters, is incomplete in LAB (Brooijmans et al., 2009). However, improvement of growth has been observed when heme is added to the medium (Brooijmans et al., 2009; Lechardeur et al., 2011).

a) F_0F_1-ATPase

F_0F_1-ATPase links the production of ATP to the transmembranar proton motive force (PMF), i.e. the driving force that promotes the movement of protons across the cytoplasmic membrane, downhill the electrochemical potential (José Pascual Abad, 2011). PMF is composed by a chemical part, the pH gradient; and an electrical part, the transmembrane potential ($\Delta\Psi$) (Lolkema, Poolman, & Konings, 1995). F_0F_1-ATPase can either generate ATP at the expense of the PMF, or consume ATP to generate PMF (Cotter & Hill, 2003; Y. Liu, Tang, Lin, & Xu, 2015).

F_0F_1-ATPase is composed of two subunits: F_0, an hydrophobic membrane channel complex composed of subunits a, b and c, that has proton-translocating activity; and F_1, an hydrophilic enzyme complex, consisting of subunits α, β, γ, δ and ε**,** responsible for ATPase activity (Cotter & Hill, 2003; Y. Liu et al., 2015).

F_0F_1-ATPase is employed by various bacteria to maintain pH_{in}, using the energy from ATP hydrolysis to extrude protons (Cotter & Hill, 2003; Y. Liu et al., 2015). In the case of LAB, F_oF_1-ATPase has been suggested to play a key role in regulating pH_{in}, may be even as the most important mechanism involved in internal pH regulation (Sullivan & Condon, 1999). Several studies have highlighted its importance under acidic conditions. For example, Martín Galano et al (2001) showed that F_oF_1-ATPase activity increased in response to acidification at sublethal external pH; in

Streptococcus pneumoniae (Martín-Galano, Ferrándiz, & G. de la Campa, 2001) as well as *Lactobacillus acidophilus*, the F_oF_1-ATPase operon is induced by exposure to acidic pH (Kullen & Klaenhammer, 1999); in *Streptococcus mutans*, this enzyme was transcriptionally upregulated on an acidic environment (Kuhnert, Zheng, Faustoferri, & Quivey, 2004) and acid tolerance has been directly related to F_oF_1-ATPase activity levels (Guzzo et al., 2000). Mutants of *Lactococcus lactis* and *Lactobacillus helveticus* without functional ATPase rapidly die (Guzzo et al., 2000), and a clear relationship between pH_{in}, ATPase and cytoplasmic levels of ATP was found for *L. lactis* (Sullivan & Condon, 1999). Moreover, in several species of oral *Streptococci* (*Streptococcus mutans*, *S. salivarius* and *S. sanguis*), acid tolerance correlates with their relative permeability to protons. Thus, the pH allowing the lowest permeabilities correspond to the highest ATPase activities (pH 6.0, 7.0 and 7.5, respectively).

Regarding *O. oeni*, a relationship between acid resistance and F_0F_1-ATPase has also been found. The ATPase activity is stronger when *O. oeni* is grown at pH 3.5 than when it is grown at pH 5.3 (Fortier, Tourdot-Maréchal, Diviès, Lee, & Guzzo, 2003). Also, Tourdot-Maréchal et al (1999) found that *O. oeni* mutants with a two-fold lower expression of F_0F_1-ATPase had only 5% viability after one hour exposure to pH 2.6, while wild-type cells were 85% viable. A relationship with F_0F_1-ATPase and malic acid was also found, as cells in medium without L-malic acid showed a 2.2-fold higher activity of F_0F_1-ATPase after 24 h of incubation at pH 3.5 (Fortier et al., 2003).

b) K^+-ATPase

K^+-ATPase is a member of the family of the P-type ATPases. K^+-ATPases exchange K^+ for H^+ by antiport transport, converting the transmembranar potential generated by the transport of potassium ions into a transmembranar pH gradient (Cotter & Hill, 2003; van de Guchte et al., 2002). By this mechanism, K^+-ATPases contribute to pH homeostasis. For example, intracellular pH of *S. mutans* during growth in TYE

(Tryptone Yeast Extract) culture medium containing glucose at pH_{out} 5.0 in the presence or absence of 25 mmol/L K^+ increased its from 5.5 to 6.14 (Dashper & Reynolds, 1992). Similar observations were reported for *L. lactis* (Bakker & Harold, 1980) and *E. hirae* (Kashket & Barker, 1977).

In the case of *O. oeni*, Guzzo et al. (2000) reported a putative P-type ATPase, probably a K^+-ATPase. To the best of our knowledge, there have not been other reports on this ATPase in this bacterium.

1.3.2 Secondary transport systems

Secondary transport systems are driven by $\Delta\Psi$ and the difference of concentration in the inside and the outside of the cell of the corresponding transported compounds. This implies that unless there is cellular regulation, these processes are reversible and highly dependent on external and internal conditions (Konings et al., 1997). These systems correspond to uniporter, symporter and antiporter transporters, and can transport solutes either neutral or charged, usually as electrogenic transport (Lolkema et al., 1995).

Fermentative bacteria, like LAB, have devised secondary PMF generating systems that depend on these secondary transporters but that do not require direct proton transport across the membrane. In these, one of the PMF components is used to drive the accumulation or extrusion of solutes by transport through the membrane, and the pH gradient is generated as a consequence of the conversion of the substrate into products in the cell. Thus, proton consumption is solely determined by the chemical properties of the substrate and products, and is affected by the pH and pKa of the compounds involved in the reaction (Lolkema et al., 1995). In these cases, the metabolism of a weak acid catalyzes the generation of a pH gradient, through the activation of this secondary PMF generating systems. These could occur through two kinds of reactions: reactions that, at a certain pH, consume protons, which will result in a proton outflux either by passive diffusion or by transport processes (Poolman,

1993); or reactions that result in the synthesis of an alkaline product, such as ammonia, which interacts with an intracellular proton and converts into ammonium, raising pH_{in} (Cotter & Hill, 2003; Y. Liu et al., 2015).

In the following paragraphs, secondary transport processes present in LAB are described. As these processes are highly dependent on pH, the reactions are presented in a range of physiological internal pH between 5.1-6.3, an interval that includes all the internal pH values reported in the literature for *O. oeni* (Augagneur et al., 2007; Bouix & Ghorbal, 2015; Salema et al., 1996).

a) Malolactic fermentation

MLF is the main reaction that characterizes the second stage of winemaking. It is worthy to mention that MLF is basically a decarboxylation. Indeed, L-malic acid, a dicarboxylic acid, is converted into the monocarboxylic L-lactic acid and CO_2 by malate decarboxylase, the malolactic enzyme. This reaction is of oenological significance, as wine naturally contains high concentrations of L-malic acid (Cotter & Hill, 2003), ranging from 2 to 8 g/L in cool climate regions; and lower than 2 g/L in warmer regions (Bartowsky, 2005).

Two mechanisms are responsible for L-malic acid uptake and L-lactic acid excretion in LAB:

- A first one, related with an electrogenic lactate-malate (Lac^--mal^{2-} or Hlac-$Hmal^-$) antiporter (ex: *Lactococcus lactis*) (Poolman et al., 1991; Zaunmüller et al., 2006); and
- A second mechanism that consists of two transporters: a L-malic acid transporter, and an L-lactic acid transporter. Regarding L-malic acid transport, studies have shown that both diffusion of monoanionic malate ($Hmal^-$), or symport of dianionic malate and a proton are possible mechanisms for this enzyme. When L-malic acid uptake is carried out by this transporter, the product of MLF, L-lactic acid, is exported via a symporter electroneutral reaction of monoanionic lactic

acid (lac^-) and a proton (Konings et al., 1997; Salema et al., 1996). It is also quite plausible that L-lactic acid excretion occurs by diffusion of its undissociated form (Konings et al., 1997; Poolman et al., 1991; Salema et al., 1996; Zaunmüller et al., 2006). These transporters are present in *O. oeni* (Konings et al., 1997; Lolkema et al., 1995).

As an electrogenic transport, malic acid uptake is driven by ΔΨ. Once inside the cell, the malolactic enzyme generates the second component of the PMF, ΔpH. This enzyme itself does not consumes a proton; it is through the differences between the pKa of the product and the substrate that a proton is consumed (Figure 1-2). For example, at physiological pH, malic and lactic acids are in their dissociated forms, as mal^{2-} and lac^-; under these conditions, MLF consumes a proton due to mass balance, resulting_in cytoplasmic alkalization (equation 1.1). If this reaction is catalyzed at low pH, when malic and lactic acid are protonated, there would be no proton consumption (equation 1.2) (Cotter & Hill, 2003; R E Kunkee, 1991; Lolkema et al., 1995). Both situations are presented in the following equations:

$$mal^{2-} + H^+ \rightarrow lac^- + CO_2 \quad (1.1)$$

$$H_2mal \rightarrow Hlac + CO_2 \quad (1.2)$$

The proton consumption that occurs at physiological pH results in a net translocation of one charge per each malate molecule and energization of the membrane, both by the consumption of a proton and by the electrogenic transport itself. The proton motive force is then used for maintenance of pH homeostasis and for the uptake of nutrients (Cotter & Hill, 2003).

The positive effect of malolactic fermentation on pH homeostasis has been experimentally validated for *O. oeni*. The presence of L-malic acid has been related to a decrease in the lag period at the beginning of fermentations (Kunkee, 1991) and to a reduction of the external pH variation when grown on FT80 medium: presence of

L-malic acid allowed a slight variation of 0.2 in the external pH when the starting pH was 5.3, whereas absence of L-malic acid resulted in an acidification of 1.7 pH units This proton consumption is probably the basis for the implication of MLF in acid tolerance (Cotter & Hill, 2003).

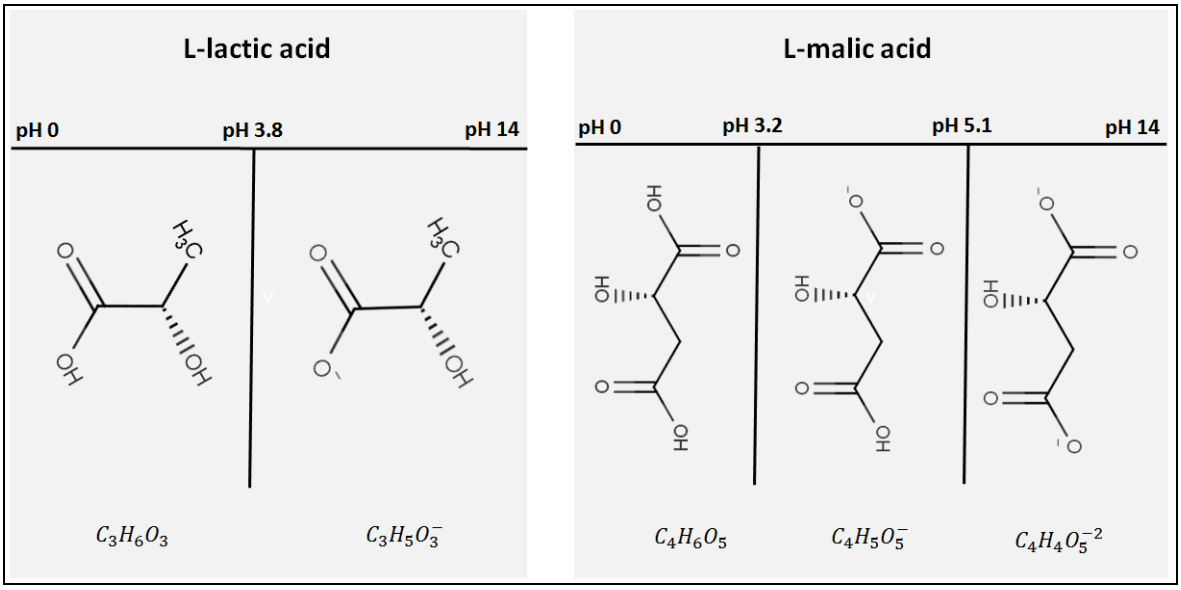

Figure 1-2**:** Major forms of L-malic and L-lactic acids according to the pH of the medium

Figure 1-2 shows the charge and chemical formula of the corresponding major microspecies for L-malic acid or L-lactic acid, according to pH. pH at which equilibrium between the protonation states is achieved (pKa) is shown over the lines. Due to the charge difference between the metabolites at their different protonation states, MLF's capacity to generate a ΔpH is pH dependent.

b) Citric acid degradation

LAB can also take advantage of citric acid for pH regulation. This organic acid is naturally present in wine at lower concentrations than malic acid, and is sometimes added artificially to increase acidity of grape musts (Kunkee, 1968). Degradation of citric acid is carried out by citrate lyase (Olguín et al, 2009), forming acetic acid and oxaloacetic acid. Oxaloacetic acid is then converted into pyruvic acid and carbon

dioxide by oxaloacetate decarboxylase (Konings et al., 1997), as described by (Zaunmüller et al., 2006):

$$citrate^{-2} + 2\,H^{+} \rightarrow oxaloacetic\ acid + acetic\ acid \quad (1.3)$$

$$oxaloacetic\ acid \rightarrow pyruvate^{-} + H^{+} + CO_2 \quad (1.4)$$

It is worthy to mention that Zaunmuller et al (2006), when postulating the charges of the compounds participating in these equations, did not consider the physiological, intracellular pH of *O. oeni*, which has been reported to vary between 5.8 and 6.3. Therefore, the equilibrated equations would be as follows:

$$citrate^{-3} \rightarrow oxaloacetate^{-2} + acetate^{-} \quad (1.5)$$

$$oxaloacetate^{-2} + H^{+} \rightarrow pyruvate^{-} + CO_2 \quad (1.6)$$

LAB cannot grow solely on citrate, and thus it is used as an electron acceptor (Zaunmüller et al., 2006). The pyruvic acid generated can be further metabolized, depending on the specific needs of the cell. If NADH is in excess, as it might occur during hexose co-metabolism, pyruvate will be used mainly for lactic acid synthesis via heterolactic fermentation (Zaunmüller et al., 2006); alternatively, pyruvate can be converted into acetyl-P or acetyl-CoA biosynthesis by pyruvate oxidase and pyruvate dehydrogenase respectively, from which ATP or $NAD(P)^{+}$ can be synthesized via heterolactic fermentation. If the external pH is low, pyruvic acid can be further metabolized downstream the citrate degradation pathway and be used for acetoin synthesis in order to maximize its contribution to the PMF (Ramos et al, 1995). In this case, two pyruvates are used to generate 2-acetolactate, in a process that releases carbon dioxide that, in *L. lactis* at least, is catalyzed by α-acetolactate synthase (Zuljan et al, 2014). 2-acetolactate is then transformed into acetoin. If the cell contains enough NADH, acetoin can be further converted into 2,3-butanediol by

butanediol dehydrogenase, an enzymatic process that regenerates NAD^+ (Zaunmüller et al., 2006).

$$2\ pyruvate^- + H^+ \rightarrow 2 - acetolactate^- + CO_2 \quad (1.7)$$

$$acetolactate^- + H^+ \rightarrow acetoin + CO_2 \quad (1.8)$$

$$acetoin + NADH + H^+ \rightarrow butanediol + NAD^+ \quad (1.9)$$

Citric acid uptake is catalyzed by an electrogenic H_2cit^-/Lac^- citric acid-lactic acid antiporter that translocates negative charges to the inside of the cell (ex: *L. lactis* subsp. *diacetylactis, Leuconostoc mesenteroides*) (Cotter & Hill, 2003; Konings et al., 1997; Zaunmüller et al., 2006), or by a uniporter transporter that translocates monoanionic citrate (H^2cit^-) (ex: *O. oeni*) (Konings et al., 1997; Lolkema et al., 1995).

The positive effect of citric acid on pH homeostasis has been experimentally validated for different LAB. For example, in *L. lactis*, a proteomic analysis showed an increase in expression for α-acetolactate synthase at low pH, whereas expression levels of lactate dehydrogenase and pyruvate dehydrogenase complex remained constant (Zuljan et al., 2014). In *L. lactis* subsp. *diacetylactis*, bacterial growth at low pH is aided by induction of the citric acid-lactic acid antiporter (Cotter & Hill, 2003). For *O. oeni*, the presence of citric acid in a FT80 culture medium allowed a decrease of the pH drop at the end of the experiment. Thus, at an initial condition of pH 5.3, in the absence of citric acid, the final pH of the culture was 3.6; on the contrary, in the presence of citric acid, a final pH of 4.6 was achieved (Augagneur et al., 2007).

c) Glutamate decarboxylase

Glutamate decarboxylase is an acid-resistant system that is present in a variety of bacteria, including Gram-negative bacteria like *Escherichia coli* and *Shigella flexneri*, and Gram-positive bacteria like *Listeria monocytogenes* and *Lactobacillus reuteri* (Y. Liu et al., 2015), and *Lactobacillus brevis* (Cotter & Hill, 2003).

Glutamate decarboxylase catalyzes the conversion of glutamate into γ-aminobutyrate (GABA) and carbon dioxide, in a reaction that consumes a proton. At physiological pH, the reaction can be formulated as follows (Y. Liu et al., 2015; Ma et al., 2012):

$$Glutamate + H^+ \rightarrow GABA^+ + CO_2 \quad (1.10)$$

Again, charges were not balanced at the intracellular pH of this LAB, and the correct equation should be:

$$Glutamate^- + H^+ \rightarrow GABA + CO_2 \quad (1.11)$$

GABA and glutamate are selectively exchanged by an antiporter (Cotter & Hill, 2003; Fernández & Zúñiga, 2006; Liu et al., 2015) that is activated at low extracellular pH; for example, in *E. coli* their highest activity was determined at pH 5.5-6.0, decreasing until pH 7.5, where activity could not be measured (Ma et al., 2012). It is thought that three successive decarboxylation-antiport cycles create a PMF sufficient for the synthesis of one molecule of ATP via the F_oF_1-ATPase (Cotter & Hill, 2003).

Glutamate decarboxylase is also present in various LAB. In *Lactobacilli*, this enzyme exhibits a sharp pH optimum at pH 4.5 and is essentially inactive at neutral pH (Gänzle, 2015). *L. lactis* subsp. *lactis* expressed *gadB* and *gadC* – which respectively encode for a glutamate decarboxylase and the antiport transporter. Maximal expression was reached at low pH and at the onset of stationary phase in the presence of sodium chloride and glutamate. *L. lactis* subsp. *cremoris* strains contains *gadB*, but it is not active as a consequence of a frameshift mutation (Nomura et al, 2000). It is interesting to note that *L. lactis* subsp. *lactis* can induce an acid tolerance response while *L. cremoris* cannot (Nomura et al, 1999). Finally, *Oenococcus oeni* contains the *gadC* genomic sequence (ID: 4415174, NCBI) but not *gadB*.

d) Glutaminase

This enzyme, together with glutamate decarboxylase, is part of the main tools for acid survival in *E. coli* (Liu et al., 2015). Glutaminase catabolizes the deamination of glutamine to glutamate and ammonium, as follows:

$$Glutamine + H_2O + H^+ \rightarrow Glutamic\ acid + NH_4^+ \quad (1.12)$$

This reaction consumes a proton under pH 4.27, when glutamate is present as uncharged glutamic acid (Liu et al., 2015). At physiological pH, however, the reaction would be the following:

$$Glutamine + H_2O \rightarrow Glutamate^- + NH_4^+ \quad (1.13)$$

There are few studies on glutaminases in LAB. Glutaminase seems to participate in acid tolerance at lower external pH than malic or citric acid. For example, in *Lactobacillus reuteri* ΔgadB, an acid tolerance effect was observed when glutamine was added at pH 2.5, which was not observed at pH 3.5 (J. S. Teixeira et al., 2014). For *Lactobacillus sanfranciscensis*, presence of glutamine increased the final pH of a culture, although in the order of 0.1 pH, and increased final biomass (Vermeulen, Gänzle, & Vogel, 2007).

Transport of glutamine has shown to be ATP-driven in *Lactobacilli*, *Streptococci* and *Lactococci* genera (Fernández & Zúñiga, 2006).

e) Biogenic amines: tyrosine, histidine and ornithine decarboxylases

In an acidic environment, LAB shifts their metabolism to amino acid utilization, as acidification of the medium limits carbohydrate metabolism (Gänzle, 2015). Under these conditions, amino acid decarboxylases are expressed, a group of enzymes that control the pH of the bacterial environment by consuming hydrogen ions as part of the decarboxylation reaction (Cotter & Hill, 2003). Glutamate, which has already

been described, plays a major role in pH homeostasis and stationary phase survival of LAB, through glutamate decarboxylase (Gänzle, 2015). Decarboxylation of other amino acids generates biogenic amines, which have negative implications for human health when consumed with alcohol (Gänzle, 2015), as they can cause a number of adverse reactions, such as low blood pressure, facial flushing, nasal congestion and/or gastrointestinal and respiratory distress (Bartowsky, 2005). Putrescine, tyramine and histamine are the most abundant biogenic amines in several fermented foods, including wine, cheese, cider, sausage, fish and meat products (Lonvaud-Funel, 1999; Romano et al, 2012). Putrescine itself does not have a direct harmful biologic activity; instead, it enhances the toxic effects of histamine and tyramine. These three biogenic amines derive from the decarboxylation of ornithine, tyrosine and histidine, respectively (Romano et al., 2012), and have been observed to increase in concentration during malolactic fermentation in wine (Lonvaud-Funel, 1999).

The decarboxylation of ornithine, tyrosine and histidine contribute to pH homeostasis due to the difference in pKa with the amino acid from which they originate, causing the consumption of a proton. Interestingly, the presence of amino acid decarboxylases within a species is strain specific, which could indicate that the genetic information in which these enzymes are encoded are present in mobile genetic elements (Lucas et al, 2003).

The enzymes that catalyze the conversion of the aforementioned amino acids into their respective amines are histidine-, ornithine, and tyrosine decarboxylases, pyridoxal-dependent enzymes (Lucas & Lonvaud-Funel, 2002). The corresponding reactions are described below.

$$L - Histidine^{+} + H^{+} \rightarrow histamine^{+2} + CO_2 \quad (1.14)$$

$$L - Ornithine^{+} + H^{+} \rightarrow putrescine^{+2} + CO_2 \quad (1.15)$$

$$L - Tyrosine + H^{+} \rightarrow tyramine^{+} + CO_2 \quad (1.16)$$

Transport of these amino acids and their respective amines occurs through electrogenic antiporters. Histidine uptake is transported through an histidine^{+}/histamine^{+2} antiporter in *Lactobacillus buchneri* (Molenaar, Bosscher, Ten Brink, Driessen, & Konings, 1993). Tyrosine uptake, through a tyrosine/tyramine^{+} antiporter in *Enterococcus durans* (Linares et al, 2009), *Enterococcus faecium* (Pereira et al, 2009) and *Lactobacillus brevis* (Wolken et al, 2006). For ornithine uptake, a similar transporter has been characterized in *E. coli* (Kashiwagi et al, 1992), but electrogenicity is unclear in its functionality (Konings et al , 1995).

Putative transporter genes have been found in the genome of different LAB, including some strains of *O. oeni* (Romano et al., 2012). These transporters also presented activity for uniport intake of their corresponding amino acid, yet at a lower rate (Linares et al., 2009; Molenaar et al., 1993; Wolken et al., 2006).

f) Arginine Deiminase pathway

The arginine deiminase (ADI) pathway, also known as the arginine dehydrolase system, is a widely reported system in LAB that is activated during acid stress (Wu et al., 2014). This pathway has been identified in a variety of bacteria, including dental ones. It catalyzes the conversion of arginine into ornithine, ammonia and carbon dioxide (Cotter & Hill, 2003; Liu et al., 2015; Wu et al., 2014) through three different reactions: arginine is first converted to L-citrulline and ammonia by arginine dehydrolase; then, L-citrulline is transformed into L-ornithine and carbamoyl phosphate by ornithine transcarbamylase; and finally, carbamoyl phosphate is catabolized to generate ammonia, carbon dioxide, and ATP by carbamate kinase (Y. Liu et al., 2015). The reactions are shown below:

$$L - Arginine + H^+ + H_2O \rightarrow L - Citrulline + NH_4^+ \quad (1.17)$$

$$L - Citrulline + HPO_4 \rightarrow L - Ornithine + Carbamoyl - P \quad (1.18)$$

$$Carbamoyl - P + ADP + H^+ \rightarrow ATP + CO_2 + NH_4^+ \quad (1.19)$$

The last reaction can consume two protons at pH closer to pH_{in}= 6.13, the pKa of carbamoyl-P. ADI allows proton consumption due to ammonia synthesis, which rapidly converts into ammonium, thus extracting a proton from the cytoplasm. It also generates metabolic energy by substrate level phosphorylation, which can be used for extrusion of cytoplasmic protons by H+-ATPase (Gänzle, 2015).

The ADI pathway is widely used by LAB involved in MLF on wine. As arginine is one of the major amino acids found in grape juice and wine (Mills et al, 2005), this system could be advantageous for survival at low pH. *L. sanfranciscensis*, *O. oeni* and other wine LAB are able to catabolize glucose and arginine concurrently (Cotter & Hill, 2003). In contrast, LAB associated with cheese fermentations, like *L. sakei*, oral LAB and *E. faecalis* are subject to catabolite repression by glucose (Cotter & Hill, 2003). The ADI pathway is more active at pH values higher than 3.5. Gene expression analysis suggests that amino acid decarboxylation is prioritized over this pathway (Gänzle, 2015).

Regarding transport, an electroneutral L-arginine+/L-ornithine+ antiporter encoded by ArcD has been widely characterized (Noens & Lolkema, 2017). The latter is present in *Lactococcus lactis* (Poolman et al, 1987) and *Lactobacillus fermentum* (Vrancken et al, 2009). Recently, the authors also characterized *ArcE* in *S. pneumoniae*, a widely distributed gene, encoding for a second L-arginine+/L-ornithine+ electroneutral antiporter able to translocate L-citrulline/L-ornithine, too (Noens & Lolkema, 2017).

Vracken et al (2009) found that *L. fermentum* has different citrulline utilization patterns when grown at different pH. They noticed that at higher pH (5.5-6.5), citrulline is excreted first and then re consumed after arginine depletion. At lower pH (3.5), citrulline was not found in the medium, which could indicate that it is consumed right after being produced.

In *O. oeni*, arginine degradation is strain specific. Strains able to degrade arginine have an increased acid tolerance when arginine is added, and produce a lower

decrease of external pH (Tonon & Lonvaud-Funel, 2000). However, there is only one gene sequence available in NCBI for *O. oeni*, corresponding to an arginine dehydrolase gene (ID: 4415326) from *O. oeni* PSU-1 strain. The arginine/ornithine transporter is absent in this strain as well as ornithine transcarbamylase and carbamate kinase. However, the genome sequence of this strain includes genes coding for transporters from the cation amino acid family of arginine (Mills et al., 2005).

g) Urease

The hydrolysis of urea into ammonia and carbon dioxide (van de Guchte et al., 2002) is catalyzed by urease, a nickel-containing oligomeric enzyme, as follows:

$$Urease + H_2O + 2\,H^+ \rightarrow 2\,NH_4^+ + CO_2 \qquad (1.20)$$

Urease is produced by a subset of oral bacteria, like *Streptococcus salivarius* and *Actinomyces naeslundii* (Cotter & Hill, 2003). Urea is present in saliva, and may be especially important for survival of *S. salivarius* under extreme acid conditions (van de Guchte et al., 2002).

In *H. pylori* and *S. salivarius*, transport of urea is carried out through a membrane-bound, H+-gated urea transporter that can facilitate uptake of urea in acidic environment. *H. pylori* urease is present not only in the cytoplasm but also in the outer surface of the cell, facilitating better efficiency of the mechanism on exposure to acid stress (Liu et al., 2015). So far, urease has not been reported in *O. oeni.*

1.4 Genome Scale Metabolic Model of *O. oeni*

A Genome Scale Metabolic Model (GSMM) is a structured format that represents the metabolism of a cell or microbial community (Orth et al, 2010), allowing the incorporation of detailed biochemical and enzymatic data in one unique structure

(McCloskey et al, 2013). These models are *in silico* representations that have been used to answer different biological questions, most frequently in the areas of metabolic engineering, interspecies interaction simulations, studies of evolutionary processes, analysis of biological network properties, prediction of cellular phenotypes and model-driven discovery (McCloskey et al, 2013). The basic structure of a GSMM will be described in this section, as well as the current model of *O. oeni*, including some applications as well.

1.4.1 Mathematical formulation of the GSMM

The mathematical formulation of a GSMM includes the representation of the metabolic network in a stoichiometric matrix S, in which every row represents a metabolite, and every column a reaction. The matrix contains the stoichiometric coefficients of these reactions, where a negative coefficient indicates consumption, and a positive coefficient indicates generation of the specific metabolite. For example, $s_{i,j}$, the coefficient in position i,j, represents the stoichiometric coefficient of a metabolite i in reaction j. For a microorganism with n metabolites and m reactions, the matrix looks as follows:

$$S = \begin{pmatrix} s_{11} & \cdots & s_{1m} \\ \vdots & \ddots & \vdots \\ s_{n1} & \cdots & s_{nm} \end{pmatrix}$$

Intracellular fluxes are represented in a vector v, and physicochemical constraints are used to describe the potential behavior of an organism, based on mass balance, energy balance and flux limitations (Kauffman, Prakash, & Edwards, 2003). These constraints are represented in the vectors lb and ub, the lower and the upper bounds of the possible values for v. Vector b represents the accumulation of the given metabolites. The mathematical formulation is thus the following:

$$S * v = b$$
$$lb \leq v \leq ub$$

This mathematical formulation represents an underdetermined problem, as there are more reactions than metabolites in the stoichiometric matrix. Because of this, precise determination of the intracellular fluxes of a cell at a given cellular phase in a specific environmental condition would require experimental determination of m – rank(S) intracellular fluxes, where rank(S) is the rank of the matrix.

Different mathematical approaches have been proposed to avoid the requirement of an extensive experimental determination. The most widely used is Flux Balance Analysis (FBA). FBA assumes that, under any given environmental condition, the organism will reach a steady state that satisfies the physicochemical constraints, thus defining a solution space that contains the multiple solutions that fulfill these conditions. Determination of a physiologically meaningful solution is key in this process, and is done through optimization by finding the optimal value of a specific objective function (Kauffman et al., 2003). Then, the optimization problem is represented as follows:

$$\max f = c^t * v$$
$$s.t \quad S * v = 0$$
$$lb \leq v \leq ub$$

Where c represents the weights of the objective function for each flux. A steady-state assumption is used to consider that b equals zero.

1.4.2 iSM454 genome-scale metabolic model

Our lab recently developed a GSMM for *O. oeni* PSU-1 strain, named iSM454 (Mendoza et al, 2017). It includes 660 reactions, 536 metabolites and 454 genes. This model uses biomass formation as objective function and it is capable of predicting nutritional requirements with an F-score of 94%, which indicates that results are predicted with high precision (fraction of correctly predicted non-essential instances among the retrieved instances) and sensitivity (fraction of correctly predicted non-essential instances over the total amount of relevant instances). iSM454 has been previously used for prediction of non-growth associated ATP (NGAM) required for growth at pH 4.8, under 0% or 12% ethanol concentration in a wine-like defined medium; identification of the distribution of the internal fluxes in the aforementioned conditions; assessment of the ATP production rates between the two pathways used by *O. oeni* to synthesize ATP: F_0F_1-ATPase and heterolactic fermentation; among others (Mendoza et al, 2017). This has been key information to understand the metabolism of *O. oeni* when grown at high concentrations of ethanol.

1.5 Motivation

The aim of this study is to aid in the understanding of the metabolic responses of *O. oeni* towards two of the main stressors present in wine: pH and ethanol. The effect of these stressors over *O. oeni* have been studied before; however, it is usually at high pH (over 4.5) and without ethanol, and thus it does not necessary represent the metabolism of *O. oeni* under wine-like conditions. Also, studies are usually done in complex medium (FT80, MRS, for example), which confounds the attribution of a biological response to a specific compound.

due to the use of different complex mediums, results are not always reproducible and can be contradictory (for example: production of erythritol by glucose (Veiga-Da-Cunha, Santos, & Van Schaftingen, 1993) or fructose (Maicas et al., 2002)). Thus, a

systemic approach based on experimental data obtained under stress, in a wine-like defined medium, will provide insight onto the metabolism of this bacterium.

As indicated before, iSM454 demonstrated its utility to understand the metabolism of *O. oeni* at two ethanol concentrations, and thus it is expected that it will give a realistic simulation of *O. oeni*'s metabolism in conditions at different ethanol concentrations. However, this is not the same with different pH values, as iSM454 is not adjusted to the internal pH of *O. oeni* reported in literature. As internal pH plays a key role in determining the effect of secondary transport mechanisms, which are key for survival at low pH, readjustment of the reactions to the biological pH conditions is a key element to improve the prediction capacity of the model.

2. HYPOTHESIS

Further curation by incorporating electronic balances and new genetic information in the recently reconstructed genome-scale metabolic model iSM454 of *Oenococcus oeni* allows to characterize *O. oeni*'s metabolic response to key environmental perturbations, in particular low pH and high ethanol concentration. This knowledge will improve the prediction of the fate of malolactic fermentation under these stressful conditions, ensuring a successful initiation and completion of this process under oenological conditions.

OBJECTIVES

3.1 General objectives

The general objective of this thesis is to contribute to a better understanding of the impact of pH and ethanol content in the physiology of *O. oeni* under oenological conditions, following both an experimental and in *silico* system-based approach.

3.2 Specific objectives

The specific objectives of this thesis are the following:

a) Systemic analysis of the metabolic response to ethanol stress in *O. oeni* using experimental data and metabolic modeling.

b) Curation of the iSM454 metabolic model of *O. oeni* accounting for electronic and mass balances.

c) Systemic analysis of the metabolic response to pH stress using experimental data and metabolic modeling.

3. MATERIALS AND METHODS

4.1 Systemic analysis of the metabolic response to ethanol stress

The following protocols correspond to the materials and methods employed during the study of the metabolic response to ethanol stress. These are divided into two sections: Protocols for experimental data acquisition and
Construction of algorithms for data analysis.

4.1.1 Protocols for experimental data acquisition

a) Microorganisms and media

Oenococcus oeni (Garvie, 1967) (PSU-1, ATCC® BAA-331™) was obtained from the American Type Culture Collection (ATCC) (Virginia, USA). Cryogenically preserved (-80°C) strains were cultured and maintained on MRS plates (Man, Rogosa and Sharpe) (De Man, Rogosa, & Sharpe, 1960) and stored at 4°C.

An *O. oeni* PSU-1 preculture was prepared from a frozen stock by inoculating 100 ml Erlenmeyer flasks containing 75 mL MRS medium supplemented with 0.5 g L^{-1} of cysteine. Before inoculation, the cells were subjected to ethanol adaptation. For this purpose, we serially passaged every culture, starting from 1% ethanol v/v to reach 0, 3, 6, 9 or 12% v/v ethanol concentration in each culture.

b) Design of a chemically defined culture medium

The developed chemically defined culture medium, named MaxOeno, was designed with the aim of simulating the wine environment, allowing *O. oeni* to grow in the presence of ethanol. However, the concentration of carbon and nitrogen used in MaxOeno was higher than that found in wine, because these concentrations allowed the growth of *O. oeni* avoiding its arrest or slowing. The vitamins and minerals were those of Terrade & Mira de Orduña (2009), but their concentration was increased

three fold. Using literature data, we verified that these concentrations were not inhibitory for the bacterium growth (Mesas, Rodríguez, & Alegre, 2004).

Carbon and energy sources were those normally found in wine, i.e. glucose, fructose, malate and citrate. Glucose and fructose are the main residual sugars present in wine. Both were added in equal concentrations (12.5 g/L) with the aim of studying their metabolic fate in *O. oeni*. Meanwhile, malate and citrate, the main organic acids in wine, were included at a concentration of 5 and 1 g/L, respectively. We verified from the literature that these concentrations were not inhibitory for the bacterium, and that they also allowed bacterial cells to grow in the presence of ethanol (Augagneur et al., 2007; Ferrer, Pardo, & Maicas, 2001; Mesas et al., 2004; Olguin, 2010; Saguir & Manca de Nadra, 1996; Salou, Leroy, Goma, & Pareilleiux, 1991).

The amino acids content was calculated using their yields in biomass. For this purpose, we employed the yields reported for *Lactobacillus plantarum* and *Lactococcus lactis* (Novak, Lindley, & Loubiere, 1997; Teusink et al., 2006), because we did not find any reported data for amino acid yields in *O. oeni*.

c) Composition of the MaxOeno culture medium

The MaxOeno culture medium contained, in g/L: 1 citrate, 5 malate, 0.4 calcium chloride (dihydrate), 1.3 magnesium sulfate, 12.5 fructose, 12.5 glucose, 2 dipotassium phosphate. 1 mL/L Tween 80 was also added, as well as 100 mL/L of a nitrogenous bases solution, 100 mL/L; 5 mL/L of a mineral salts solution; and 1 mL/L of a vitamins solution.

The vitamin solution contained the following, in g/L: 1 thiamine, 1 biotin, 2 nicotinic acid, 20 pyridoxine hydrochloride, 2 C-D-pantothenate, 1 folic acid, 2 choline chloride, 1 riboflavin, 0.1 4-aminobenzoic acid, 0.1 cyanocobalamine and 5 xanthine. The nitrogenous bases solution contained 0.5 g/L of each of the following: adenine sulphate, uracil, cytosine, thymine and guanine. Mineral salts solution contained, in g/L: 60 $MgSO_4*7H_2O$; 12 $FeSO_4*7H_2O$; 0.015 $CuSO_4*5H_2O$; and 0.135

$ZnSO_4*7H_2O$. The medium was sterilized by membrane filtration (pore size < 0.22 µm, Millipore, USA).

Besides, the culture medium was supplemented with 1,060 mg/L of assimilable nitrogen prepared with the following amino acids, in g/L: 0.4 L-arginine, 0.24 L-serine, 0.27 L-threonine, 0.33 L-glutamic acid 0.33 mg/l, 0.3 L-aspartic acid 0.3, 0.33 L-lysine, 0.3 L-asparagine, 0.3 L-leucine, 0.5 L-glutamine, 0.2 L-alanine, 0.54 cysteine, 0.27 glycine, 0.53 histidine, 0.3 isoleucine, 0.34 methionine, 0.37 phenylalanine, 0.67 proline, 0.46 tryptophan, 0.41 tyrosine and 0.27 valine.

Before sterilization, the pH of the medium was adjusted to 4.8.

d) *O. oeni* cultivation in different ethanol conditions

Ethanol-adapted cells were inoculated in 50 mL flasks containing 35 mL of MaxOeno culture medium to achieve an initial optical density at 600 nm (OD600) of approximately 0.2. The flasks were of glass, airtight and with a sampling port. The cultures were incubated at 25°C, without stirring. Samples were collected aseptically through the flask sampling port, and bacterial growth was estimated by OD600, the optical density of the culture measured at 600nm. At the same time, the content from each flask was centrifuged; the supernatant was collected and frozen at -20°C, for future chemical analyses.

The biomass was determined as dry weight of cells through a calibration curve of OD_{600} versus dry weight (g/L). The latter was previously carried out as described in Li and Mira de Orduña (2009), to obtain equation 3.1, where both parameters are related.

$$X\ (gDCW/L) = 0.8105*(OD_{600}) + 0.0104 \qquad (3.1)$$

e) Chemical analyses

L-lactate, D-lactate and amino acids were quantified by UHPLC/MS using a Dionex unit model Ultimate-3000 (Dionex Corp., Sunnyvale, USA) coupled to a mass spectrometer Exactive™ plus (Thermo Fisher Scientific, San Jose, CA). The UHPLC

system was controlled using the Xcalibur™ 2.13 software (Thermo Fisher Scientific, San Jose, CA). The methods utilized for compound identification and quantification are detailed below:

L- and D- lactate: 50 µl of sample were dried and then derivatized by adding 50 µl of (+)-*O,O´*-diacetyl-L-tartaric anhydride solution (≥97%) (DATAN) (Sigma-Aldrich, USA) (100 mg/mL, where DATAN was dissolved in dichloromethane:acetic acid (4 : 1, by volume)). The samples were incubated for 40 min at 75°C, under agitation. Subsequently, the samples were dried and reconstituted in 200 µl of a solution of acetonitrile and water (1:2). L-lactate and D-lactate (≥98%) (Sigma-Aldrich, USA) were used as external standards. A 10 µl derivatized sample was injected in the equipment and separated using a UPLC BEH C18 (100 × 2.1 mm, 1.7 µm, Waters) analytical column at a flow of 0.5 mL/min and oven temperature of 31°C. Solvents used for separation were: solvent A: ammonium formate 1.5 mM, pH was adjusted at pH 3.6 using formic acid. Solvent B: acetonitrile.

Amino acids: A 10 µL sample was directly injected in the equipment and separated using a LiChrospher® 100 RP-18 (5µm) (Merck) analytical column with a flow of 0.35 mL/min and oven temperature of 30°C. Solvents used for separation were: solvent A: formic acid 0.1% v/v. Solvent B: methanol.

Cysteine: A 50 µl sample was derivatized using 100 µl 5,5´-dithiobis(2-nitrobenzoic acid) (Ellman's reagent) (Sigma-Aldrich, USA). The reagent solution for derivatization was prepared using 4 mg Ellman's reagent dissolved in 10 mL buffer phosphate 0.01 M (pH 7.0). All samples were derivatized at the time of being taken. The chromatographic conditions were the same of those employed for amino acids analysis.

Sugars (glucose, fructose), organic acids (malate, acetate, citrate, total (L- + D-) lactate and alcohols (ethanol, mannitol and erythritol) were separated and quantified in a Lachrom L-700 HPLC system (Merck Hitachi, Japan) equipped with Diode Array and Refractive Index detectors (Hitachi, Japan). An Aminex HPX-87H ion

exchange column (Bio-Rad, USA) was used, as described previously (Varela *et al*, 2003). For sugars, malate, citrate, acetate and ethanol, the mobile phase used was sulphuric acid 5 mM with a flow of 0.450 ml/min and oven at 35°C. For mannitol and erythritol, the mobile phase was milliQ™ water with a flow rate of 0.450 ml/min at a constant temperature of 75°C. External standards were used to quantify the required compounds in all cases.

f) Statistical analysis: mood test

As it was not possible to assume normal distribution of the data due to not enough data points, significant difference of consumption, production, growth and specific growth rates was analyzed by mood median's non-parametric test with 95% confidence interval.

4.1.2 Construction of algorithms for data analysis

a) Flux Balance Analysis (FBA)

To perform FBA of the different growth phases at each ethanol level, the following fluxes (mmol $gDCW^{-1}$ h^{-1}) were set with experimental values: the substrates glucose, fructose, citrate, malate, cysteine, threonine, valine, phenylalanine and serine; and the products mannitol, erythritol, L-lactate, R-lactate and acetate. For the three phases determined for growth at 0% ethanol, ethanol rate was also measured and thus constrained with experimental data. To minimize experimental error, linear regressions were determined for each of the metabolites at each growth phase and used to predict the phase's final value. Initial values were taken from the initial concentration of the experiment for phase I, and from the final values of the former phase for phases II and III. Also, experimental data showed that there was accumulation of mannitol or fructose, as there was higher mannitol production during phase II and III than fructose consumption in the same phase. The same happened with L-malic acid and L-lactic acid production. Cysteine, threonine, phenylalanine and valine are essential amino acids that were not consumed in all phases, and thus

experimental data also showed accumulation of these compounds. Thus, to represent these phenomena, accumulation reactions were added for each of the phases as follows: sink for phases 2 and 3, and demand for phases 1 and 2. These reactions represent influxes and/or outfluxes from the model for the following six metabolites: mannitol, malate, cysteine, threonine, phenylalanine and valine.

b) Estimation of the accumulation reactions

As it was necessary to limit the flux that could pass through the accumulation reactions (i.e the sink and demand reactions described in FBA), an extended model was generated to allow simultaneous simulation of the three phases observed for each ethanol level. Similar approaches have been used before to model microbiome interactions (Shoaie et al., 2013) and multi-tissues of *Arabidopsis thaliana* (Gomes de Oliveira Dal'Molin, Quek, Saa, & Nielsen, 2015). These approaches present differences with the current work in the interaction spaces added during the construction of the extended stoichiometric matrix. For example, when microbiomes are modelled it is important to include metabolic interactions, and thus a shared extracellular space is defined in which all subtracts and products are available, and thus the model is able to simulate bacterial interactions (i.e mutualism, competition, amensalism, commensalism, etc). For multi-tissue modelling, a similar extracellular common space is constructed between tissues who are able to interact, and thus there are different spaces generated for each binary interaction. Here, our objective was to model intracellular accumulation of the same bacteria at different temporalities, and thus we did not include a common external space per se; in this case, new reactions were added that allowed unidirectional transfer of specific cytoplasmatic compounds – those that were accumulated, based on our experimental results – from one phase to the other. Storage was not allowed, and thus, the surplus of a product generated in one phase had to be excreted in the following phase, or passed onto the next phase. The pseudo-stationary postulation was applied for the totality of the phases, and thus all accumulation had to be depleted – by utilization or excretion – at the third phase.

Another difference with the other modelling approaches is that this extended model was only intended for limitation of the fluxed carried by the accumulation reactions defined for FBA, and not for finding the optimal result; thus, biomass was fixed and the objective function used was maximization and minimization of each specific flux carried through these added accumulation reactions.

The extended model possesses a stoichiometric matrix Z, which contains three "S" sub matrices (Figure 3-1), each associated to a specific growth phase. These "S" sub matrices were taken from iSM454 and represent three independent problems solved simultaneously in the extended model. Then, to allow interaction between these three problems and thus lose independency, accumulation reactions were added, which allow flux to pass from $phase_n$ to $phase_{n+1}$, and that correspond with the sink and demand reactions added to the iSM454 model. Moreover, accumulation reactions were added for the six metabolites of interest: mannitol, malate, cysteine, threonine, phenylalanine and valine, to allow interaction between the phases.

These reactions had the following structure:

mannitol _cytosol1 -> mannitol _cytosol2

where *mannitol _cytosol1* represents cytosolic mannitol flux in growth phase I, and *mannitol _cytosol2* represents corresponding cytosolic mannitol flux in growth phase II.

Additionally, Flux Variability Analysis (FVA) was carried out to determine the maximum and the minimum flux that each accumulation reaction was able to carry in constrained conditions. These values were used to constrain the accumulation reactions in FBA simulation for each of the three phases.

c) Incorporating experimental data into the Model

To determine internal flux distributions for each of the phases present on each ethanol levels, we used the GSMM iSM454 previously constructed for *O. oeni* strain

PSU-1 (Mendoza et al., 2017) and constrained the model with the specific production/consumption rates determined experimentally. For the amino acids, the exchange reactions related to cysteine, threonine and serine were fixed as these amino acids are used for pyruvate generation, i.e. needed for mass balance, and the essential amino acids valine and phenylalanine were constrained to limit biomass formation. Due to experimental accumulation of mannitol, malate and amino acids, we added accumulation reactions for these metabolites, represented as demand (phases 1 and 2) and/or sink (phases 2 and 3) reactions.

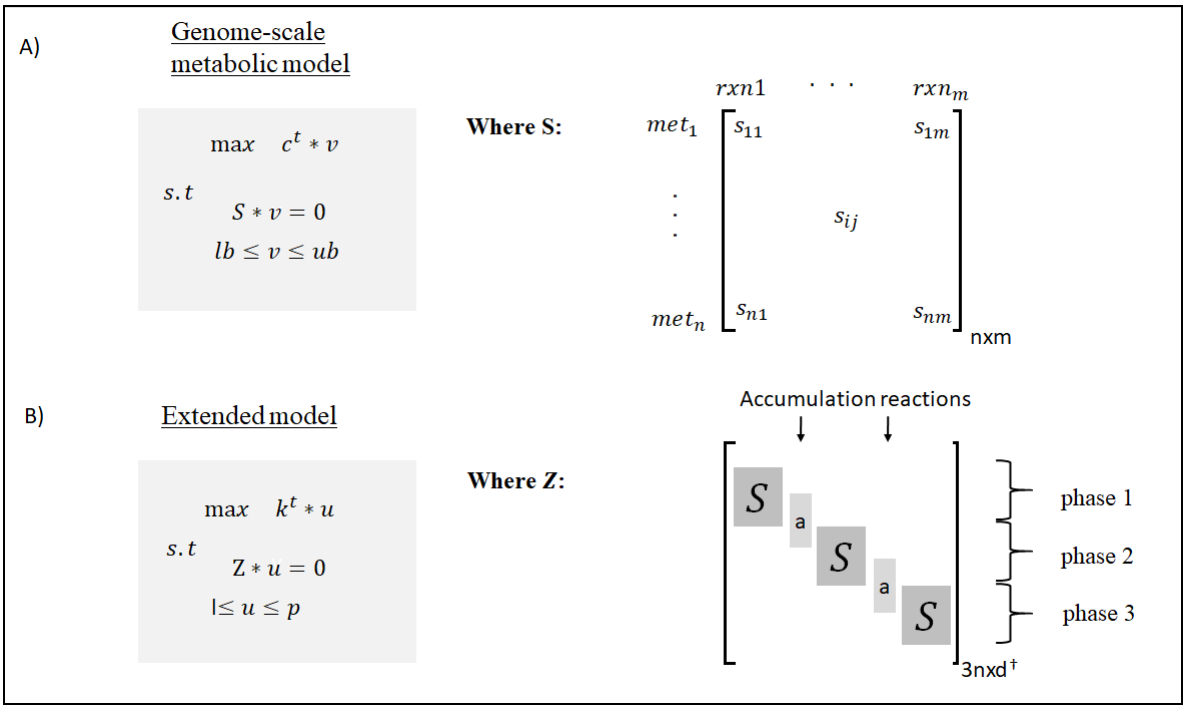

Figure 3-1: Equation and matrices considered in the construction of the extended model Construction of the extended model

A) Shows the structure of the genome-scale metabolic model iSM454. This model includes a stoichiometric matrix "S" (nxm), where n is the number of metabolites and m the number of reactions; a vector "v" (1xm) of internal fluxes; vectors "lb" and "ub" that limit the values of vector "v"; and a vector "c" of weights (1xn) for the objective function. **B)** Shows the extended model, which is able to simulate simultaneously the three phases identified for each ethanol level, and thus includes similar components: a matrix "Z" that contains three "S" matrix, one per phase, and 2 ''a" vectors (1xh),

where “a” represents the accumulation reactions that allows interaction between phases; thus, matrix sigma has a size (3nxd), where d=3m+2h. The extended model also includes vector “u” (1xd) of internal fluxes, limited by vector “l” and “p” (1xd), and a vector “k” of weights (1x3n).

d) Prediction of Non-Growth Associated Maintenance (NGAM)

NGAM was estimated by setting the specific production and consumption rates of the experimentally measured compounds in iSM454, as described above for FBA. Thereby, flux through the NGAM reaction was progressively increased from 0 to 4 mmol $gDCW^{-1}$ h^{-1}. In each cycle, biomass production rate was maximized and the prediction error was assessed. The NGAM flux that allowed the lowest biomass prediction error was selected.

e) Sensitivity analysis for NGAM

Sensitivity of estimated NGAM was assessed for each of the specific consumption/production rates set in the model. For this purpose, each rate was varied independently by increasing and decreasing its value in 1%, and then NGAM was recalculated each time.

f) Flux Variability Analysis (FVA)

FVA was carried out by maximizing and minimizing the flux under the same constrained conditions, like for NGAM estimation. This technique was used for each of the accumulation reactions present in the extended model, and in iSM454 to analyze changes of production of ATP, NADH, NADPH; and separately, in F_0F_1-ATPase and diacetyl synthase. To assess variation of ATP, NADH and NADPH, the sum of the following reactions was subjected to FVA: Malate dehydrogenase, glyceraldehyde-3P dehydrogenase, threonine dehydrogenase, NADH quinone oxidoreductase transhydrogenase and the pathway for methylglyoxal degradation for NADH formation; Glucose-6P dehydrogenase, phosphogluconate dehydrogenase and

GMP reductase for NADPH formation; and acetate kinase, pyruvate kinase, F_0F_1-ATPase and phosphoglycerate kinase for ATP formation.

g) Determination of energetic requirements

FBA was performed using the estimated NGAM values as constraints to determine internal flux distribution. Accumulation reactions were also limited with the constraints determined in the extended model. In *O. oeni*, ATP is produced by the F_0F_1-ATPase and/or by three reactions of the phosphoketolase pathway (reactions that involve the following enzymes: acetate kinase, pyruvate kinase and 3-phosphoglycerate kinase). Moreover, this bacterium produced NAD^+/NADH through reactions that involve the following enzymes: malate dehydrogenase, glyceraldehyde-3P dehydrogenase, threonine dehydrogenase, NADH quinone oxidoreductase transhydrogenase and the pathway for methylglyoxal degradation for NADH formation; Glucose-6P dehydrogenase, phosphogluconate dehydrogenase and GMP reductase for NADPH formation. This knowledge was considered for the determination of the maximum intracellular fluxes for NAD+/NADH and ATP synthesis at different growth phases.

4.2 Systemic analysis of the metabolic response to pH stress

The following protocols correspond to the additional materials and methods used specifically during the study of the metabolic response to pH stress. Again, these are divided into two sections: Construction of algorithms for Data Analysis and Protocols for experimental data acquisition.

4.2.1 Construction of algorithms for Data Analysis

a) Construction of metabolite-specific tables

For each metabolite included in the iSM454, we searched its chemical formula and charge at pH 7.2, as it is the standard pH at which this information is presented. This information was obtained from Marvin™ (ChemAxon, 2016). SMILES, InChI, KeggID and CHEBIiD metabolite identifiers were also added for each metabolite when available in the data bases Chemical Entities of Biological Interest (ChEBI) (Hastings et al, 2013) and/or Kyoto Encyclopedia of Genes and Genomes (Kegg) (Kanehisa and Goto, 2000). This information was assembled in the corresponding vectors metFormula, metCharge, CheBiID, InChi, KeggID and SMILES. An extract of this table is available in Appendix B.

b) Model curation

Mass and charge imbalances were assessed with the command checkMassChargeBalance included in CobraToolbox. Reactions were then manually curated when there was discordance between mass and charge imbalances. In this case, reactions were compared with MetaCyc (Caspi et al., 2016) or balanced manually. Reactions that were only mass imbalanced in protons, and that have the same imbalance in charge, were fixed automatically by adding or resting free protons to each reaction. All these curations were done in MATLAB™ R2015a.

c) Development of AUTOPAD, an algorithm for automatic pH adjustment

We developed AUTOPAD, an algorithm for pH adjustment that is able to change the internal and external pH of a given model. To this end, the protonation state of the metabolites included in the model is changed to adjust the behavior expected at the given pH. Then, the reactions are rebalanced to cope for mass imbalances resulting from these modifications. The inputs of the algorithm are: a GSMM file in .mat format; the new internal and external pH values to be fixed (pH_{set}); and a table that

includes the pKas of each metabolite in the corresponding order of the GSMM, sorted from higher to lower pKa. To adjust the protonation state of metabolites, we assume that when the pH value is higher or equal to a given metabolite pKa, the metabolite exists only in that protonation state.

Charge and mass modifications by protonation changes are carried out as follows:

i. Metabolites. The row of the pKa table that corresponds to a metabolite i is selected. This row contains all the known pKa for this metabolite. Then, the algorithm searches two pKa values in this row: the pKa value which is closest to and is also higher than the original pH (7.2); and the pKa value which is closest to and is also higher than the pH_{set}. The position of both pKas in the row is stored. Then, the difference between both positions is estimated by subtracting these values. For this analysis, a difference in one position is considered as a difference of one charge, as there is one protonation state of difference between the pKas. A negative value indicates dissociation of one proton, and a positive value, acquisition of a proton. Mass and charge of each metabolite are modified to adjust to pH_{set}.

ii. Reactions. After all metabolites have been evaluated - and adjusted, if required - the reactions are checked with Cobra Toolbox's checkMassChargeBalance to identify possible reaction imbalances caused by the changes in the metabolite protonation states. In this step, mass imbalances are fixed by adding free hydrogen atoms as substrates or products. The algorithm output is a GSMM that is mass and charge rebalanced, that has internal reactions balanced at a given pH_{in} and external reactions balanced at the given external pH, as well. This algorithm was built on MATLAB™ R2015a, and requires Cobra Toolbox.

d) Internal pH estimation

For internal pH estimation, a second algorithm that calls AUTOPAD was built. The input of the internal pH estimation algorithm is a GSMM, a set of experimental data, a fixed external pH, and a range of probable internal pH values to test. At each iteration, a model solution with the fixed external pH and one of the possible pH_{in}

values is generated with the algorithm for pH adjustment. Then, experimental data is used to carry out FBA in order to predict biomass formation. Cumulative percentage prediction error (CPPE) (in case the data set includes different conditions, otherwise this value would represent percentage prediction error) is calculated. The output is an excel archive that contains the tested pH_{in} values and the corresponding CPPE of each calculation.

4.2.2 Protocols for experimental data acquisition

a) Characterization of culture kinetics

An O. *oeni* PSU-1 preculture was prepared from a glycerol frozen stock of cells in a 100 ml Erlenmeyer flask containing 70 ml of MRS medium at pH 4.8 for one week. The cells were then cultivated in 250 ml Erlenmeyer flasks containing 170 ml of the defined medium MaxOeno at pH 4.0 for pH adaptation.

The adapted cells were inoculated into 100 ml flasks to a final OD of 0.2. These flask contained 70 ml of MaxOeno at the following pH: 4.0, 3.5 and 3.2, in triplicate. Cells were incubated at 25 ºC without stirring. Samples were taken every eight hours the first two days and every twelve hours the next days, until stationary phase was reached. Each sample's OD was measured at 600 nm, and then the samples were centrifuged at 10000 rpm for 4 minutes at 4 ºC to isolate biomass.

b) Statistical analysis

As it was not possible to assume normal distribution of the data due to not enough data points, significant difference of consumption, production, growth and specific growth rates was analyzed by the non-parametrical version of one factor ANOVA, the Kruskal-Wallis test. Then, Tuckey test was used to evaluate the difference between the three pH levels with 95% confidence interval.

5. RESULTS

This chapter describes the studies we carried out to improve our understanding of the physiology of *O. oeni*. For this purpose, the response of *O. oeni* to increasing ethanol content and low pH was assessed. In both cases, experimental data was collected and then a GSMM was used to analyze the physiological response of *O. oeni* to each variable. The first section refers to the adaptation to increasing ethanol concentrations. In this case, *O. oeni* was grown in a wine-like defined culture medium containing either 0, 3, 6, 9 or 12% v/v ethanol concentrations. In the second section, adaptation to low pH was analyzed by cultivating *O. oeni* at pH 4.0, 3.5 and 3.2. An improved version of iSM454 model was used for Flux Balance Analysis in this case, iMR453. The steps that end with the construction of iMR453, which include an extensive curation procedure and the incorporation of new genetic information, are also reported.

5.1 Adaptation of *Oenococcus oeni* to high ethanol concentrations

5.1.1 Cell growth of *O. oeni* PSU-1 strain in defined wine-like culture medium

The ability of *O. oeni* to grow in the defined, wine -like culture medium designed here, named MaxOeno, was followed by biomass concentration (measured as optical density, OD_{600nm}) and specific growth rates. Additionally, we compared the performance achieved in this medium with the defined medium previously described by Terrade & Mira de Orduña (2009). The growth in both media was evaluated either with 12% v/v of ethanol and without ethanol; and at pH 3.5. In both cases, *O. oeni* PSU-1 cultivated in MaxOeno´s grew more (OD_{600nm} = 0.75 vs OD_{600nm} = 0.25) and faster (μ= 0.012 h^{-1} vs. μ= 0.004 h^{-1}) than Terrade´s. Therefore, the MaxOeno culture medium was employed for all experiments of this work.

5.1.2 Growth of *O. oeni* PSU-1 strain cultivated in the presence of increasing ethanol concentrations

O. oeni PSU-1 was grown in MaxOeno culture medium with increasing ethanol concentrations (0, 3, 6, 9 or 12% v/v ethanol), at pH 4.8. Cell growth kinetics featured four growth phases for all culture conditions, *i.e.* phases I, II, III and stationary; ranging from 0 to 50 hours, 50 to 104 hours, 104 to 164 hours and 164 to 255 hours cultivation, respectively. These phases were marked by substrate depletion (phase I to II) or by significant change in specific growth rate (phase II to III, table 5-1). A lag phase was not observed in all cases (Figure 5-1). Besides, all cultures reached maximum biomass titers after 164 hours (6.8 days) cultivation; thereafter, growth arrested.

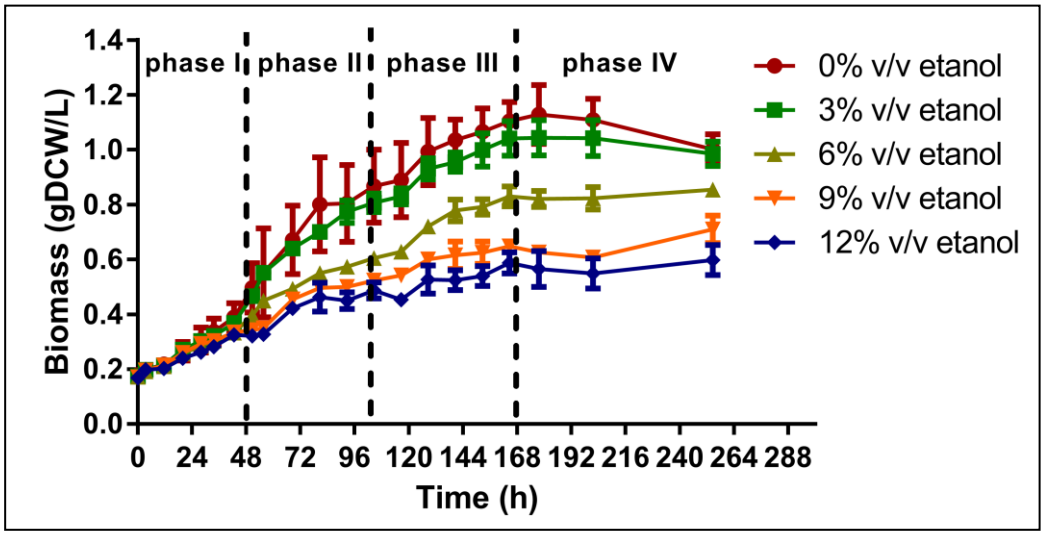

Figure 5-1: Effect of ethanol concentration on the growth of *O. oeni* PSU-1 strain cultivated in MaxOeno, a defined wine-like culture medium.

Each growth phase is delimited by discontinued vertical lines. Phases I, II and III last between 0 to 50 hours, 50 to104 hours and 104 to164 hours of cultivation, respectively.

A clear, linear relationship ($r^2 = 0.98$) between ethanol concentration and cell growth was found, when considering each phase. Moreover, the higher the ethanol content, the slower the specific growth rate and the biomass production (**Error! Reference source not found.**). During phase I, cultures without ethanol and low ethanol (3 and 6 % ethanol) achieved the maximum biomass production and specific growth rate (Table 5-1).

The IVth, *i.e.* stationary, phase was not considered in further metabolic studies because neither growth, nor consumption or production of compounds was observed.

Table 5-1**:** Biomass production (gDCW L^{-1}) and specific growth rates (h^{-1}) of the three growth phases determined for *O. oeni* PSU-1 cultivated in MaxOeno defined medium with increasing concentrations of ethanol

Ethanol content (%v/v)	**Biomass production(¥) (gDCW/L)**				**Specific growth rate(¥) (h^{-1})**		
	I	**II**	**III**	**Total**	**I**	**II**	**III**
0	0.366^{a1}	0.31^{b1}	0.178^{c1}	0.854^{1}	0.021^{a1}	0.008^{b1}	0.003^{c1}
3	0.292^{a2}	0.256^{b2}	0.212^{c1}	0.76^{2}	0.018^{a2}	0.008^{b1}	0.004^{c1}
6	0.225^{a3}	0.169^{b3}	0.191^{b1}	0.585^{3}	0.016^{a3}	0.006^{b2}	0.005^{c1}
9	0.171^{a4}	0.175^{a3}	0.106^{b2}	0.452^{4}	0.014^{a4}	0.007^{b2}	0.003^{c1}
12	0.153^{a5}	0.16^{a3}	0.134^{b2}	0.447^{4}	0.013^{a5}	0.007^{b2}	0.005^{c1}

(¥) All assays were carried out in triplicate and its coefficients of variation (CV) were <20%. Shared superscript letters in the same row indicate no significant difference between cultures with different ethanol level. Shared superscript numbers in the same column indicate no significant difference between growth phases in a same ethanol level (Mood test, $p < 0.05$).

5.1.3 Metabolism of sugars and organic acids by *O. oeni* PSU-1 strain

O. oeni employs three metabolic pathways to obtain energy: phosphoketolase pathway (heterolactic fermentation), malolactic fermentation (MLF) and citrate degradation. The end-products of these catabolic pathways are D-lactate, L- lactate, acetate, ethanol, mannitol, erythritol and CO_2. To tackle the metabolic response of *O. oeni* to ethanol concentration, we followed the consumption and production of the major metabolites of these pathways.

a) Glucose and fructose consumption

As expected, the higher the ethanol concentration in the medium, the lower the sugar consumption. However, regardless of the ethanol concentration, the largest amounts of sugars were consumed during phase I. In this phase, total sugar consumption was similar for all culture conditions (Figure D-1, appendix D), although specific consumption rates for fructose were twice as fast than for glucose, regardless of the ethanol content (Figure 5-2 A and B).

During phase II, both glucose and fructose consumption increased as ethanol content lowered in the culture medium (Figure D-1, appendix D). Furthermore, during this phase, *O. oeni* PSU-1 consumed glucose faster than fructose. Specific consumption rate of fructose was reduced by 50% compared to the previous phase, although specific glucose consumption rate decreased less, regardless of culture conditions (Figure 5-2 A and B).

Finally, in phase III, specific consumption rate of glucose was generally faster than fructose. Specific glucose consumption rates in cultures without and with 3% and 6% v/v ethanol were similar than phase II; but decreased significantly in cultures with 9% and 12% v/v ethanol (Figure 5-2 A and B). On the other hand, specific fructose consumption rates in cultures without and with 3 % v/v ethanol decreased around 90% and 60%, respectively. Similar rates than in phase II were found for cultures with 6%, 9% and 12% ethanol.

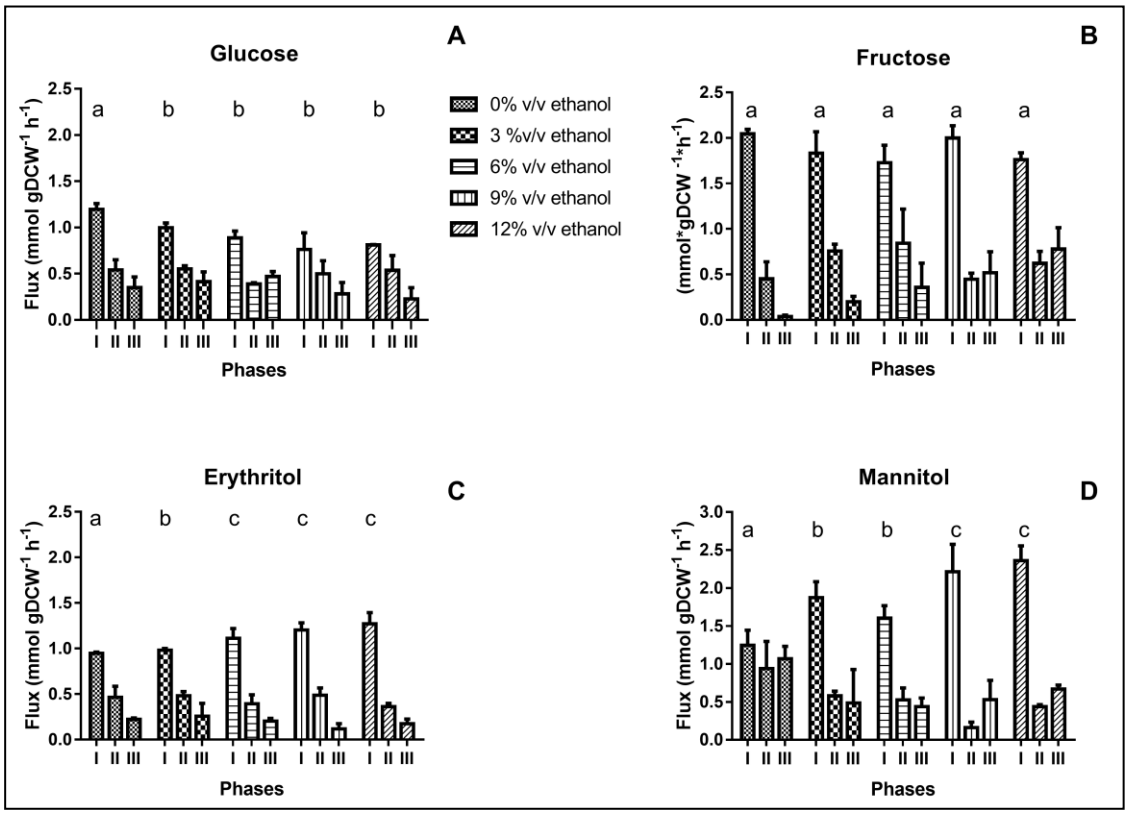

Figure 5-2: Specific consumption rates of glucose (A), and fructose (B) and concomitant specific production rates of the related products, erythritol (C) and mannitol (D) during cultivation of *O. oeni* PSU-1 under increasing ethanol contents.

Growth phases I, II and III are represented by 1, 2 and 3, respectively.

b) Mannitol and erythritol production

These polyols are mainly produced through fructose catabolism - although they could also be synthesized from glucose. Again, the fastest production of mannitol and erythritol was achieved during phase I. The production of both metabolites increased concomitantly, with ethanol content (Figure 5-2, C and D). Total mannitol concentration - the most abundant metabolite produced - was higher than erythritol concentration. In the absence of ethanol, specific production rates for mannitol and

erythritol were 1.25 mmol $gDCW^{-1}h^{-1}$ and 0.95 mmol $gDCW^{-1}$ h^{-1}, respectively. Production rates of both polyols raised concomitantly with ethanol increment, during phase I (Figure 5-2 D).

In phase II, production rates of both poyols dropped by half of the previous phase in the absence of ethanol in the culture medium. Once again, mannitol production increased with ethanol content, except for cultures with 6% ethanol (Figure 5-2 D). On the contrary, erythritol production decreased sharply in this phase for cultures containing 9 and 12%v/v ethanol (Figure 5-2 C).

c) L-malate and citrate metabolism

L-malate and citrate are the main organic acids in wine that support the growth of *O. oeni* under nutritional stress conditions. Lactate is synthesized by *O. oeni* as L- or D-enantiomers, according to its origin. L-lactate is produced in one step from L-malate through malolactic fermentation; and D-lactate towards the phosphoketolase pathway.

L-malate and citrate were metabolized during phase I (Figure 5-3 A and B), their consumption being triggered at the very beginning of the cultivation. Total acid consumption, expressed in concentration units (g/L), suggests that all cultures behaved similarly, both acids being completely consumed at the end of phase I, i.e. after 50 hour cultivation (Figure D-2, appendix D). Specific consumption rates, however, clearly show that the higher the ethanol content, the faster the metabolism of these organic acids.

Surprisingly, malate consumption was larger than L-lactate production; and the specific consumption rate of the former was *circa* 30 % faster than the latter, for all culture conditions (Figure 5-3 A and E). This suggests that one of these compounds is either accumulating intracellularly or being transformed into another metabolite (Figure 5-3 A, D and E).

On the other hand, the specific production rate of D-lactate (0.15 to 0.20 mmol. $gDCW^{-1}$ h-1) was more than tenfold slower than the corresponding one for L-lactate

(1.5 to 3.0 mmol. $gDCW^{-1}$ h^{-1}), at least during phase I. Also, during this phase D-lactate production is lower at 9 and 12% ethanol content. Contrary to L-lactate, D-lactate is still significantly synthesized in later phases, although at variable rates (Figure 5-3 E).

Acetate was the second most abundant metabolite produced, reaching a maximum of 50 mmol $gDCW^{-1}$ in cultures without ethanol (appendix D). *O. oeni* produces acetate from citrate and from sugars through the phosphoketolase pathway. During phase I, citrate uptake and acetate synthesis rates were higher than other phases (Figure 5-3 B and C), suggesting that acetate was formed using all citrate consumed. However, acetate synthesis was faster than citrate uptake, which indicates that another pathway, such as the phosphoketolase pathway, was used additionally for its production. However, in phases II and III acetate was mainly produced through phosphoketolase pathway, using other compounds, such as glucose.

5.1.4 Metabolism of amino acids

All the amino acids were metabolized during the cultivation of *O. oeni* in MaxOeno culture medium at increasing concentrations of ethanol. Histidine, lysine, cysteine and aspartic acid were the most consumed amino acids, with over 50% of its original concentration consumed. Also, the highest specific consumption rates were those of histidine and proline (Figure 5-4 D and F) and their rates increased concomitantly with increasing ethanol contents in culture medium.

Amino acids were mostly consumed (almost 90%), during phase I, with the exception of cysteine, which was consumed during phases I and II (Figure 5-4, Figure D-3 from appendix D). Interestingly, specific consumption rate of cysteine was the only one that was higher for phase II than for phase I, even increasing with ethanol content (Figure 5-4 A). Threonine was consumed faster in cultures with 9 and 12% ethanol; and serine was consumed faster in cultures with 6% ethanol (Figure 5-4 C and E).

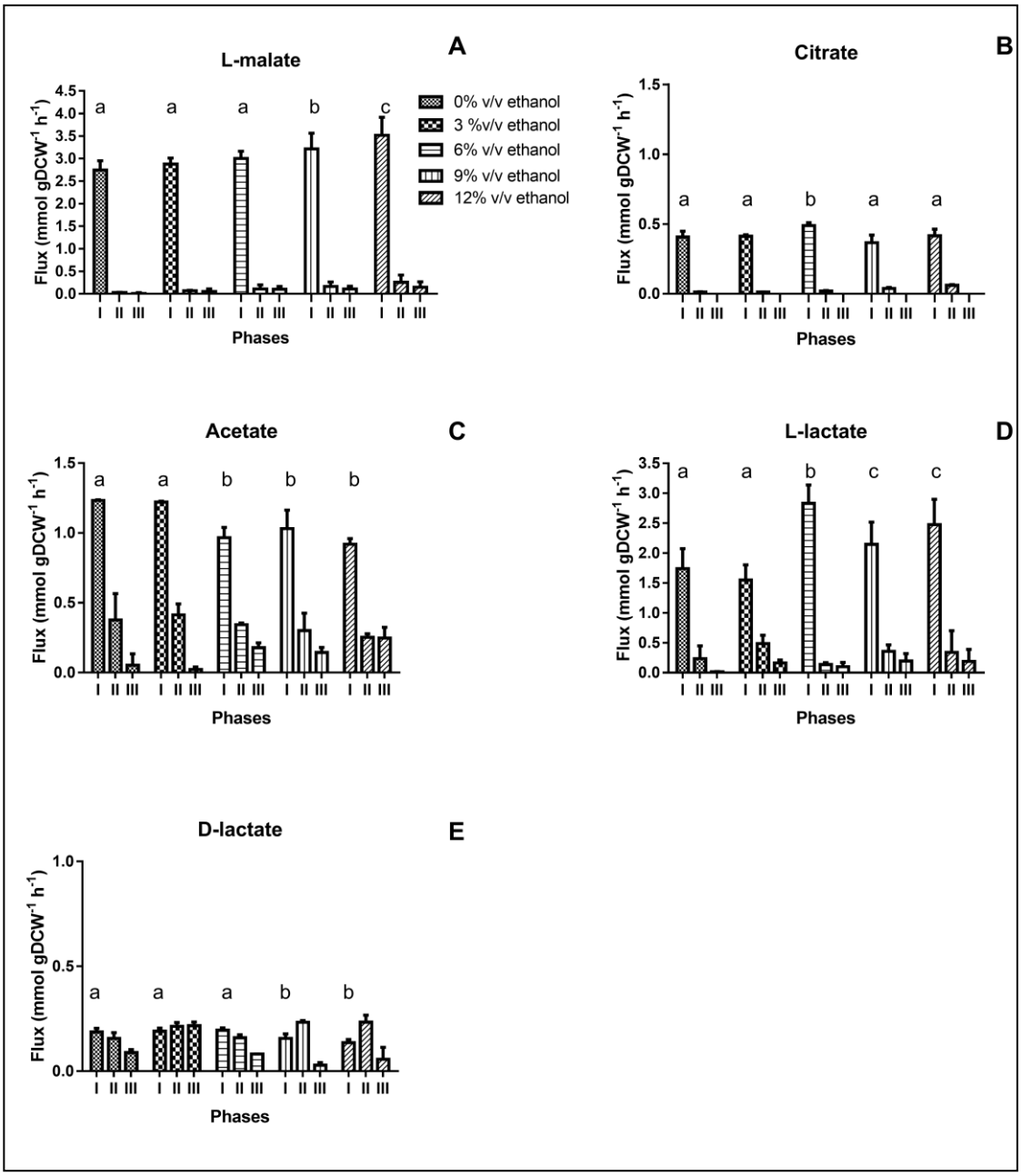

Figure 5-3: Specific consumption rates of malic (A) and citric (B) acids and specific production rates of acetate (C) L-lactate (D) and D- lactate (E) during growth of *O. oeni* PSU-1, under increasing ethanol contents.

Growth phases I, II and III are represented by 1, 2 and 3, respectively.

Besides, histidine and lysine consumption increased with ethanol. It is noteworthy that histidine was the most consumed amino acid in the cultures with 12% ethanol, reaching 18 mmol $gDCW^{-1}$. Cysteine, lysine, methionine and tryptophan were imported at similar amounts, regardless of the ethanol content (Table 5-2). However, their specific consumption rates increased with ethanol content (Figure 5-4 G, Figure D-3 from appendix D). Alanine and aspartic acid were also consumed faster in cultures with higher ethanol content (Figure 5-4 B and H).

Finally, the consumption of aspartic acid, arginine, glutamic acid and isoleucine decreased as ethanol content was incremented in the culture medium.

5.1.5 Analysis of intracellular fluxes

a) Non-Growth Associated Maintenance (NGAM)

FBA was carried out in iSM454 model to predict NGAM for each experimental data set. Thereby, a range of possible NGAM values was tested and biomass formation rate was predicted. The NGAM value that allowed the minimal biomass prediction error was selected for each data set. Biomass was predicted correctly, with an average biomass prediction error of 0.05%.

Estimated NGAM values significantly increased in all phases, although differently, depending on the ethanol content of the culture medium. In phase I, NGAM increased 3 fold in cultures with 3 and 6% ethanol; and 10 and 17 fold in cultures with 9 and 12% ethanol. In phase II, it sequentially increased from 6 to 11 fold in cultures from 3 to 12% ethanol, respectively. In phase III, a maximum NGAM increase of 7 fold was achieved for cultures with 12% ethanol content. Regardless of the ethanol level, NGAM was the lowest for phase I and the largest for phase III (Figure 5-5 A).

Table 5-2: Amino acid requirements by *O. oeni* PSU-1 cultured in medium with different ethanol content

		Consumed amino acids [%] ¥				
	Amino acid	**Ethanol (% v/v)**				
		0%	**3%**	**6%**	**9%**	**12%**
	Histidine	72.1^{a}	68.8^{b}	82.9^{b}	79.3^{c}	67.8^{d}
>50%	Lysine	77.6^{a}	69.8^{a}	74.7^{a}	66.5^{a}	64.9^{a}
	Cysteine	67.9^{a}	64.3^{a}	68.2^{a}	64.4^{a}	64.4^{a}
	Aspartic acid	65.0^{a}	68.8^{a}	62.1^{b}	46.5^{c}	24.7^{d}
	Arginine	39.3^{a}	39.3^{a}	40.1^{a}	36.4^{a}	31.5^{b}
	Methionine	32.7^{a}	37.9^{a}	37.0^{a}	39.4^{a}	36.8^{a}
	Proline	36.3^{a}	34.7^{ab}	34.5^{ab}	32.8^{ac}	29.5^{c}
30-50%	Alanine	31.7^{a}	30.0^{b}	30.2^{b}	28.3^{c}	25.5^{d}
	Glutamic acid	41.3^{a}	37.5^{a}	36.4^{a}	32.0^{b}	25.5^{c}
	Serine	46.6^{a}	43.3^{ab}	44.6^{ac}	41.7^{ad}	39.2^{d}
	Glutamine	18.1^{a}	21.4^{ab}	22.4^{b}	23.3^{bc}	25.9^{c}
	Valine	28.5^{a}	27.2^{a}	26.4^{a}	23.7^{c}	18.3^{d}
	Tyrosine	13.4^{a}	15.3^{b}	17.4^{b}	18.9^{b}	16.4^{c}
<30%	Leucine	6.8^{a}	5.8^{a}	13.5^{b}	24.3^{c}	19.5^{d}
	Isoleucine	27.8^{a}	21.0^{b}	19.3^{b}	16.9^{bc}	14.3^{c}
	Phenylalanine	24.8^{a}	25.2^{a}	25.0^{a}	22.4^{b}	18.7^{b}
	Threonine	23.9^{a}	20.9^{ab}	17.0^{a}	20.7^{b}	19.3^{b}
	Tryptophan	23.5^{a}	23.2^{a}	24.0^{a}	23.4^{a}	20.4^{a}

¥ All assays were performed in triplicate and all coefficients of variation (CVs) were <10%. Shared superscript letters (a, b, c) in the same row indicate no significant difference (Mood test, $p < 0.05$). Consumption of amino acids highlighted in light gray are independent consumed of ethanol content present in the culture medium. Consumption of amino acids highlighted in dark gray are dependent consumed of ethanol content present in the culture medium.

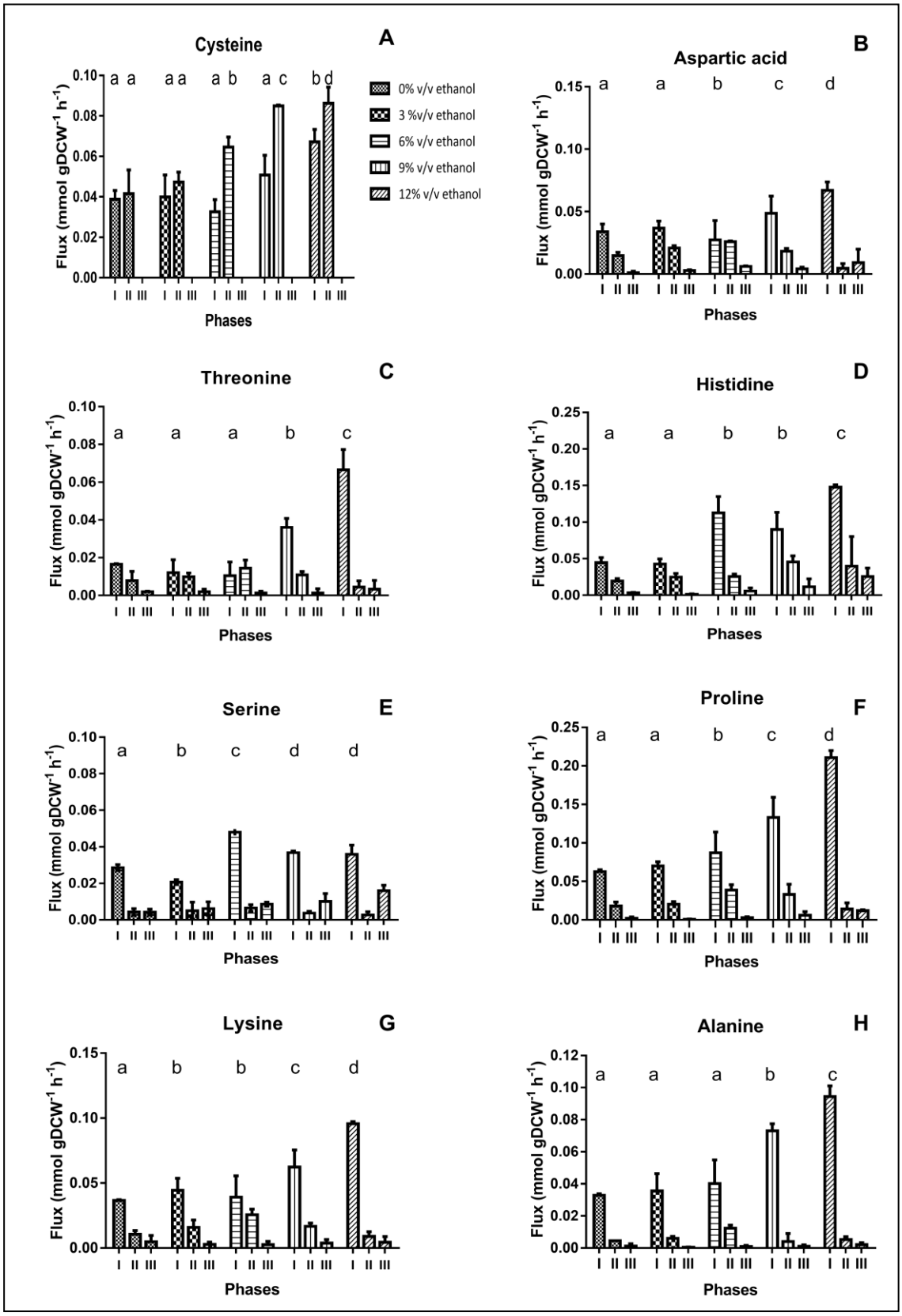
A
Cysteine
a a a a a b a c b d
B
Aspartic acid
a a b c d
C
Threonine
a a a b c
D
Histidine
a a b b c
E
Serine
a b c d d
F
Proline
a a b c d
G
Lysine
a b b c d
H
Alanine
a a a b c
0% v/v ethanol
3 %v/v ethanol
6% v/v ethanol
9% v/v ethanol
12% v/v ethanol
Flux (mmol gDCW-1 h-1)
Phases
I II III

Figure 5-4**:** Specific consumption rates of amino acids during cultivation of *O. oeni* PSU-1 under increasing ethanol contents.

A) Cysteine. B) Aspartic acid. C) Threonine. D) Histidine. E) Serine. F) Proline. G) Lysine. H) Alanine. Growth phases I, II and III are represented as 1, 2 and 3, respectively. Statistical analysis was only performed for phase I and shared letters indicate no significant difference (Mood test, $p< 0.05$).

b) NGAM Sensitivity analysis

Sensitivity of NGAM values towards the experimental data was evaluated by varying each constrained flux independently in 1% of its value, and then repeating NGAM prediction. NGAM prediction variation was assessed by calculating the relative prediction error (in %), and the highest prediction error was taken as representative of the NGAM's sensitivity of the corresponding data set (appendix G).

Phase I was the most sensitive phase at every ethanol level, reaching the highest NGAM prediction variation in the absence of ethanol (130%). The largest variations were obtained when fructose and mannitol fluxes were varied.

c) Energetic requirements

The model predicted that ATP requirements increase with ethanol content at each phase. Higher ATP requirement is predicted during phase I, regardless of the ethanol content.

ATP is synthesized either by F_0F_1-ATPase or phosphoketolase pathway. In phase I, the specific production rate of ATP (r_{ATP}) produced by F_0F_1-ATPase was higher than ATP produced through the phosphoketolase pathway. In cultures with 0 to 12% ethanol, fluxes through ATPase increased from 2.9 to 4.8 mmol $gDCW^{-1}$ h^{-1}, respectively; and fluxes through the phosphoketolase pathway decreased from 2.1 to 1.3 mmol $gDCW^{-1}$ h^{-1}, for the same cultures (Figure 5-5 C and D).

In phase II, r_{ATP} occurring through F_0F_1-ATPase decreased by 50% in all cultures. On the contrary, r_{ATP} through the phosphoketolase pathway increased in all cultures with ethanol content. Finally, during phase III, r_{ATP} by F_0F_1-ATPase continues to decrease – by another 50% compared to phase II; and r_{ATP} through phosphoketolase pathway also decreased in cultures containing less than 6 % v/v of ethanol content, but remained constant in cultures with higher ethanol contents (Figure 5-5 C and D).
Interestingly, during phase I, the ATP flux through F_0F_1-ATPase increased from 58% to almost 80% of total ATP flux in cultures without ethanol and cultures with ethanol content, respectively. Besides, during phases II and III there was a preference for synthesis by the phosphoketolase pathway; on average, 56% of ATP was produced from this pathway (Figure 5-5 C, D and E).

d) Impact of ethanol on the redistribution of intracellular fluxes

Distribution of carbon intracellular fluxes was analyzed for all the growth phases, considering the major central metabolic pathways, which includes phosphoketolase pathway, fructose reduction, citrate degradation and malolactic fermentation. FBA showed that a significant redistribution of intracellular fluxes occurred in *O. oeni* in response to ethanol content (Figure 5-6; Figure D-4 and Figure D-5, appendix D). Fluxes were normalized over specific growth rates.

The model showed that fructose, the sugar that was most consumed, was mainly used – around 70% of the total - for mannitol biosynthesis during phase I; however, in later phases, fructose was redirected to glucose-6P synthesis, and then into the phosphoketolase pathway (Figure D-4 and Figure D-5, appendix D).
Erythritol biosynthesis arises from ribulose-5P and glyceraldehyde-3P in almost all cases (Figure D-5, appendix 0). It was highest during phase I, and increased with ethanol content, from 42 to 84 mmol $gDCW^{-1}$ in cultures without and with 12% ethanol, respectively.

The model also predicted diacetyl synthesis. This specific production rates incremented with ethanol content and thus were highest at 12% ethanol in all phases. This compound is produced from pyruvate.

Interestingly, pyruvate production increased in phase II, and even more in phase III by the following routes: amino acid degradation, citrate degradation, and L-malate conversion into oxaloacetate (Figure 5-6; Figure D-4 and Figure D-5, appendix D). All of these fluxes also incremented as ethanol increased in the culture medium (Figure D-4 and Figure D-5, appendix D).

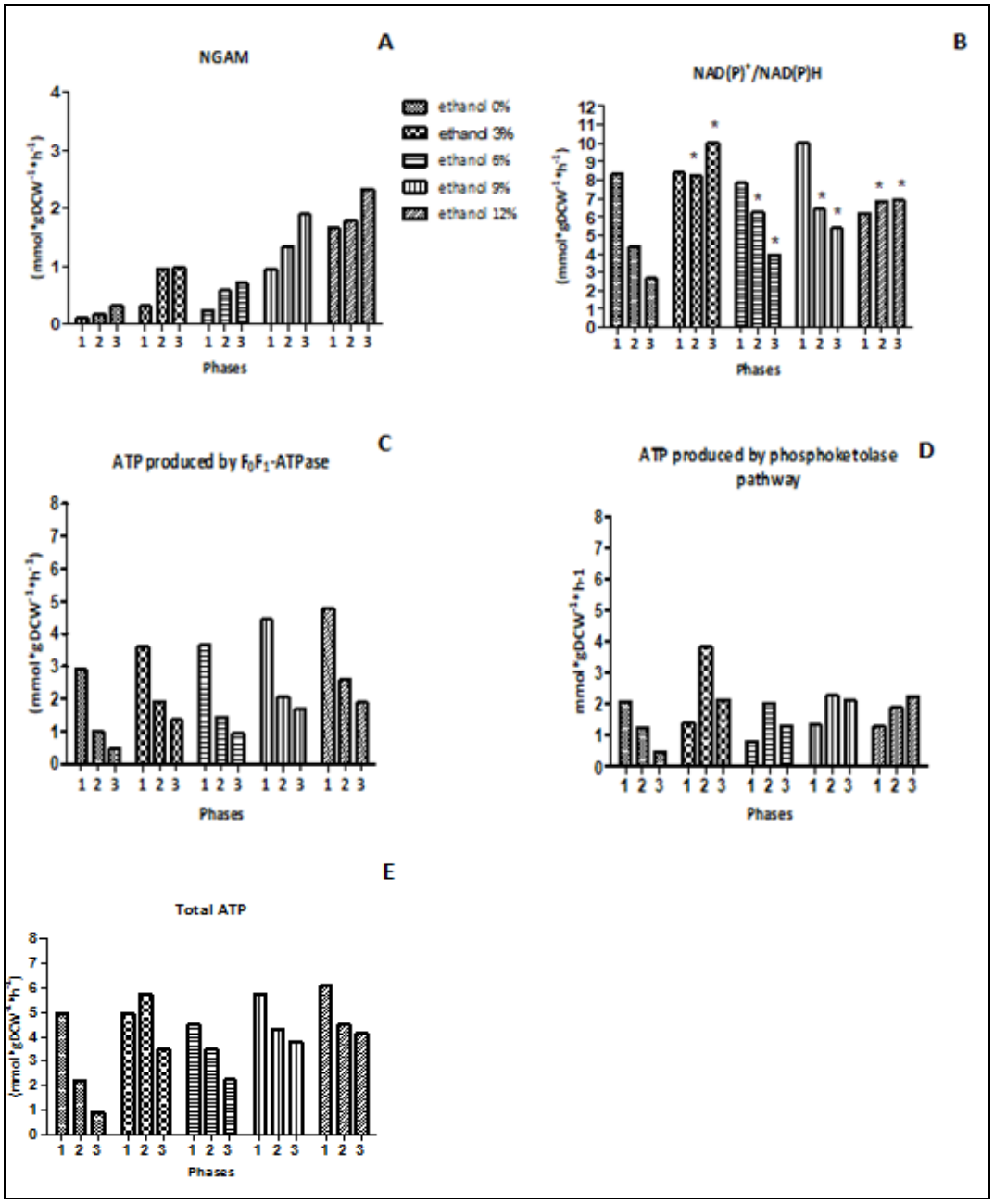

Figure 5-5: NGAM and in silico determined specific production rates of key metabolites of *O. oeni* PSU-1

A) NGAM, B) NAD(P)+/NAD(P)H, C) ATP produced by F0F1-ATPase, D) ATP produced by phosphoketolase pathway, E) Total ATP, i.e ATP produced by both ATPase and phosphoketolase pathways. FVA was applied to determine the production span of these compounds at the optimum

biomass production rate. A span that was higher than 10% of the estimated flux is marked by an asterisk (*).

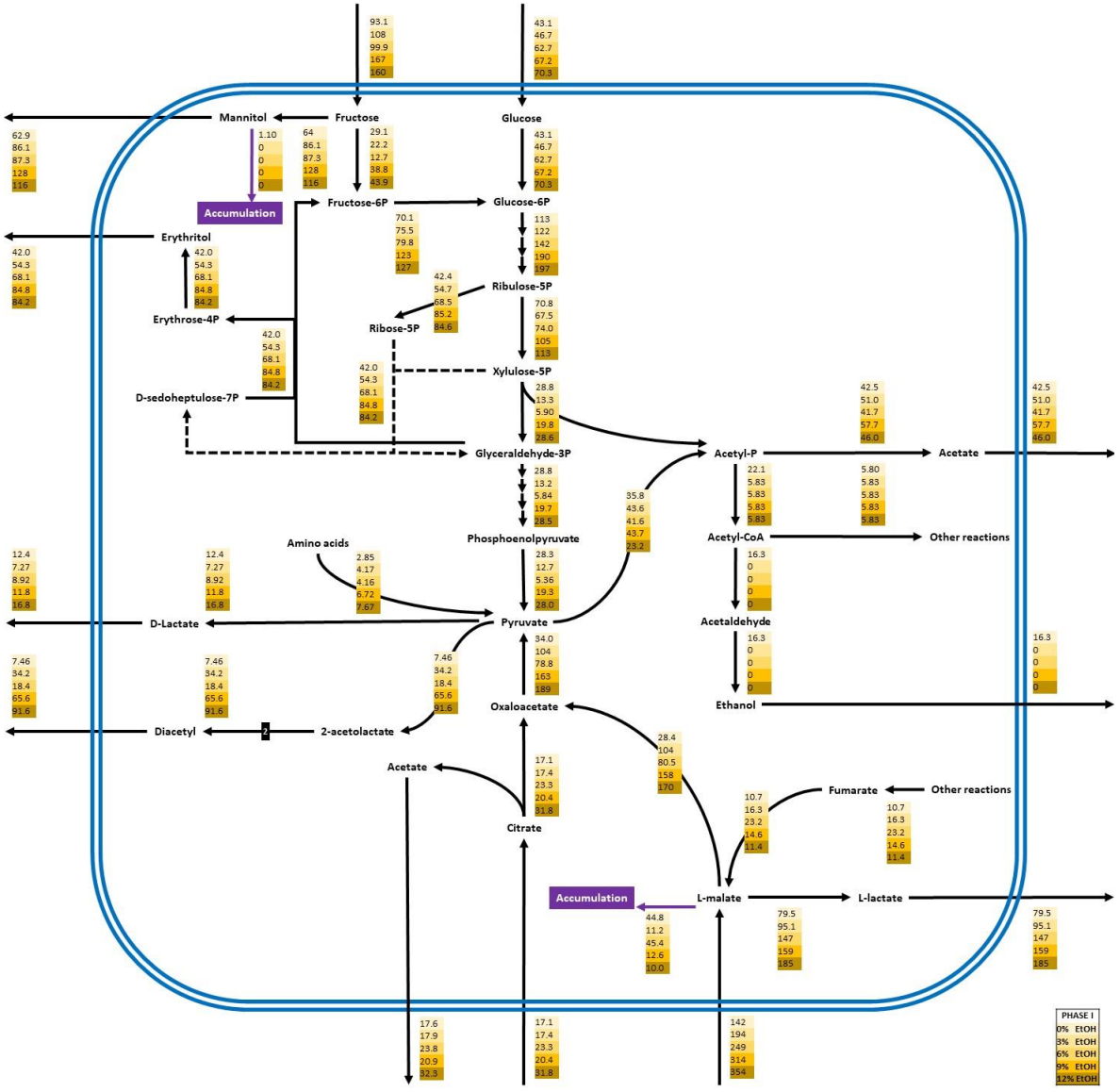

Figure 5-6: Metabolic flux redistribution of the central carbon metabolic pathways of *O. oeni* PSU-1 upon cultivation in a culture medium without and with 3, 6, 9 and 12% (yellow boxes, from top to bottom) ethanol concentration, during growth phase I.

5.2 Adaptation of *Oenococcus oeni* to low pH

In this chapter, the adaptation of *O. oeni* to low pH is studied with the aid of iMR453. In order to do so, this part is divided in four sections: Curation of the iSM454 model, Modification of internal pH, Characterization of culture kinetics, and Analysis of intracellular fluxes. The first section, Curation of the iSM454 model, includes the assessment of mass and charge imbalances present in iSM454, and the modifications performed to reduce blocked reactions and improve biological relevance. This step ends with the generation of the model iMR453. Then, in the second section, Modification of internal pH, an algorithm for internal and external pH modifications was generated, and then iMR453 was employed to estimate the pH_{in} value that minimized biomass prediction error. In the third sectio, Characterization of culture kinetics, we characterized the growth features of *O. oeni* at different pH culture conditions (4.0, 3.5 and 3.2) and the resulting changes of specific consumption and production rates of main compounds. Finally, in the fourth section, Analysis of intracellular fluxes, the experimental data collected in the third subsection is analyzed with the aid of the iMR453 model.

5.2.1 Curation of the iSM454 model

The first step in curation of iSM454 was to correct mass and charge imbalances. As iSM454 does not have the charges neither the masses associated to the metabolites present in the model, the first step was to search and include this information. This was carried out by searching through Marvin™ (ChemAxon, 2016). Metabolite identifiers were recollected from CheBi (Hastings *et al*, 2013) and Kyoto Encyclopedia of Genes and Genomes (KEGG) (Kanehisa, M. and Goto, 2000) to facilitate compound identification. Once mass and charge were assigned to each metabolite, then mass and charge imbalances were evaluated for each reaction included in the iSM454 model. Of the 660 reactions, 163 were imbalanced. These

were classified in two types: type I, reactions whose mass and charge imbalances could be fixed by incorporation of hydrogen ions; and type II, reactions where mass imbalances were not only protons, or where hydrogen imbalances were not the same as charge imbalances (Table 5-3). First type reactions were easily corrected by automated curation, and second type reactions required manual curation.

Table 5-3**:** Example of type I and type II imbalances

	Reaction Name	**Reaction**	**Mass imbalance**	**Charge imbalance**
Type 1	ASPARAGHYD-RXN	1 L-Asn [c] + 1 H2O [c] -> 1 L-Asp [c] + 1 NH4+ [c] + 1 H+ [c]	1	1
	CTPSYN-RXN	1 UTP [c] + 1 L-Gln [c] + 1 ATP [c] + 1 H2O [c] -> 1 CTP [c] + 1 L-Glu [c] + 1 ADP [c] + 1 P [c] + 1 H+ [c]	3 H	3
	UDPNACETYLGLUCOSA	1 UDP-N-acetylglucosamine [c] + 1 phospho-enolpyruvate [c] -> 1 UDP-N-acetylglucosamine-enolpyruvate [c] + 1 P [c]	-1 H	-1
Type 2	TRANS-RXNK9E-432	1 D-mannose [e] + 1 phospho-enolpyruvate [c] -> 1 D-mannose [c] + 1 pyruvate [c]	1 H, -3 O, -1 P	2
	TRANS-RXNK9E-454	1 Fe2+ [e] + 1 H+ [e] -> 1 Fe2+ [c] + 1 H+ [c]		-2
	RXNK9E-138	1 NO3 [e] + 1 ATP [c] -> 1 NO3 [c] + 1 ADP [c] + 1 P [c]	1 H, 1 O	-1

A negative imbalance indicates that the imbalance is due to lack of charge/mass in the product side and a positive one, to lack in the substrate side. Type I reactions are only mass imbalanced in hydrogen ions, and have the same charge imbalances. Type II have major imbalances, and require manual curation.

Of the 163 imbalanced reactions, 29 required manual curation (Appendix C). Of these reactions, seven were discarded - four involved in processes not needed for modeling: 'FOLYLPOLYGLUTAMATESYNTH_RXN', 'METHIONYL_TRNA_FORMYLTRANSFERASE_RXN', 'RXN_11811' and '_1_11_1_12_RXN'; and three exchange reactions of external metabolites, i.e. not needed: 'dextran (glucose)n_ex_', 'putrescine_ex_' and 'spermidine_ex_'. In this process, two genes were removed from the model as they belonged to reactions of DNA reparation, which shouldn't have been included in the model: OEOE_1391 and OEOE_0787. Also, four additional reactions were modified by changing their reversibility (Appendix C).

Regarding metabolites, the following metabolites were discarded during the curation as they only participated in the removed reactions: Mannose [c], NH3 [c], THF-Glu [c], lipid_hydroperoxide [c], lipid [c], 'dextran__glucose_n[e]', 'spermidine[e]' and 'putrescine[e]'; a new metabolite, D-mannose-P, was added to balance the PTS-mannose transporter ('TRANS-RXNK9E-432', present in Table 5-3); and the names of three metabolites were changed to facilitate identification (Appendix C).

Additionally, the pathways in the model were compared with the recent work of Cibrario *et al* (2016), in which sugar degradative pathways in different strains of *O. oeni* were reviewed. Thus, we found out that the phosphomannose isomerase reaction (E.C. 5.3.1.8), gene OEOE_0249, (NCBI geneID 4415535) was absent in the model, and was included.

As a final step of curation, reactions were classified into 89 subsystems to facilitate reaction identification (appendix C0). This information was added to the model in the vector subSystems.

The result of all these curation steps was the generation of the iMR453 model, which includes 453 genes, 655 reactions and 529 metabolites, all mass and charge balanced.

5.2.2 Modification of internal pH

The internal pH of *O. oeni* is expected to be dependent of the external pH, and thus the algorithm AUTOPAD for pH modification was constructed in MATLAB™ 2015a to analyze this reaction. AUTOPAD generates multiple models that have metabolites in the protonation state corresponding to a given internal and external pH, and which reactions are mass and charge balanced. This algorithm requires the pKa of each metabolite present in the model, and thus pKa were recollected for each metabolite present in the model from MarvinSketch™ (ChemAxon, 2016).

We evaluated iMR453, by searching the pH_{in} that minimized the cumulative biomass prediction error from the experimental data provided by Gutiérrez (unpublished data). This data included twelve batch experiments of *O. oeni* grown in MaxOeno at the following conditions: eight were done at external pH 4.8 with one of the following ethanol concentrations: 0, 3 , 9, 12% v/v, in duplicates; and four cases at external pH 3.5, with 0 and 12% v/v ethanol, in duplicates (Appendix A). Figure 5-7 shows the errors obtained for pH_{in} values in a range of 5.6-6.3. In both cases the minimum error was observed when pH_{in} was 6.26-6.27, indicating that pH_{in} remains stable when external pH varies.

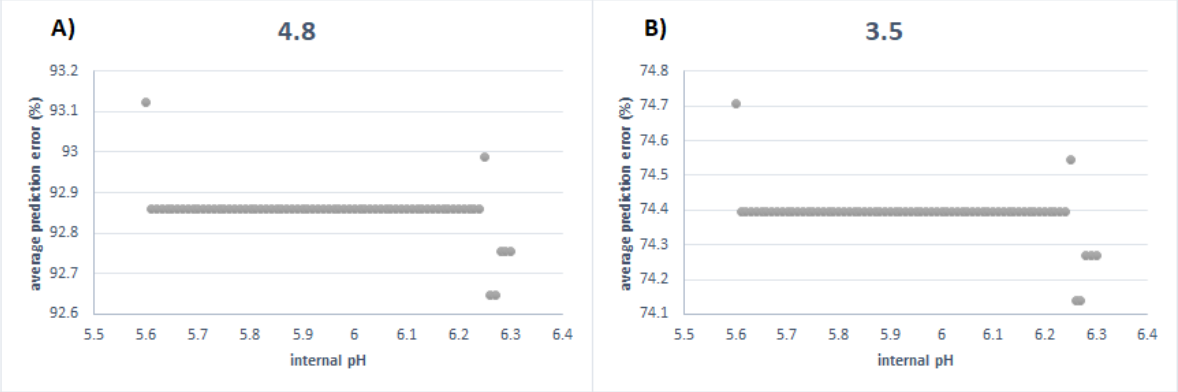

Figure 5-7: Estimation of internal pH at two conditions of external pH (4.8 and 3.5) by minimizing biomass prediction error

Figure 5-7 illustrate the average biomass prediction error from biomass predicted with iMR453 fixed with the experimental data provided by Gutiérrez (2015) for two different external pH, 4.8 and 3.5, at a range of possible internal pH values. Each point in the figure represents the biomass prediction error estimated from iMR453 adjusted to external pH 4.8 (a) or 3.5 (b) and at the internal pH indicated in the x-axis.

To the best of our knowledge, there are three studies that have measured pH_{in} for *Oenococcus oeni* (Table 5-4). These studies show that, even at low pH_{out}, pH_{in} is maintained (Bouix & Ghorbal, 2015). These experimental results agree with our *in silico* determinations. In particular, Salema *et al* (1996) measured a pH_{in} of 6.1 and 6.3 when pH_{out} was 4.6 and 5.2, respectively. For pH_{out}=3.5, our results are higher than Salema's *et al* (pH_{in}=5.8), but closer to the results of Bouix & Gorbal (2015), i.e. pH_{in}=6.1.

Table 5-4**:** Internal pH of *Oenococcus oeni* cultivated at different external pH according to the literature

	Salema *et al* (1996)	**Augnaugneur *et al* (2007)**	**Bouix & Gorbal (2015)**
External pH	**Internal pH**		
3.0	5.8		
3.2		5.8	6.1
3.5	5.8		
4.1	6.0		
4.5		6.5	
4.6	6.1		
5.2	6.3		
5.3		6.8	
5.6	6.3		

5.2.3 Characterization of culture kinetics

To evaluate the physiological response of *O. oeni* to increasingly acidic pH, *O. oeni* PSU-1 was grown in MaxOeno defined culture medium (Contreras *et al*, submitted) at pH = 4.0, 3.5 and 3.2. In this section, we first described the adaptation routine employed to prepare the cells to grow at the desired pH values. Then, the experimental results are reported. Specific growth rates, biomass concentration, substrates consumption and metabolites production found at each pH condition are presented to allow for comparison of differential physiological responses.

a) Adaptation

To prepare cells for survival at low pH, two different adaptation protocols were tested for pH 3.2 and 3.5. *O. oeni* pre-culture was first cultured at pH 3.5 or 4.0 in MaxOeno medium for seven days. Then, each set of cells were cultivated at pH 3.5 and 3.2 in 100 ml flasks, at an initial OD of 0.1 (Figure 5-8). Growth at both pH 3.2 and 3.5 seemed to improve when prior adaptation at pH 4.0 was carried out.

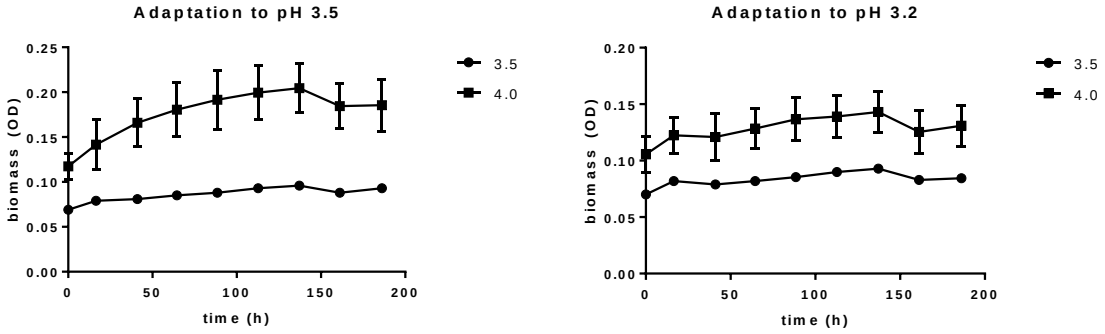

Figure 5-8: Evaluation of the effectiveness of pH adaptation for growth of O. oeni PSU-1 at pH 3.2 and 3.5

Results are the average of a biological duplicate. Sample for final pH 3.5, adaptation at pH 3.5 is the result of a single experiment.

b) Cultivation of O. oeni at pH 4.0, 3.5 and 3.2

O. oeni was grown at pH 4.0, 3.5 and 3.2 in the MaxOeno culture medium, and samples were taken until stationary phase was reached. The results of this experiment are shown in the following subsections. Experiments were carried out in triplicates.

i. Biomass

Cells cultured at pH 4.0 were the first to reach stationary phase after 290 h, achieving the highest biomass (X(pH 4.0) = 0.63 gDCW L^{-1}). Both cultures grown at pH 3.5 and pH 3.2 reached stationary phase at 435 h; the former with a final biomass X (pH 3.5) = 0.53 gDCW L^{-1}, and the latter X (pH 3.2) = 0.39 gDCW L^{-1}(Figure 5-9). Interestingly, during the first 52 h of cultivation, the biomass concentration was similar for all pH conditions.

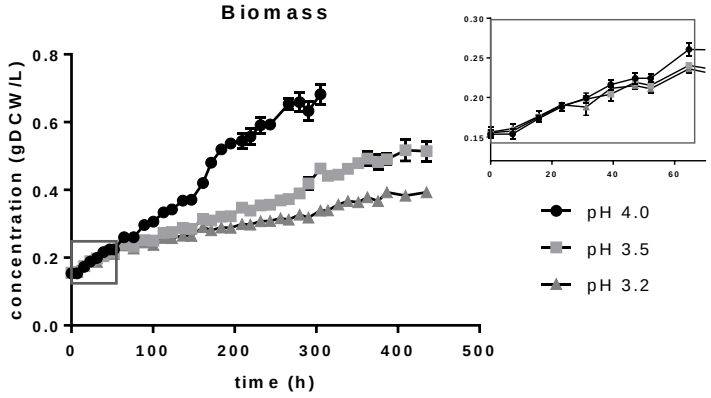

Figure 5-9: Biomass formation during the cultivation of *O. oeni* PSU-1 in MaxOeno at pH 4.0, 3.5 and 3.2

Figure shows a zoom of the first 50 hours, in which biomass production is constant between the three experimental phases.

In all experimental conditions biomass showed four growth phases: phase I, phase II, phase III and stationary phase (Figure 5-10). Cells grown at pH 3.5 and 3.2 share the same duration for each phase: 0-52 h for phase I; 52-195 h for phase II; 195-362 h for phase III; and 362-435 h for stationary phase. Cells grown at pH 4.0 presented the same four phases, at different timing: 0-65 h for I; 65-147h for II; 147-232 h for III; and 232- 305 h for stationary phase. Maximum specific growth rate (μ_{max}) was observed at phase I in all three cases (Table 5-5). As expected, pH 4.0 had the highest

μ_{max} (pH 4.0) =0.0083 h^{-1}; and μ_{max}(pH 3.2) = μ_{max}=0.0064 h^{-1}, the lowest, with a 23% reduction. μ_{max} did not show significant differences between cultures at pH 3.2 and 3.5.

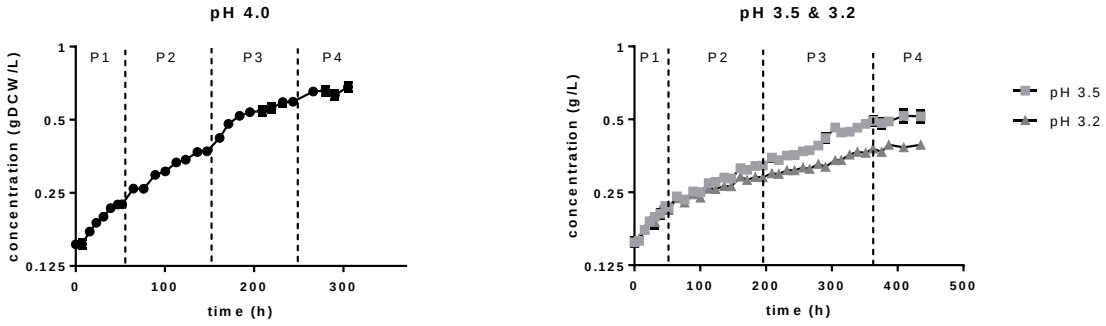

Figure 5-10: Biomass formation at different pH in log scale

Biomass formation is shown in logarithmic scale, in order to distinguish the four growth phases. pH 3.5 and 3.2 have the same time lapses for each phase, and thus are presented in the same image. pH 4.0 shows the same phases, at different time lapses.

Each phase was, as observed during different ethanol concentrations, marked by differences in the specific consumption and production rates of the compounds; during phase I there was the highest malic and citric acid consumption. The differences between phase II and phase III, as the compounds are maintained, could be attributable to inhibition.

Table 5-5**:** Final biomass titer and maximum specific growth rates of *O. oeni* PSU-1 cultivated at different acidic pH in MaxOeno culture medium.

	Final biomass (gDCW L^{-1})	**maximum specific growth rate (h^{-1})**
pH 4.0	$0.683^{a} \pm 0.0301$	$0.00829^{a} \pm 0.000235$
pH 3.5	$0.522^{b} \pm 0.0243$	$0.00693^{b} \pm 0.000241$
pH 3.2	$0.393^{c} \pm 0$	$0.00641^{b} \pm 0.000352$

Table 5-5 shows a characterization of biomass growth by indicating final biomass concentration and maximum specific growth rate, which was achieved during phase I. Same superscript in the same column indicates no significant difference as assessed by Dunnet's test with a 95% confidence interval. Experiments were done in triplicate for pH 4.0 and 3.5, and in duplicate for pH 3.2.

ii. Organic acids

Malic and citric acids were the organic acids present as substrates in the medium. Almost all L-malic acid was consumed during phase I for the three pH conditions (Figure 5-11 a), concomitant with undifferentiated biomass formation. Highest specific consumption rate was observed at pH 3.5 and 3.2, and the lowest at pH 4.0. Then, during the following phases organic acids were differentially consumed: for cultures at pH 4.0, L-malic acid was consumed at a slower rate during phase II until its depletion at 100 h. For cultures carried out at pH 3.5 and 3.2, L-malic acid was minimally consumed during phase II, and during phase III consumption restarted, but at a lower rate. Total depletion was only observed at pH 4.0 (Figure 0-2 a, appendix E). It is noteworthy that the highest specific L-malic acid consumption, i.e.

normalized by biomass, occured at pH 3.2 = 59.8 mmol $gDCW^{-1}$), followed by pH 3.5= 41.1 mmol $gDCW^{-1}$) and pH 4.0 = 30.8 mmol $gDCW^{-1}$) (Table 5-6).

Citric acid was depleted in all cases (Figure 0-2 b, appendix E), although at different times; at pH 4.0, citric acid was depleted at the end of phase I, and thus presented the higher specific consumption rate of this phase. For pH 3.5 and 3.2, depletion was reached after during phase II. Total citrate consumption showed a similar behavior than malic acid, i.e. higher at pH 3.2, than pH = 3.5 and pH = 4.0 (Table 5-6).

Acetic and lactic acid concentrations were measured to assess organic acid production. For production. For lactic acid, although lactic acid production by unit of biomass was similar similar for all three cases (

Table 5-7), during phase I there was higher specific production rate during pH = 3.5 and pH = 3.2 (Figure 5-11 c). During phase II and III, the highest specific production rate was observed at pH = 4.0.

Total acetic acid production was more important at pH 3.2 (
Table 5-7). However, during phase I the lowest production rate was observed during pH 3.2. During phase II and III, highest production was during pH = 4.0.

Lactic acid is both produced from malolactic fermentation (L-lactic acid) and heterolactic fermentation (D-lactic acid). During phase I, specific consumption rate of malic acid was higher than specific production rate of lactic acid (Figure 5-11). This indicates a possible accumulation of malic acid in the inside of *O. oeni*. The same occurs with acetic acid at pH 3.2. This compound is produced through two reactions: by acetate kinase as part of the heterolactic fermentation, and by citrate lyase in the citrate degradation pathway. Because of these reactions, acetate production should be higher or equal to citric acid consumption; however, this is not shown at this phase at pH 3.2, which indicates a possible accumulation of either acetate or citrate.

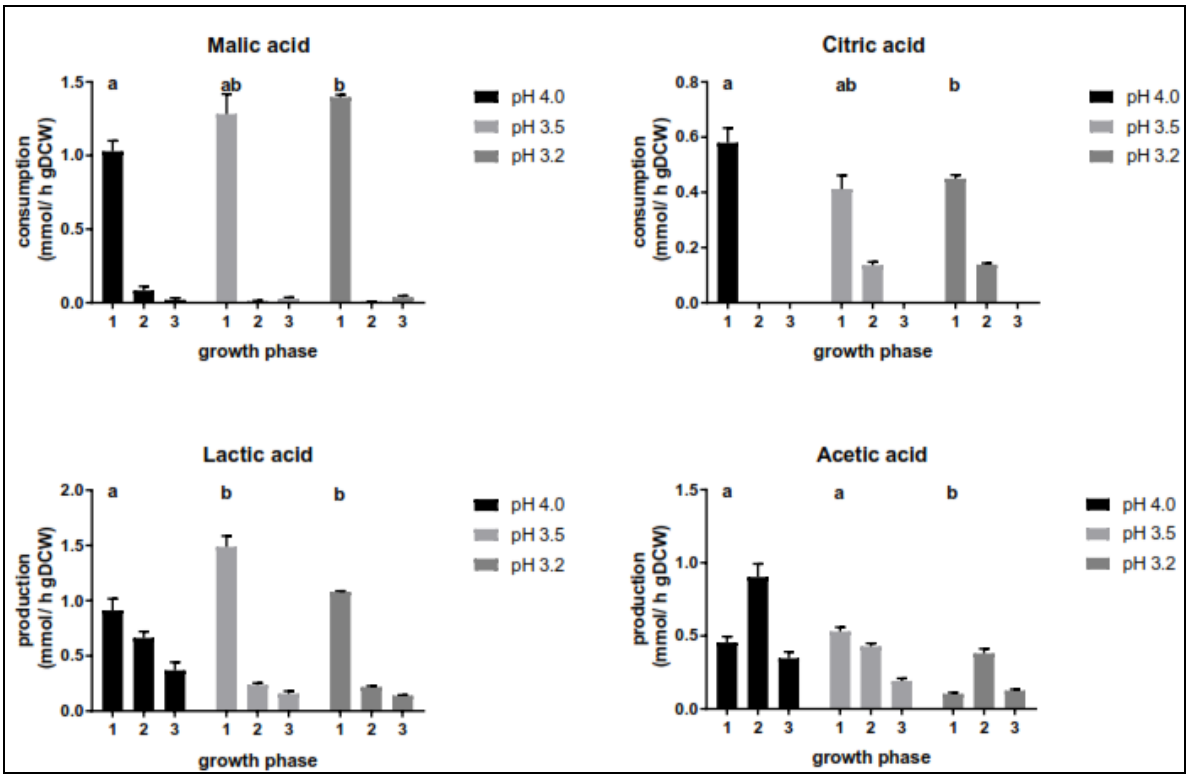

Figure 5-11: Organic acid production and consumption at pH 4.0, 3.5 and 3.2 for the three growth phases.

Graphs correspond to: A) Malic acid consumption, B) Citric acid consumption, C) Lactic acid production, D) Acetic acid production.

Table 5-6: Substrate consumption normalized by biomass content during the cultivation of *O. oeni* PSU-1 at pH 4.0, 3.5 and 3.2

	Glucose (mmol $gDCW^{-1}$)	**Fructose (mmol $gDCW^{-1}$)**	**Malic acid (mmol $gDCW^{-1}$)**	**Citrate (mmol $gDCW^{-1}$)**
pH 4.0	$73.85^{a} \pm 2.80$	$95.37^{a} \pm 1.45$	$30.78^{a} \pm 1.63$	$14.14^{a} \pm 1.14$
pH 3.5	$78.68^{a} \pm 13.24$	$203.20^{b} \pm 19.80$	$41.12^{b} \pm 4.83$	$24.14^{b} \pm 1.95$
pH 3.2	$70.71^{a} \pm 13.62$	$231.66^{b} \pm 12.89$	$59.79^{c} \pm 4.39$	$38.00^{c} \pm 2.46$

Same letter as superscript indicate no significant difference according to Dunnet's test with a 95% confidence interval.

iii. Sugars

Glucose and fructose were the two carbon sources added in the medium, and as expected, consumption of both of these sugars increased the higher the external pH was, with 63, 43 and 22% of glucose consumed for pH 4.0, 3.5 and 3.2, respectively, and 100, 67 and 57% for fructose. Only fructose was completely consumed at pH 4.0 (Figure E-1Figure 5-11 b, in appendix E). When normalizing by biomass (Table 5-6), glucose shows a similar consumption in all cases. Fructose, however, was more consumed at pH 3.5 and 3.2. During phase I, there is higher consumption of both of these sugars during pH = 4.0. During phase II and III, there is higher consumption of glucose at pH 4.0; however, fructose consumption is the lowest at this pH.

Two polyols were measured as products of the metabolism of *O. oeni*: mannitol and erythritol. Both of these are derived from fructose and glucose. Mannitol was found since since the first sample, which indicates that *O. oeni* started producing mannitol immediately; and erythritol since 15.7 h (pH 4.0 and 3.5) and 23.2 h (pH 3.2) (Figure E-1 c E-1 c & d, in appendix E). Normalization by biomass showed that both sugars had their their lowest production at pH 4.0 (

Table 5-7); Total mannitol production significantly increased when pH decreased, from 84.62 mmol $gDCW^{-1}$ at pH 4.0, 137.63 mmol $gDCW^{-1}$ at pH 3.5 and 160.7 mmol $gDCW^{-1}$ at pH 3.2. During phase I, however, mannitol specific production rate was kept constant at all the experimental cases. During phase II, highest specific production rate is present at pH 3.2.

Total erythritol production was similar at pH 3.2 and 3.5, in both cases higher than at pH 4.0. During phase I, the lowest specific production rate of erythritol was observed at pH 4.0. Erythritol specific production rate was low for all cases during phase II and III.

i. Amino acid consumption

Total amino acid consumption was analyzed for the three experimental conditions. Among these, glutamine and tryptophan showed significantly different consumption, according to the pH condition (Table 5-8). Also, seven amino acids – aspartate, glycine, glutamate, proline, leucine, methionine, isoleucine and arginine - showed similar consumption at pH 3.2 and 3.5, but significantly higher than at pH 4.0; and cysteine was the only that showed significant higher consumption only at pH 3.2. Arginine only showed significant differentiated consumption between pH 4.0 and 3.2. It is interesting to notice that glutamine, aspartate, arginine and glutamate participate in mechanisms of survival at low pH, as described above in the Introduction (section 1.3.2 Secondary transport systems).

There are three amino acids that *O. oeni* PSU-1 could use as carbon source: serine, threonine and cysteine. Also, cysteine was the only amino acid that was fully

consumed in all three cases. Threonine and serine were consumed equally in the three conditions.

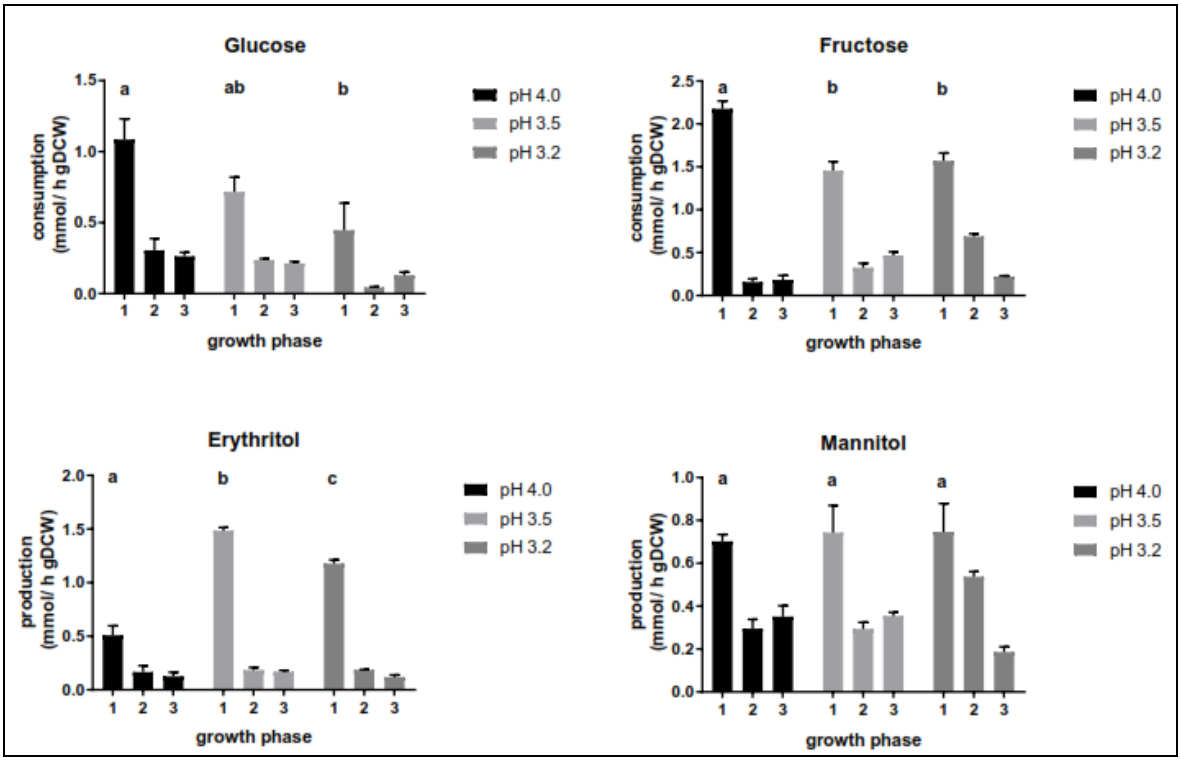

Figure 5-12: Sugar consumption (glucose and fructose) and polyol production (erythritol and mannitol) at pH 4.0, 3.5 and 3.2 for the three growth phases.

Graphs correspond to: A) Glucose consumption, B) Fructose consumption, C) Erythritol production, D) Mannitol production.

Table 5-7: Product formation normalized by biomass formation

	Lactic acid (mmol gDCW^{-1})	**Acetic acid (mmol gDCW^{-1})**	**Mannitol (mmol gDCW^{-1})**	**Erythritol (mmol gDCW^{-1})**
pH 4.0	97.86^{a} ± 7.80	91.29^{a} ± 7.57	84.62^{a} ± 6.15	49.03^{a} ± 6.68
pH 3.5	96.75^{a} ± 10.23	103.08^{a} ± 10.05	137.63^{b} ± 10.73	96.01^{b} ± 7.13

pH 3.2	$110.72^{a} \pm 1.48$	$166.08^{b} \pm 2.21$	$160.70^{c} \pm 3.92$	$104.10^{b} \pm 6.62$

Table shows product formation until the end of the experiment, normalized by biomass formation. Same letter as superscript indicate no significant difference according to Dunnet's test with a 95% confidence interval.

Table 5-8: Specific amino acid consumption (mmol $gDCW^{-1}$) during the cultivation of *O. oeni* PSU-1 at 3 different pH 4.0, 3.5 & 3.2.

Amino acids	pH 4.0 (mmol $gDCW^{-1}$)	pH 3.5 (mmol $gDCW^{-1}$)	pH 3.2 (mmol $gDCW^{-1}$)
Glutamine	2.031^{a}	6.028^{b}	8.507^{c}
Tryptophan	0.747^{a}	1.589^{b}	2.352^{c}
Cysteine	7.652^{a}	7.022^{a}	15.754^{b}
Aspartate	2.589^{a}	4.735^{b}	5.108^{b}
Glicine	2.346^{a}	8.244^{b}	4.549^{b}
Glutamate	1.097^{a}	3.335^{b}	2.635^{b}
Proline	1.046^{a}	4.387^{b}	3.528^{b}
Leucine	0.936^{a}	2.605^{b}	2.405^{b}
Methionine	0.320^{a}	1.431^{b}	1.913^{b}
Isoleucine	0.117^{a}	1.950^{b}	1.215^{b}
Arginine	0.469^{a}	0.908^{ab}	1.839^{b}
Valine	0.511^{a}	2.010^{b}	0.839^{a}
Serine	0.970^{a}	2.063^{b}	1.212^{a}
Alanine	0.437^{a}	3.028^{b}	1.732^{ab}
Lisine	0.141^{a}	1.589^{b}	0.974^{ab}
Threonine	0.433^{a}	0.520^{a}	0.719^{a}
Tyrosine	0.596^{a}	1.422^{a}	2.278^{a}

Histidine	0.611 [a]	1.367[a]	1.706[a]
Phenilalanine	0.700 [a]	1.288[a]	1.545[a]

Different superscript letters in the same row indicate when there is a significant difference between the three experimental cases according to Tuckey's test with a 95% confidence interval. Dark gray rows show amino acids that have significant difference in the consumption rates between the three experimental cases; light gray rows indicate when pH 4.0 shows significant difference with both pH 3.5 and 3.2 as a group; and white rows indicate when there was not a difference. Red text marks the amino acids who have been related with survival at acidic pH.

5.2.4 Analysis of intracellular fluxes

To gain a better understanding of the metabolism of *O. oeni*, three versions of the iMR453 model were constructed: iMR453 6.26-4.0; iMR453 6.26-3.5 and iMR453 6.26-3.2. These models were adjusted to the external pH that corresponded to each specific experimental case, and an pH_{in}= 6.26 as determined above. Because of this, 120 reactions were modified at iMR453 6.26-4.0; five additional reactions were modified at iMR453 6.26-3.5, all of them corresponding to transport reactions; and two additional transporter reactions were modified at iMR453 6.26-3.2. Then, as accumulation was observed in these experiments (similar to what happened at different ethanol levels), an extended model was built for each pH value and constraints for the accumulation reactions were estimated, following the methodology used in the previous section (Adaptation of *Oenococcus oeni* to high ethanol concentrations). Sink and/or demand reactions were added when corresponded for the following compounds: mannitol, malic acid, acetic acid, cysteine, threonine, phenylalanine, and valine.

a) NGAM estimation

NGAM values were estimated following the same methodology used for ethanol levels, and are shown in Table 5-9. For phase I, NGAM values increase as pH

decrease, showing NGAM values of 0.998, 1.056 and 1.312 for pH 4.0, 3.5 and 3.2, respectively. However, during phases II and III the opposite occurred, i.e. NGAM decreased when external pH decrease (for phase II: 2.66, 1.83 and 1.63; for phase III: 2.39, 1.55 and 1.1). Interestingly, the difference between NGAM values within the same growth phase is maximum two-fold, which is very different from the 36-fold increase found between 0 and 12% ethanol concentration. This small difference suggests a limited influence of pH on non growth associated maintenance.

Table 5-9: Estimation of non-growth associated maintenance (NGAM) (mmol ATP $gDCW^{-1}$ h^{-1}) for *O. oeni* PSU-1 cultivated at pH 4.0, 3.5 and 3.2

	pH 4.0	pH 3.5	pH 3.2
Phase I	1	1.06	1.31
Phase II	2.66	1.83	1.63
Phase III	2.39	1.55	1.1

NGAM values were estimated by fixing the experimental data obtained for each respective growth and pH in one of the three pH-adjusted version of the iMR453 model: iMR453 6.26-4.0; iMR453 6.26-3.5 and iMR453 6.26-3.2. Then, biomass formation was left unrestrained and was fixed as the objective function. Flux through the NGAM reaction was increased by 0.001 and biomass was predicted, iterating between a range of 0 to 3 mmol $gDCW^{-1}$ h^{-1}. The NGAM value that allowed the lowest biomass prediction error was selected.

b) NGAM sensitivity towards intracellular pH

To evaluate the effect of pH_{in} in the estimation of NGAM, NGAM was recalculated for a range of possible values for pH_{in}, which was a range composed by 6.4 as upper bound - as a value higher than those previously reported for pH_{in} at these pH_{out} values

- (Augagneur et al., 2007; Bouix & Ghorbal, 2015; Salema et al., 1996; refer to Table 5-4) and by the medium pH as lower bound, which was 4.0, 3.5 or 3.2 as defined. A similar variation range was reported empirically by Bouix & Ghorbal (2015): *O. oeni*'s intracellular pH was shown to be the same as the medium pH at the beginning and at the end of the fermentation, increasing while malic acid was consumed, and decreasing after its depletion. Figure 5-13 summarizes the results obtained.

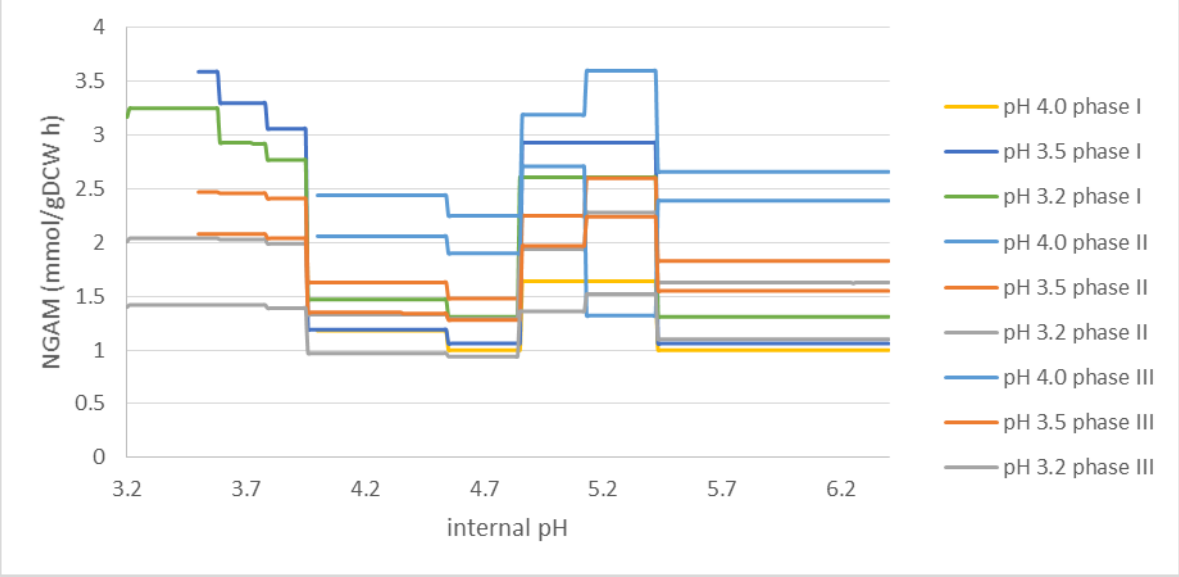

Figure 5-13: Sensitivity of NGAM values (mmol ATP $gDCW^{-1}$ h^{-1}) in response to internal pH variation for *O. oeni* PSU-1 cultivated at pH 4.0, 3.5 and 3.2

Figure 5-13 shows the NGAM values estimated at each internal pH for the nine experimental data. Prediction was executed for models adjusted to the mediums pH as external pH, and to a ranging values of internal pHs. These were varied from the medium's pH to 6.4.

As the figure shows, NGAM is maintained constant inside specific ranges, and it abruptly changes when pH_{in} is decreased 0.01 from that range. To understand the causes of these variations, we searched for the reactions that changed when pH_{in} crossed from one interval to the other (for example: by comparing a model adjusted

to a pH_{in} 5.42 with one model adjusted at pH_{in} 5.43, in order to understand the differences between the first two intervals). Each NGAM variation could be attributed to a specific set of reactions, and the variations of each set of reactions could be attributed to one specific compound that changed its protonation state. These compounds were: NADPH for the first and second interval (18 reactions modified); malic acid for the second and third (6 reactions); $NADP^+$ for the third and fourth (18 reactions); acetic acid for the fourth and fifth (9 reactions); NADPH for the fifth and sixth (18 reactions); lactic acid for the sixth and seventh (7 reactions); and ADP for the seventh and eighth (104 reactions).

c) Redistribution of internal fluxes

To simulate the distribution of internal fluxes for each experimental case, specific consumption and production rates were fixed, with the predicted NGAM values and biomass formation (Figure 5-14).

The model predicted ethanol formation during phase I for all pH conditions; and during phase II and III at pH 3.2.

L-malic acid, as indicated in the previous analysis, increased during phase I the lower the external pH was. The model predicted two main active reactions that consumed this compound: malic enzyme, which converts L-malic acid into oxaloacetic acid, allowing its utilization as carbon source; and malolactic enzyme, which allows conversion into L-lactic acid and thus proton extrusion. During phase I and as expected, the model predicted that malolactic enzyme was more active at pH 3.5 and 3.2 than at pH 4.0. Notably, the activity of malic enzyme incremented the lower the external pH was for all growth phases, which indicates more carbon requirement at acidic conditions.

As lactic acid was measured, the model indicated the distribution of both, L-lactic acid, produced from L-malic acid by the malolactic enzyme; and D-Lactic acid, produced from pyruvate by lactate dehydrogenase. D-lactic acid was produced mainly in phase I in all conditions, and its production increased with lower pH. L-

lactate was also mainly produced during phase I, and continued to be produced during phases II and III. This continuous release resulted from the predicted malate accumulation, as consumption stagnated during phase II.

Regarding fructose utilization, this metabolite can either be used to produce erythritol and mannitol, or to be phosphorylated and then converted into glucose-6P by glucose isomerase, and thus enter the heterolactic fermentation. Similarly to what we observed at different ethanol concentrations, erythrose-4P, erythritol's direct precursor, was produced by transaldolase instead of the classical pathway. This enzyme is part of the pentose phosphate pathway and generates fructose-6P and erythrose-4P from sedoheptulose-7P and glyceraldehyde-3P, instead of direct conversion of fructose-6P into acetyl-P and erytrose-4P, as the classical pathway. Interestingly, the model predicted that mannitol was only produced during growth I, and erythritol production, even if found at all growth phases, was also higher during growth I. These compounds are produced in order to regenerate $NAD(P)^+$, and thus indicate higher cofactor requirement during growth I. It also indicates that other pathways could be more active during growth II and III for cofactor regeneration. When other active reactions that produced NADP+ were searched, high flux through the enzyme transhydrogenase was observed. This enzyme catalyzes the conversion of NAD^+ and NADPH into NADH and $NADP^+$.

Regarding acetate production, the model predicted two active reactions that synthetize this compound: acetate kinase, which uses acetyl-P as substrate and regenerate ATP in the process; and citrate lyase, which uses citrate to generate ATP and oxaloacetate. The model indicated that almost all acetic acid is generated by citrate lyase in phase I, the first enzyme of the citrate degradation pathway. The activity of acetate kinase increased as the fermentation continued, probably due to citrate depletion. Also, the activity of this enzyme decreased the lower the external pH was.

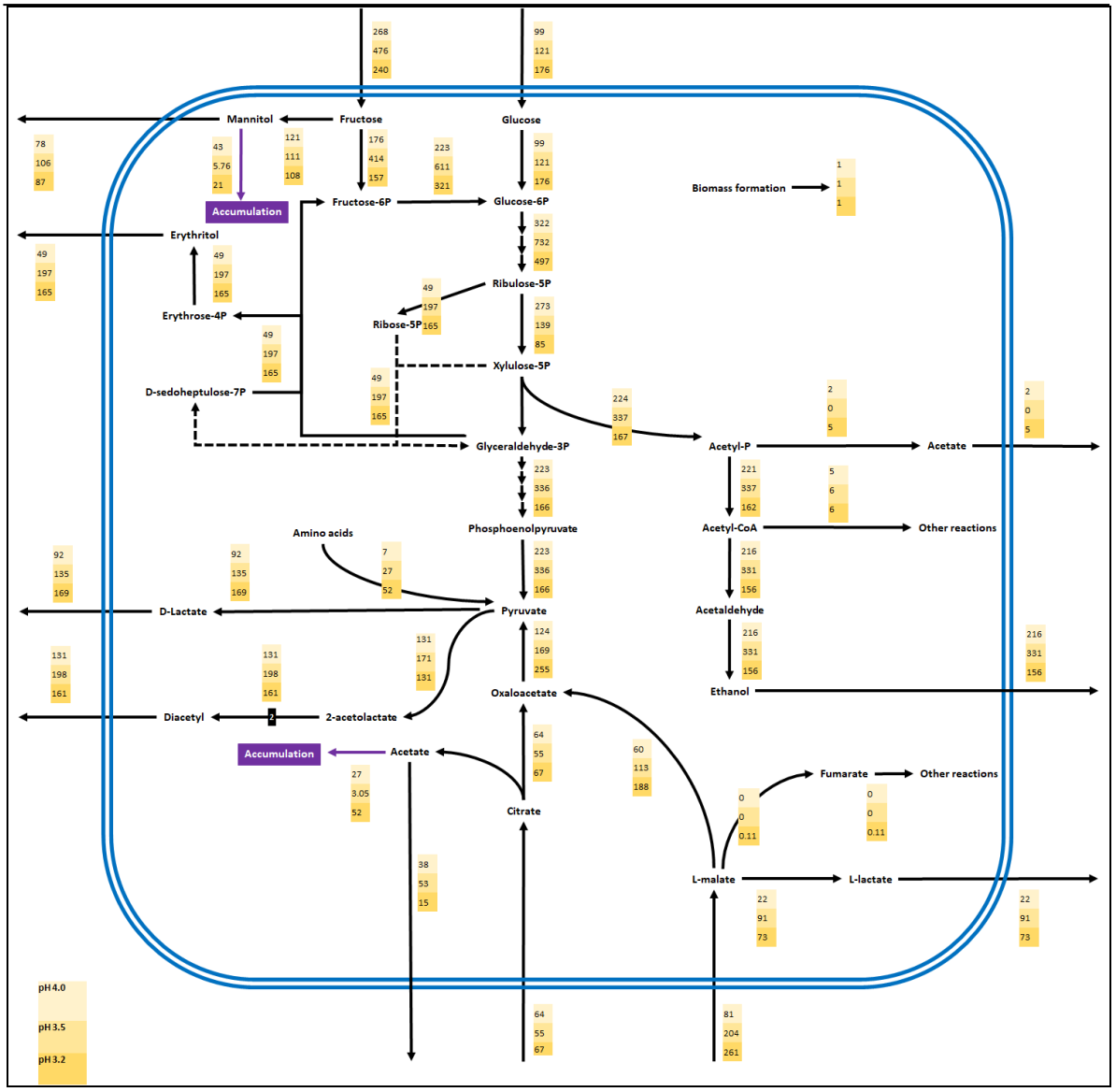

Figure 5-14: Metabolic flux redistribution of the central carbon metabolic pathways of *O. oeni* PSU-1 upon cultivation in a culture medium at pH 4.0, 3.5 and 3.2 (from top to bottom), during growth phase I.

The model also predicted diacetyl formation. As it seemed that there was a tendency regarding diacetyl production, Flux Variability Analysis (FVA) was carried out to determine the range of possible fluxes for this compound. Interestingly, all cases

allowed zero diacetyl formation. However, when FVA was carried out on acetolactate synthase, then the flux was found substantial for all cases (Figure 5-15). Acetolactate synthase is the enzyme that catalyzes the reaction that converts pyruvate into 2-acetolactate, which is the precursor of both diacetyl and 2-butanediol. This shows that the model was indifferent whether to produce diacetyl or 2-butanediol but that either one or the other is needed.

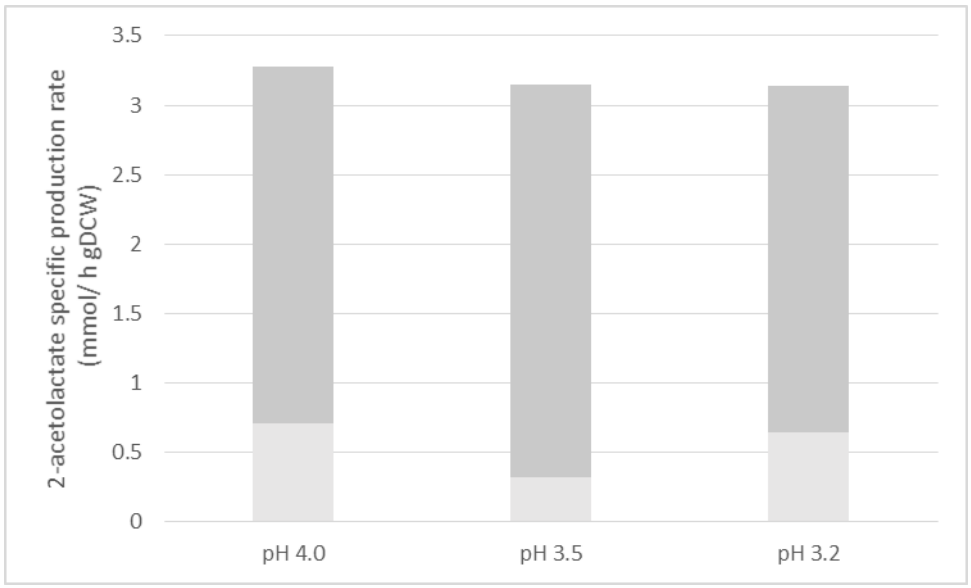

Figure 5-15: FVA for synthesis of 2-acetolactate for growth of *O. oeni* PSU-1 at pH 4.0, 3.5 and 3.2

2-acetolactate is the precursor of both diacetyl and butanediol, products which synthesis can extrude protons. The gray bar indicates the factible specific production rate of this compound.

d) ATP synthesis

O. oeni produces ATP by two methods: by using the F_0F_1-ATPase, which uses the proton motive force to generate ATP; and by heterolactic fermentation, through three reactions: acetate kinase, pyruvate kinase and phosphoglycerate kinase. As F_0F_1-ATPase is one of the mechanisms for survival at low pH (Cotter & Hill, 2003; Y. Liu

et al., 2015; van de Guchte et al., 2002), the flux distribution between these two mechanisms was studied.

The flux towards F_0F_1-ATPase was found to increase the lower the external pH was, and in all cases had a minimum during phase I, a maximum during phase II, and a medium level at phase III (Figure 5-16). However, when the two methods of ATP production were compared, a clear tendency to increase ATPase utilization instead of heterolactic fermentation was found the lower the pH was for phase I and II (Figure 5-17). Phase III, which had the lowest growth, showed a decrease between pH 4.0 and pH 3.5, yet was maintained between pH 3.5 and pH 3.2.

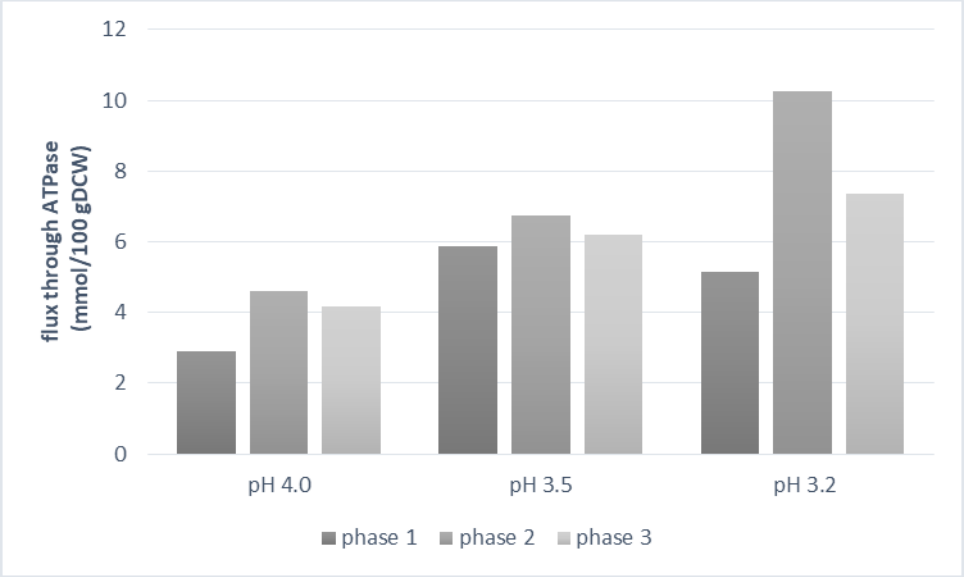

Figure 5-16: Prediction of ATP production through F_0F_1-ATPase at acidic conditions, normalized by biomass

Fluxes were obtained by simulation of each phase on the model iMR453, and then normalized by biomass formation.

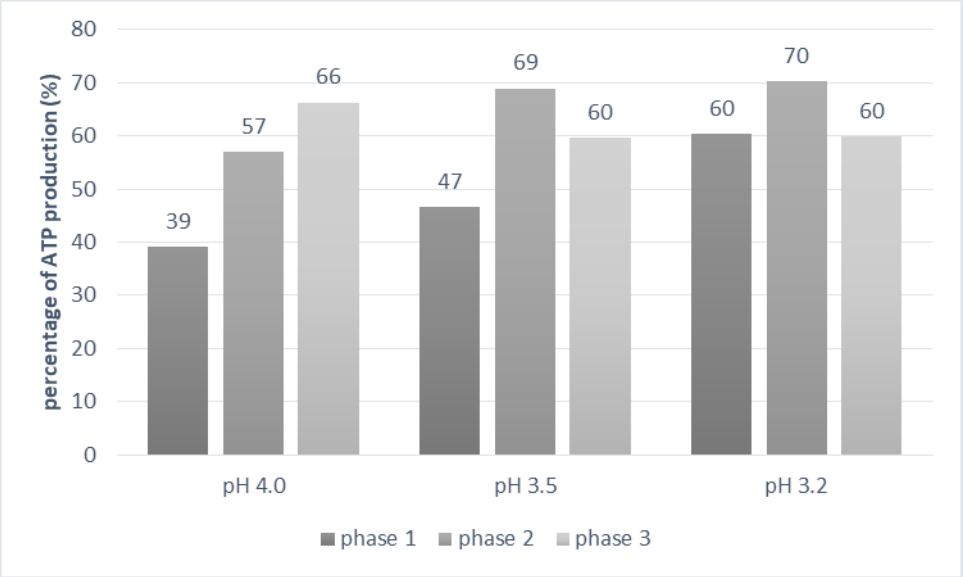

Figure 5-17: Percentage distribution of the synthesis of ATP through F_0F_1-ATPase as predicted by iMR453 during growth at pH 4.0, 3.5 and 3.2

6. DISCUSSION

6.1 Adaptation of *Oenococcus oeni* to high ethanol concentrations

In this work, we determined the effect of ethanol on nutritional and energetic requirements of *O. oeni* to ensure its growth. For this end, we cultivated *O. oeni* PSU-1 strain in a wine-like, defined culture medium spiked with 0, 3, 6, 9 or 12% v/v ethanol. Moreover, we took advantage of our recently constructed genome-scale metabolic model (Mendoza et al., 2017) that allowed assessing the redistribution of the intracellular metabolic fluxes and the energetic factors at increasing ethanol concentrations.

As expected, cell growth was closely correlated (r^2 = 0.98) to ethanol content. Specific growth rate and maximal biomass content decreased progressively as ethanol concentration in the medium increased. Moreover, both decreased during the time course of the batch cultivation. In general, specific growth rates and biomass production were larger during phase I, which was consistent with the highest metabolic activity of *O. oeni* observed during this phase, for all the tested culture conditions.

Changes in ethanol level strongly impacted *O. oeni's* requirements of Non-Growth Associated Maintenance (NGAM), $NAD(P)^+$/NAD(P)H cofactors and energy, reflected in higher production of ATP by ATPase.

Energetic demand for NGAM dramatically increased in *O. oeni* cells cultured under alcoholic stressful conditions. Indeed, cultures containing 9 and 12% ethanol required 10 and 17 times more NGAM during phase 1, respectively, than cultures without ethanol. The latter indicates that the ATP produced was principally used to cope with cell maintenance resulting from this stress. This agrees with our previous work, where the genome –scale metabolic model (GSMM) indicated that NGAM was 30-fold higher in cultures with 12% ethanol than in cultures without ethanol (Mendoza

et al., 2017). Notably, the model predicted that the cells cultivated with 6% ethanol would require a lower NGAM than those grown at 3% ethanol. This agrees with Cavin, Divies, & Guzzo (1998) that reported that low concentrations of ethanol activate bacterial growth, i.e. ethanol improves exchanges between the cell and the external medium. In addition, significant cellular changes normally occur when at least 8% ethanol is present in the medium, coinciding with changes in membrane lipid composition (Da Silveira, A., Folkert, Rombouts, & Abee, 2003; Grandvalet et al., 2008; H. Teixeira, Gonçalves, Rozès, Ramos, & San Romão, 2002).

F_0F_1-ATPase is the preferred route employed for the synthesis of ATP during phase I. Indeed, even in the absence of ethanol in the culture, 58% of the total ATP is generated by this route. Moreover, to overcome the strong ATP demand for NGAM at higher ethanol concentrations, the model predicts that this pathway produces almost 80% of the required ATP. As F_0F_1-ATPase produces ATP at the expense of proton translocation to the inside of the cell, this indicates a higher requirement for proton extrusion. In this regard, the malolactic reaction is usually considered the major pathway for proton extrusion and ATP production in lactic acid bacteria (Tourdot-Maréchal et al., 1999; van de Guchte et al., 2002). In this process, one mole of malic acid is consumed and generates equivalent amounts of L-lactate and CO_2; and, because of pKa differences between the substrate and the products, a proton is consumed (Augagneur et al., 2007; W. N. Konings, 2002; Marty-Teisset et al., 1996). This positive effect is augmented by L-lactate transport, a symporter that extrudes protons (Salema et al., 1996). We found that malic acid was almost totally depleted during phase I in each condition, in concordance with the higher F_0F_1-ATPase flux predicted by the model. Moreover, in this phase, specific consumption rates of malic acid were the fastest in cultures with 9 and 12% ethanol, as well as specific production rates of L-lactic acid. The key role of malic acid for proton extrusion is confirmed by the model, as it predicts that 74-95% of the protons translocated by ATPase are extruded by malolactic fermentation and L-lactic transport in all the experimental conditions; and that the flux through this reaction increases

concomitantly with the ethanol content in the medium, to overcome higher energetic requirements. This confirms that malolactic reaction is the main pathway for ATP synthesis in the presence of high ethanol content.

For reducing power regeneration, ethanol formation is the main pathway for reoxidation of $NAD(P)^+$ in *O. oeni*, although at high metabolic rates this process becomes limiting (Richter et al, 2003); therefore, other external electron acceptors are used for $NAD(P)^+$ reoxidation (Maicas et al., 2002; Richter, Vlad, & Unden, 2001; Versari et al., 1999). Several studies have reported that one of the main limitations in $NAD(P)^+$ regeneration through the ethanol biosynthetic pathway is the deficiency of D-pantothenate in the culture medium, an essential precursor for HSCoA in *O. oeni* (Richter et al., 2001; Terrade & Mira de Orduña, 2009). The latter is the cofactor of acetaldehyde dehydrogenase (Garvie, 1967). Nevertheless, the MaxOeno culture medium employed in this work contains enough D-panthotenate to allow optimal growth of *O. oeni* and ethanol pathway activation. Another cause could be the limited availability of HSCoA due to its preferential use for fatty acid production, to overcome the damage of cell membrane that could result from ethanol.

When ethanol production pathway is non-functional, a lack of reduced cofactors occurs. Our results show that *O. oeni* uses fructose, glucose and citrate as electron acceptors for cofactors reduction. In particular, the specific production rates of mannitol and erythritol incremented as ethanol concentrations increased during phase I. However, fructose, which is the main precursor of mannitol and erythritol, showed similar specific consumption rates during phase I, regardless of the culture conditions; and glucose, which can also be used for erythritol formation, displayed slower consumption rates at higher ethanol concentrations. This indicates that there is a preferential consumption of carbon sources towards mannitol and erythritol formation at higher ethanol concentrations rather than biomass formation, which

could be caused by the higher cofactor requirement, because of a possible negative regulation over ethanol synthesis, or both of them. Indeed, the model predicts that cofactor regeneration due to mannitol and erythritol formation countervail for almost 50% of the cofactors used for sugar catabolism in conditions without ethanol, and for 51-57% of this usage in ethanol-containing cultures.

Citric acid consumption is also related with cofactor regeneration. Consumption of this chemical compound is used for pyruvate formation, which is then used for either production of D-lactate or diacetyl. D-lactate is used for $NAD(P)^+$ regeneration, while diacetyl is related with consumption of intracellular protons and thus increase of internal, as well as external pH, as diacetyl is less acidic than citric acid (Saguir & Manca de Nadra, 1996; Versari et al., 1999). Citric acid was mainly consumed during phase I at similar specific consumption rates, regardless of the ethanol content. During this phase, D-lactate formation showed a different behavior: the highest flux towards D-lactate synthesis - which arises from both citrate degradation and phosphoketolase pathway - was observed when ethanol was absent in the medium, where 72% of the consumed citrate was directed towards the synthesis of lactate, instead of the 38% and 58% observed at 9% and 12% v/v ethanol, respectively. On the contrary, the model predicted higher diacetyl production fluxes when ethanol was higher in the medium. As citric acid consumption was similar in all conditions, this indicates that, at high ethanol concentrations, citric acid consumption was not sufficient to supply all the pyruvate required for diacetyl synthesis. Indeed, in the absence of ethanol, 44% of the citrate consumed was used for diacetyl formation; however, at 9 and 12% ethanol, there were 3.2 and 2.9 moles of diacetyl produced per mole of consumed citrate. This clearly indicates that pyruvate was redirected to the formation of this compound. For this end, the required pyruvate is produced from L-malate, as at increasing ethanol conditions the flux through malic enzyme, which uses L-malic acid for oxaloacetate synthesis, increases. Thus, a 3.7-fold higher

synthesis of oxaloacetate was achieved through this route in cultures containing 12% ethanol, as compared to those without ethanol.

Thus, citric acid was mainly used for internal ionic balance through diacetyl production under ethanolic conditions; and not for $NAD(P)^+$ cofactor regeneration. In lactic acid bacteria, diacetyl formation requires intracellular protons, resulting in an increase in the internal pH. In addition, its extrusion increases external pH because it is less acidic than citric acid. In general, D-lactate production is privileged with regards to diacetyl, probably to allow the cells to obtain NAD+; however, when lactate dehydrogenase (LDH) function is reduced, pyruvate accumulates and diacetyl is produced (García-Quintáns, Magni, De Mendoza, & López, 1998; Tsakalidou & Papadimitriou, 2011). Thus, high ethanol content could limit the function of LDH, allowing diacetyl production, as demonstrated here. Another possible cause is that higher diacetyl formation results from the larger energetic requirements caused by higher NGAM requirements. As F_0F_1-ATPase generates ATP by translocating protons to the inside of the cell, higher ethanol concentrations imply a higher necessity to extrude these protons by alternative pathways. In fact, at the highest ethanol concentrations, diacetyl generation consumes 20 and 25%, respectively, of the protons introduced into the cell by F_0F_1-ATPase; opposite to only 5% for cells grown in the absence of ethanol. This shows that the increment of diacetyl formation and the resulting proton consumption in this reaction allows to increment the proton gradient. This gradient can then be used to produce, through F_0F_1-ATPase, the energetic requirements needed to overcome the challenging environment of this elevated ethanol concentration in the medium. From a biological perspective, proton consumption can also be used to compensate for the proton influx caused by the higher permeability of the plasmatic membrane at high ethanol concentrations.

Additionally, the specific consumption rate of cysteine, one of the most consumed amino acids, increased with ethanol content in the medium. Genomic studies of *O. oeni* PSU-1 reported that this strain is unable to synthesize cysteine, because sulfur

cannot be transported inside of the cell (Garvie, 1967; Mills et al., 2005). Cysteine can be used as a source for pyruvate formation, together with serine and threonine. The model predicted a 2.7-fold increase in pyruvate formation from these amino acids at 12% ethanol than in cultures without ethanol. Additionally, cysteine can be used in reactions of CoA synthesis, where this amino acid is added to D-4-P-phantothenate generating R-4-P-phantothenosyl-L-cysteine, and *O. oeni* does have the genes to this synthesize (Mills et al., 2005). CoA functions as an acyl group carrier and carbonyl activating group in numerous reactions central to cellular metabolism, and provides the 40-phosphopantetheine prosthetic group incorporated by carrier proteins that play key roles in fatty acid and non-ribosomal peptides biosynthesis (Spry, Kirk, & Saliba, 2008).

In conclusion, we found that under ethanol stress conditions, *O. oeni* favors anabolic reactions related with cell reconstruction pathways and/or production of stress protectors; consequently, the requirements of NAD(P)+, NGAM and ATP increase with ethanol content, unrelated with biomass increment.

Finally, in this work we were able to integrate in the model specific consumption/production rates and specific growth rates for each of the determined growth phases. As there were only feasible solutions, the model was able to integrate experimental data and represent the different phenotypes of *O. oeni* in each of the growth phases. To the best of our knowledge, this is the first report where experimental data from the entire exponential curve has been integrated to the model (Mendoza et al., 2017). Even if GSMMs and FBA are usually applied to data obtained from steady state experiments, these strategies have been previously used to model data from batch growth, based on the assumption of a pseudo-steady state of the cellular metabolism (Pastink, M. I. et al., 2009; R. Pereira, Nielsen, & Rocha, 2016; Teusink et al., 2006). This study shows how this approach can be used to

tackle growth and metabolic changes of the different phases occurring within a batch culture.

6.2 Adaptation of *Oenococcus oeni* to low pH

In this work, the second version of the GSMM of *O. oeni* PSU-1 was generated, the model iMR453. This model is mass and charge balanced, has been further curated manually, and is in accordance with the last works on carbohydrate metabolism for PSU-1. iMR453 was used to determine the pH_{in} value that minimized biomass prediction error for two sets of experimental data sets, and in both cases pH_{in} was determined to be 6.26, which is in accordance with current data (Augagneur et al., 2007; Bouix & Ghorbal, 2015; Salema et al., 1996).

Also, successful growth of *O. oeni* at pH 4.0, 3.5 and 3.2 was achieved in a medium containing the substrates citric and malic acid as organic acids, and fructose and glucose as sugars. This is not trivial, as Augagneur *et al* (2007) tried and failed to grow *O. oeni* at pH 3.2 in FT80 medium containing glucose, fructose, L-malic and citric acid. The authors attributed the absence of growth to the production of acetate that occurs due to citric acid utilization, as they did observe growth when the same medium was used, minus citric acid. In this study, the highest synthesis of acetic acid was also observed at pH 3.2, with 166.1 mmol $gDCW^{-1}$ produced at the end of the fermentation, showing a significant difference with production at pH 4.0 and 3.5, with 91.3 and 103.1 mmol $gDCW^{-1}$ of acetic acid, respectively. We consider that the main difference between the work of Augagneur *et al* and the one carried out in this thesis is the adaptation protocol, which allowed expression of stress mechanisms that avoid rapid inhibition due to product formation. Acetic acid in its undissociated form can permeate the membrane and dissociate in the cytoplasm, increasing pH_{in}. At pH 3.2, 95.7% of the total concentration of acetic acid is non-dissociated (ChemAxon, 2016), and thus membrane permeation can be lethal. To harness the difficulties of survival at acidic conditions, *O. oeni* has been reported to increase membrane

presence of C19cyc11 fatty acids and decrease C16:0 fatty acids (Hua et al, 2009), and increase membrane anisotropy (Chu-Ky et al., 2005), mechanisms that could have been activated during previous adaptation.

Similar growth behavior was observed between cells grown at pH 3.2 and 3.5. These experiments reached stationary phase at the same time, and also showed similar μ during phase I, the phase that presented μ_{max}. Final biomass concentration, however, was different: pH 3.2 presented 0.303 gDCW L^{-1}, which corresponds to 75% of the biomass reached at pH 3.5, 0.522 gDCW L^{-1}. As both experiments reached stationary phase when sugar was still available in the medium, growth stagnation could be attributable to product inhibition. Incomplete sugar consumption at low pH has been observed before, and attributed to product inhibition due to acetate (Augagneur et al., 2007). Different is the case of pH 4.0: this experiment reached growth stagnation at 305 h, 130 h before the other experiments, and fructose was depleted but not glucose. Fructose is used as an electron acceptor that allows cofactor regeneration by the synthesis of mannitol and erythritol, and thus the absence of fructose harness growth, yet does not limit it (Maicas et al., 2002). Then, growth stagnation could have been caused by a combined effect of product inhibition and fructose depletion, and thus inability to synthetize $NAD(P)^+$.

It is interesting to notice that a similar growth curve was obtained during phase I for all pH conditions. This phase had the highest metabolic activation, observed by higher production and consumption of compounds, and also the highest consumption of both malic and citric acid. Both of this organic acids have been described to aid in maintenance of pH_{in}, and in some cases to even increase external pH (Augagneur et al., 2007; Hua et al., 2009; Salema et al., 1996), and thus could be responsible of this undifferentiated growth.

Regarding ATP synthesis, a higher percentage of ATP was produced by F_0F_1-ATPase the lower the external pH was. This was expected, as F_0F_1-ATPase is vital for survival at low pH (Cotter & Hill, 2003; Y. Liu et al., 2015). A similar result was observed when the flux towards F_0F_1-ATPase was analyzed, which showed that at

each growth phase there was higher flux the lower the external pH was. This type of behavior is exactly what Fortier et al. (2003) found: they identified a 1.6-fold F_0F_1-ATPase activity when comparing cells growing at pH 5.3 and 3.5 in the presence of malic acid, which is closer to the 1.8-fold observed in this experiment when comparing ATPase flux at pH 4.0 and 3.2 for phase I, the phase with higher malic acid consumption. Higher ATPase expression has also been observed in cells that survived at pH 2.9 (Drici-Cachon, Guzzo, Cavin, & Divies, 1996), and no acidurance was reported for mutants without ATPase activity (Galland, Tourdot-Maréchal, Abraham, Son, & Guzzo, 2003; Raphaëlle Tourdot-Maréchal et al., 1999).

Lower synthesis of acetic acid was observed at pH 3.2. iMR453 predicted two active reactions for acetate synthesis: acetate kinase, which uses acetyl-P and regenerate ATP in the process; and citrate lyase, which uses citrate to generate acetate and oxaloacetate. As the flux of acetate was lower than citrate consumption, this indicated that an accumulation of either citrate or acetate happened in the inside of the bacteria. This is not the first time that this has been observed (Olguín et al., 2009). The model predicted that almost all acetic acid was generated by citrate lyase during phase I for all cases. This indicates that during phase I *O. oeni* was able to generate enough energy for survival from glycolysis and F_0F_1-ATPase, without the use of acetate kinase, as the flux through this enzyme increased during the next phases. It is expected that there would be a preference for F_0F_1-ATPase as it does not require carbon sources to generate energy, if a method for proton extrusion is available.

In this regards, during phase I there was higher specific consumption rate of malic acid the lower the external pH was, which is coherent with the positive effect of this organic acid in conditions of low pH reported previously. The model predicted that this L-malic acid had two main destinies: oxaloacetic acid due to malic enzyme, for utilization as carbon source; and L-lactic acid due to malolactic enzyme, for proton extrusion. The latter carried a higher flux during phase I at pH 3.2 and 3.5 than at pH 4.0. Indeed, at pH 3.2, 73% of the protons imported to the inside of the cell due to

F_0F_1-ATPase are extruded by malolactic fermentation and lactic acid transport, and at pH 4.0, 67%. This shows the importance of malic acid for energy generation, as it allows higher ATP formation due to proton extrusion, and provides an explanation for the low flux predicted for acetate kinase during this phase.

Moreover, malic enzyme also incremented its flux the lower the external pH was for all growth phases. This could indicate higher carbon requirement at lower pH. This is also supported by the higher pyruvate production from amino acids (serine, threonine and cysteine, specifically) observed the lower the external pH was, and the decrease in glucose consumption observed at phase II during pH 3.2. Some authors have reported that at low pH, there is lower glucose utilization due to glycolysis inhibition in lactic acid bacteria (Zuljan et al., 2014) and in *O. oeni* (Bartowsky, 2005; Firme, Leitão, & Romão, 1994).

Lactic acid presented higher specific production rate at pH 3.2 and 3.5 during phase I. iMR453 was used to predict lactic acid distribution, and it showed that D-lactic acid was mainly produced at phase I in all cases. Production of D-lactic acid has been related with citrate fermentation, as this process generates pyruvate (Hugenholtz, 1993; S. Q. Liu, 2003), so this is a reasonable prediction. L-lactate was mainly produced during phase I, and was produced continually during phase II and III. This continuous release is due to the predicted malate accumulation, as L-malic acid consumption stagnated during phase II.

Diacetyl production was predicted for all conditions during phase I. This compound is related with citrate consumption, and yet, there were 2, 3.6, and 2.4 molecules of diacetyl generated per molecule of citrate consumed for pH 4.0, 3.5 and 3.2 respectively. D-lactate was also predicted to be higher than citrate consumption, with 1.4, 2.5 and 2.3 molecules of this compound per molecule of citrate consumed. The model showed that all the pyruvate generated from heterolactic fermentation, malic acid conversion into oxaloacetic acid, citric acid consumption and amino acid consumption was directed into these two compounds. Diacetyl synthesis produced proton extrusion during phase I, and was responsible for 23, 17 and 16% of the

extrusion of the protons introduced into the cytoplasm by F_0F_1-ATPase; and synthesis of D-lactic acid produces cofactor regeneration.

Regarding sugars, both fructose and glucose have a lower specific consumption rate during phase I at pH 3.2 and 3.5 than at pH 4.0. This is especially interesting as synthesis of erythritol is enhanced at low pH during phase I, which indicates higher cofactor requirement at lower pH. A similar enhanced production of erythritol was previously observed when comparing pH 3.5 and pH 4.0 on a complex medium containing fructose and glucose (Zhang & Lovitt, 2005). The synthesis of mannitol is only predicted to occur during phase I, and thus it was slowly released during the following phases. Accumulation of mannitol has been previously reported in bacteria as a measure to cope with osmotic pressure (Beales, 2004), and in LAB also as an antioxidant (Wisselink et al., 2002). A possible accumulation for acid survival has not been reported.

As mannitol and erythritol are mainly produced during phase I, other pathways for cofactor regeneration were analyzed, and transhydrogenase was found to have high flux at phase II and III. This enzyme catalyzes the conversion of NAD^+ and NADPH into NADH and $NADP^{+,}$ and has three genes related with its activity present in the genome of *O. oeni* (Richter, Hamann, & Unden, 2003). To date, there are not studies that have analyzed the relation between survival at acidic conditions with the expression of transhydrogenase.

There were two amino acids that were consumed significantly higher the lower the external pH was, glutamine and tryptophan. Also, there were eight that had increased consumption at pH 3.2 and 3.5 when compared to pH 4.0, which are aspartate, glycine, glutamate, proline, leucine, methionine, isoleucine and arginine. Four out of ten of these amino acids have been previously described to have a positive effect during low pH: glutamine, glutamate, aspartate and arginine. These four participate, respectively, in the following responses: glutaminase, glutamate decarboxylase, aspartase, and arginine deiminase system. Of these responses, it is interesting to notice that only glutaminase is present in the model, and it was only active at pH 3.2

and 3.5. Arginine deiminase system has been reported for other strains of *O. oeni* (Tonon & Lonvaud-Funel, 2000), but the other responses has not been observed before in this genera. Regarding the other differently consumed amino acids, tryptophan is an interesting case. In some strains of *Lactobacillus spp*., the activity of a tryptophan decarboxylase (EC 4.1.1.28) has been reported (Fernández & Zúñiga, 2006). This enzyme can decarboxylate tryptophane into tryptamine, a biogenic amine that has also been observed in wine (Landete, Ferrer, & Pardo, 2007). It has not been reported that this enzyme is either present in *O. oeni* or that it aids in survival at acidic conditions; however, as tryptophan is negatively charged (-1) at the internal pH of *O. oeni*, and tryptamine is positively charged (+1) (ChemAxon, 2016), this reactions could potentially consume two protons per tryptophan, and thus its possible positive effects at low pH cannot be discarded. The other amino acids have been reported to be used as substrates for aromatic compounds generation (Methionine, Leucine and Isoleucine), or have unknown catabolic pathways in LAB (proline, glycine) (Fernández & Zúñiga, 2006).

NGAM was estimated for each experimental data set. Contrary to the case of different ethanol concentrations, the differences between the estimated NGAM were lower, reaching only a maximum range of a 2-fold in the same growth phase. This shows that NGAM values remain relatively constant along the different experimental pH tested in this experiment. Sensitivity analysis of NGAM toward pH_{in} showed that pH_{in} could affect NGAM through key compounds. There were eight intervals found in the range of pH_{in} = 3.2 to 6.4. The difference between each interval was found to be attributed to a specific set of reactions, and the variations of each set of reactions was attributed to one specific compound that changed its protonation state. All these compounds are key metabolites of the metabolism of *O. oeni*, as they are either cofactors ($NADP^+$, NADPH, ADP) or are related to proton extrusion mechanisms (malic and lactic acid to malolactic fermentation; acetic acid as a product of citrate metabolism). Variations in the protonation state of each of these metabolites caused a readjustment of all the reactions in which these compounds participate, as a proton

had to be added or taken out of the reaction. For ADP, its charge variation impacts 104 reactions. $NADP^+$/NADPH are only present in 18 reactions; however, these are important for fatty acid formation (and thus biomass formation) and for the first steps of heterolactic fermentation, and thus have a high impact in the metabolism. Acetic, malic and lactic acid are only present in 9, 6 and 7 reactions, respectively; however, variations in their protonation states have an impact in transport reactions, either improving or harnessing proton extrusion.

The case of malic acid is particularly interesting: when pH_{in} is higher than 5.13, due to differences in internal and external pH, malic uptake results in the release of a proton, acidifying the cytoplasm. This negative effect is counteracted by malolactic fermentation, which consumes a proton, and by lactic transport, which also consumes a proton, therefore ending in a net translocation of one proton. When internal pH is lower than 5.12, malate uptake does not result in proton release; however, malolactic fermentation does not result in proton consumption either, thus maintaining a net translocation of one proton due to lactic acid transport. This explains why NGAM was maintained for phase I at the third interval, as it is during this phase – phase I – where the higher specific consumption rate of malic acid was carried out, and thus the effect on NGAM estimation was counteracted.

The sensitivity of NGAM towards pH_{in} shows how delicate is the inner balance of internal pH and secondary transport systems, as the latter is highly dependent of pH_{in} in order to be effective for proton extrusion, and the former requires these secondary transport systems to avoid cytoplasm acidification. These results also remark the importance of correct identification of pH_{in} for the construction of GSMMs, especially in the case of acidophilic bacteria, as pH is a key determinant of the correct functioning of reactions for proton extrusion.

To our knowledge, this is the first time the impact of variations in pH_{in} has been analyzed by using a GSMM. There are three previous works that have analyzed the effect of pH on bacterial growth through GSMMs: Andersen, Lehmann & Nielsen (2009) analyzed the preference of organic acid production at external pH = 6.0, 4.5

and 2.5 for *Aspergillus niger*. To do this, they incorporated the different ratios of dissociated and undissociated forms of each organic acid released as product in the external section of the model, reactions that had to be manually adjusted to each external pH. Großeholz et al. (2016) evaluated pH adaptation in *Enterococcus faecalis* at pH 6.5 and 7.5. To include pH modification, they adjusted two transport reactions according to the protonation of the external pH, and included a proton influx. These previous works do not consider modification of internal reactions due to pH_{in} variations. The last work is the closest to this thesis: Park, Kim, & Lee (2011) evaluated polyhydroxyalkanoate biosynthesis in *Ralstonia eutropha* at pH 6.0, 7.0 and 8.0. To do this, they adjusted all the reactions included in the model to the external pH evaluated. However, they do not include different internal and external pH, and adjusted all reactions in unison. Thus, this work is novel in the independent adjustment of both external and internal pH and in the generation of models that show the effect of cytoplasm acidification. This step is key for the understanding of acidophile bacteria, as they are usually subjected to increased energetic expenses due to cytoplasm acidification. This is also important for bacteria that depend on secondary transport processes such as *O. oeni*, as these processes are affected by internal and external pH and thus the positive effect on cytoplasm deacidification could go unnoticed if pH is not considered accordingly.

7. CONCLUSIONS

Through this work, two novel approaches for *in silico* analysis were developed: first, the generation of an extended GSMM able to simulate simultaneously different growth phases of an organism, including intracellular accumulation. This approach was proven useful to simulate phenotypes from organisms that present complex behavior like intracellular accumulation and to whom traditional strategies were not effective. Second, the construction of AUTOPAD, the algorithm for automatic pH adjustment. This algorithm allowed a better analysis of the metabolic response of a microorganism growing at acidic conditions by incorporating pH as a variable, and thus allowing the inclusion of the variations of the protonation state. This techniques were used to understand the metabolism of *O. oeni* PSU-1 growing in a wine-like defined medium under two of the main stressors present in its natural habitat: ethanol and pH.

Empirical and *in silico* results showed that citric and malic acid are key for growth at extreme conditions, as highest biomass formation and specific growth rate was observed when these compounds were present in the medium for all ethanol concentration and pH values. This positive effect is mainly attributed to energy generation, as they were responsible for at least 80% of the proton extrusion required for energy generation through F_0F_1-ATPase in all cases.

Mannitol and erythritol production was shown to be vital for $NAD(P)^+$ regeneration in conditions of high ethanol concentrations, as its synthesis was responsible for 50-57% of the cofactor requirements for sugar degradation. This percentage was not the same in acidic conditions, which shows a clear differentiation into these two stresses, thus relating ethanol stress to a lack of cofactors.

Of the amino acids, cysteine was the only one that was completely depleted in all cases, showing that it could also be of importance for survival at stressful conditions. Aspartic acid and proline were also consumed differentially in both cases.

NGAM prediction showed that to overcome ethanol stress there was a high expense of ATP that is redirected into maintenance and stress mechanisms. However, this is not the

same with acidic conditions, which indicated that there are some metabolic processes that are more active at low pH and that are thus countervailing for processes that are affected by low pH.

8. FUTURE WORK

This work highlighted the importance of some compounds for survival at stress conditions that are currently unknown of its effect for stress survival and that thus required further investigation. In particular, the amino acids aspartic acid and proline could be related with stress responses, as consumption of both was higher during ethanol and pH stress; and tryptophan, as the presence of a tryptophan decarboxylase is suspected. Also, the enzyme transhydrogenase is of interest to be analyzed, as could be of special importance for cofactor regeneration during stress.

These studies could aid to gain a better understanding of the importance of amino acids in the metabolism of *O. oeni* during stress, and allowed a better phenotype prediction in the models iMR453 and iSM454.

Also, a future challenge is to apply a consortium metabolic model to winemaking, as a simulation of *O. oeni* and other microorganisms that share its ecological niche would aid in the understanding of the interactions between these species and the effects on wine quality.

REFERENCES

Alakomi, H., Skyttä, E., Saarela, M., & Helander, I. M. (2005). Lactic Acid Permeabilizes Gram-Negative Bacteria by Disrupting the Outer Membrane. *Applied and Environmental Microbiology*. http://doi.org/10.1128/AEM.66.5.2001-2005.2000.Updated

Andersen, M. R., Lehmann, L., & Nielsen, J. (2009). Systemic analysis of the response of Aspergillus niger to ambient pH. *Genome Biology*, *10*(5), R47. http://doi.org/10.1186/gb-2009-10-5-r47

Augagneur, Y., Ritt, J. F., Linares, D. M., Remize, F., Tourdot-Maréchal, R., Garmyn, D., & Guzzo, J. (2007). Dual effect of organic acids as a function of external pH in Oenococcus oeni. *Archives of Microbiology*, *188*(2), 147–157. http://doi.org/10.1007/s00203-007-0230-0

Bakker, E. ., & Harold, F. M. (1980). Energy coupling to potassium transport in Streptococcus faecalis.pdf. *The Journal of Biological Chemistry*, *225*(2), 433–440.

Bartowsky, E. J. (2005). Oenococcus oeni and malolactic fermentation – moving into the molecular arena. *Australian Journal of Grape and Wine Research*, *11*, 174–187. http://doi.org/10.1111/j.1755-0238.2005.tb00286.x

Bartowsky, E. J., Costello, P. J., & Chambers, P. J. (2015). Emerging trends in the application of malolactic fermentation. *Australian Journal of Grape and Wine Research*, *21*, 663–669. http://doi.org/10.1111/ajgw.12185

Bauer, R., & Dicks, L. M. T. (2004). Control of malolactic fermentation in wine. A review. *South African Journal of Enology and Viticulture*, *25*(2), 74–88.

Beales, N. (2004). Adaptation of Microorganisms to Cold Temperatures, Weak Acid Preservatives, Low pH, and Osmotic Stress: A Review. *Comprehensive Reviews in Food Science and Food Safety*, *3*, 1–20. http://doi.org/10.1111/j.1541-4337.2004.tb00057.x

Bouix, M., & Ghorbal, S. (2015). Rapid assessment of Oenococcus oeni activity by measuring intracellular pH and membrane potential by flow cytometry, and its application to the more effective control of malolactic fermentation. *International Journal of Food Microbiology*, *193*, 139–146. http://doi.org/10.1016/j.ijfoodmicro.2014.10.019

Breeuwer, P., Drocourt, J., Rombouts, F. M., & Abee, T. (1996). A Novel Method for Continuous Determination of the Intracellular pH in Bacteria with the Internally Conjugated Fluorescent Probe 5 (and 6-) -Carboxyfluorescein Succinimidyl Ester . A Novel Method for Continuous Determination of the Intracellular pH in B. *Applied and Environmental Microbiology*.

Brooijmans, R., Smit, B., Santos, F., van Riel, J., de Vos, W. M., & Hugenholtz, J. (2009). Heme and menaquinone induced electron transport in lactic acid bacteria. *Microbial Cell Factories*, *8*, 28. http://doi.org/10.1186/1475-2859-8-28

Caspi, R., Billington, R., Ferrer, L., Foerster, H., Fulcher, C. A., Keseler, I. M., … Karp, P. D. (2016). The MetaCyc database of metabolic pathways and enzymes and the BioCyc collection of pathway/genome databases. *Nucleic Acids Research*, *44*(D1), D471–D480. http://doi.org/10.1093/nar/gkv1164

Cavin, J. F., Divies, C., & Guzzo, J. (1998). La fermentation malolactique In: Oenologie. Fondaments scientiques et technologiques (Flanzy, C., Coordinateur). *Technique et Documentation Lavoisier, Paris.*, 503–511.

ChemAxon. (2016). Marvin 16.3.28. Retrieved from http://www.chemaxon.com

Chu-Ky, S., Tourdot-Marechal, R., Marechal, P. A., & Guzzo, J. (2005). Combined cold, acid, ethanol shocks in Oenococcus oeni: Effects on membrane fluidity and cell viability. *Biochimica et Biophysica Acta - Biomembranes*, *1717*(2), 118–124. http://doi.org/10.1016/j.bbamem.2005.09.015

Cibrario, A., Peanne, C., Lailheugue, M., Campbell-Sills, H., & Dols-Lafargue, M. (2016). Carbohydrate metabolism in Oenococcus oeni: a genomic insight. *BMC Genomics*, *17*(1), 984. http://doi.org/10.1186/s12864-016-3338-2

Cordente, A. G., Curtin, C. D., Varela, C., & Pretorius, I. S. (2012). Flavour-active wine yeasts. *Applied Microbiology and Biotechnology*, *96*(3), 601–618. http://doi.org/10.1007/s00253-012-4370-z

Cotter, P. D., & Hill, C. (2003). Surviving the Acid Test : Responses of Gram-Positive Bacteria to Low pH Surviving the Acid Test : Responses of Gram-Positive Bacteria to Low pH. *Microbiology and Molecular Biology Reviews : MMBR*, *67*(3), 429–453. http://doi.org/10.1128/MMBR.67.3.429

Da Silveira, M. G., A., G. E., Folkert, A., Rombouts, F. M., & Abee, T. (2003). Membrane Fluidity Adjustments in Ethanol-Stressed Oenococcus oeni Cells. *Appl. Environ. Microbiol*, (69), 5826–5832. http://doi.org/10.1128/AEM.69.10.5826

Dashper, S. G., & Reynolds, E. C. (1992). pH regulation by Streptococcus mutans. *Journal of Dental Research*, *71*(5), 1159–1165. http://doi.org/10.1007/s002030000233

Davis, C. R., Wibowo, D. J., Lee, T. H., & Fleet, G. H. (1986). Growth and Metabolism of Lactic Acid Bacteria during and after Malolactic Fermentation of Wines at Different pH Growth and Metabolism of Lactic Acid Bacteria during and after Malolactic Fermentation of Wines at Different pH, *51*(3), 539–545. Retrieved from http://aem.asm.org.kuleuven.ezproxy.kuleuven.be/content/51/3/539.full.pdf+html

De Man, J. C., Rogosa, M., & Sharpe, M. E. (1960). A medium for the cultivation of lactobacilli. *J. Appl. Bact.*, *23*(1), 130–135.

Drici-Cachon, Z., Guzzo, J., Cavin, & Divies, C. (1996). Acid tolerance in Leuconostoc oenos. Isolation and characterization of an acid-resistant mutant. *Appl. Microbiol.*

Biotechnol., (44), 785–789.

Fernández, M., & Zúñiga, M. (2006). Amino acid catabolic pathways of lactic acid bacteria. *Critical Reviews in Microbiology*, *32*(3), 155–83. http://doi.org/10.1080/10408410600880643

Ferrer, S., Pardo, I., & Maicas, S. (2001). Malolactic fermentation in wini with high densities of non-proliferating Oenococcus oeni. *World Journal of Microbiology and Biotechnology*, *16*(8–9), 805–810.

Firme, M. P., Leitão, M. C., & Romão, M. V. S. (1994). The metabolism of sugar and malic acid by Leuconostoc oenos: effect of malic acid, pH and aeration conditions. *Journal of Applied Bacteriology*, *76*(2), 173–181. http://doi.org/10.1111/j.1365-2672.1994.tb01613.x

Fleet, G. (1993). *Wine Microbiology and Biotechnology*. CRC Press. Retrieved from https://books.google.cl/books?id=vd_0mtncl0QC&pg=PA313&dq=alcoholic+fermentation+wine&hl=en&sa=X&redir_esc=y#v=onepage&q=alcoholic fermentation wine&f=false

Fortier, L. C., Tourdot-Maréchal, R., Diviès, C., Lee, B. H., & Guzzo, J. (2003). Induction of Oenococcus oeni H+-ATPase activity and mRNA transcription under acidic conditions. *FEMS Microbiology Letters*, (222), 165–169. http://doi.org/10.1016/S0378-1097(03)00299-4

Galland, D., Tourdot-Maréchal, R., Abraham, M., Son, C.-K., & Guzzo, J. (2003). Absence of Malolactic Activity Is a Characteristic of H+-ATPase-Deficient Mutants of the Lactic Acid Bacterium Oenococcus oeni. *Applied and Environmental Microbiology*, *69*(4), 1973–1979. http://doi.org/10.1128/AEM.69.4.1973-1979.2003

Gänzle, M. G. (2015). Lactic metabolism revisited: metabolism of lactic acid bacteria in food fermentations and food spoilage. *Current Opinion in Food Science*, *2*(Figure 2), 106–117. http://doi.org/10.1016/j.cofs.2015.03.001

García-Quintáns, N., Magni, C., De Mendoza, D., & López, P. (1998). The citrate transport system of Lactococcus lactis subsp. lactis biovar diacetylactis is induced by acid stress. *Appl. Environ. Microbiol*, (64), 850–857.

Garvie, E. I. (1967). Leuconostoc oenos sp.nov. *J. Gen. Microbiol.*, (48), 431–438.

Gomes de Oliveira Dal'Molin, C., Quek, L.-E., Saa, P. A., & Nielsen, L. K. (2015). A multi-tissue genome-scale metabolic modeling framework for the analysis of whole plant systems. *Frontiers in Plant Science*, *6*(January), 1–12. http://doi.org/10.3389/fpls.2015.00004

Grandvalet, C., Assad-García, J. S., Chu-Ky, S., Tollot, M., Guzzo, J., Gresti, J., & Tourdot-Maréchal, R. (2008). Changes in membrane lipid composition in ethanol- and acid-adapted Oenococcus oeni cells: characterization of the cfa gene by heterologous complementation. *Microbiology*, (154), 2611–2019. http://doi.org/10.1099/mic.0.2007/016238-0

Großeholz, R., Koh, C., Veith, N., Fiedler, T., Strauss, M., Olivier, B., … Kummer, U. (2016). Integrating highly quantitative proteomics and genome-scale metabolic modeling to study pH adaptation in the human pathogen Enterococcus faecalis, (December 2015). http://doi.org/10.1038/npjsba.2016.17

Gutiérrez Hernández, G. D. (2015). *Diseño y optimización de un medio de crecimiento definido para Oenococcus oeni en condiciones enológicas*. Pontifica Universidad Católica de Chile. Retrieved from https://repositorio.uc.cl/handle/11534/15712

Guzzo, J., Jobin, M. P., Delmas, F., Fortier, L. C., Garmyn, D., Tourdot-Marechal, R., … Divies, C. (2000). Regulation of stress response in Oenococcus oeni as a function of environmental changes and growth phase. *International Journal of Food Microbiology*, *55*(1–3), 27–31.

Hastings, J., de Matos, P., Dekker, A., Ennis, M., Harsha, B., Kale, N., Muthukrishnan, V., Owen, G., Turner, S., Williams, M., and Steinbeck, C. (2013). The ChEBI reference database and ontology for biologically relevant chemistry: enhancements for 2013. Retrieved from https://www.ebi.ac.uk/

Hua, L., WenYing, Z., Hua, W., ZhongChao, L., & AiLian, W. (2009). Influence of culture pH on freeze-drying viability of Oenococcus oeni and its relationship with fatty acid composition. *Food and Bioproducts Processing*, *87*(1), 56–61. http://doi.org/10.1016/j.fbp.2008.06.001

Hugenholtz, J. (1993). Citrate metabolism in lactic acid bacteria. *FEMS Microbiology Reviews*, *12*(1–3), 165–178. http://doi.org/10.1016/0168-6445(93)90062-E

José Pascual Abad. (2011). Proton Motive Force. In M. V. Muriel Gargaud, Prof. Ricardo Amils, José Cernicharo Quintanilla, Henderson James (Jim) Cleaves II, William M. Irvine, Prof. Daniele L. Pinti (Ed.), *Encyclopedia of Astrobiology* (1st ed., p. pp 1355-1356). Springer. Retrieved from https://link.springer.com/referenceworkentry/10.1007%2F978-3-642-11274-4_141

Kanehisa, M. and Goto, S. (2000). KEGG: Kyoto Encyclopedia of Genes and Genomes. *Nucleic Acids Res.*, (28), 27–30.

Kashiwagi, K., Miyamoto, S., Suzuki, F., Kobayashi, H., & Igarashi, K. (1992). Excretion of putrescine by the putrescine-ornithine antiporter encoded by the potE gene of Escherichia coli. *Proceedings of the National Academy of Sciences of the United States of America*, *89*(10), 4529–4533. http://doi.org/10.1073/pnas.89.10.4529

Kashket, E. R., & Barker, S. L. (1977). Effects of Potassiu Ions on the Electrical and pH Gradients Across the Membrane of Streptococcus lactis Cells. *Journal of Bacteriology*, *130*(3), 1017–1023.

Kauffman, K. J., Prakash, P., & Edwards, J. S. (2003). Advances in flux balance analysis. *Current Opinion in Biotechnology*, *14*(5), 491–496. http://doi.org/10.1016/j.copbio.2003.08.001

Konings, W. N. (2002). The cell membrane and the struggle for life of lactic acid bacteria. *Antonie van Leeuwenhoek*, *82*(3), 3–27. Retrieved from http://link.springer.com/chapter/10.1007/978-94-017-2029-8_2

Konings, W. N. (2006). Microbial transport: adaptations to natural environments. *Antonie van Leeuwenhoek*, *90*(4), 325–42. http://doi.org/10.1007/s10482-006-9089-3

Konings, W. N., Lolkema, J. S., Bolhuis, H., van Veen, H. W., Poolman, B., & Driessen, A. (1997). The role of transport processes in survival of lactic acid bacteria Energy transduction and multidrug resistance. *Antonie van Leeuwenhoek*, *71*, 117–128.

Konings, W. N., Lolkema, J. S., & Poolman, B. (1995). The generation of metabolic energy by solute transport. *Archives of Microbiology*, *164*(4), 235–242. http://doi.org/10.1007/BF02529957

Konings, W. N. N., Lolkema, J. S. S., Bolhuis, H., Veen, H. W. van W. Van, Poolman, B., & Driessen, A. J. M. (1997). Energy transduction and multidrug resistance F pH mv. *Antonie van Leeuwenhoek*, *71*(1–2), 117–128. http://doi.org/10.1023/A:1000143525601

Kuhnert, W., Zheng, G., Faustoferri, R., & Quivey, R. (2004). The F-ATPase Operon Promoter of Streptococcus mutans Is Transcriptionally Regulated in Response to External pH. *Journal*, *186*(24), 8524–8528. http://doi.org/10.1128/JB.186.24.8524-8528.2004

Kullen, M. ., & Klaenhammer, T. . (1999). Identification of the pH-inducible, proton-translocating F1-FO-ATPase (atpBEFHAGDC) operon of lactobacillus acidophilus by differential display: gene structure, cloning and characterization. *Molecular Microbiology*, (33), 1152–1161.

Kunkee, R. E. (1968). Malo-Lactic Fermentation. *Advances in Applied Microbiology*, *9*(C), 235–279. http://doi.org/10.1016/S0065-2164(08)70530-6

Kunkee, R. E. (1991). Some roles of malic-acid in the malolactic fermentation in wine-making. *FEMS Microbiol Rev*, *88*(1), 55–72.

Lafon-Lafourcade, S., Carre, E., & Ribéreau-Gayon, P. (1983). Occurrence of Lactic Acid Bacteria During the Different Stages of Vinification and Conservation of Wines Occurrence of Lactic Acid Bacteria During the Different Stages of Vinification and Conservation of Wines, *46*(4), 874–880.

Landete, J. M., Ferrer, S., & Pardo, I. (2007). Biogenic amine production by lactic acid bacteria, acetic bacteria and yeast isolated from wine. *Food Control*, *18*(12), 1569–1574. http://doi.org/10.1016/j.foodcont.2006.12.008

Lechardeur, D., Cesselin, B., Fernandez, A., Lamberet, G., Garrigues, C., Pedersen, M., … Gruss, A. (2011). Using heme as an energy boost for lactic acid bacteria. *Current Opinion in Biotechnology*, (22), 143–149. http://doi.org/10.1016/j.copbio.2010.12.001

Linares, D. M., Fernández, M., Martín, M. C., & Álvarez, M. A. (2009). Tyramine biosynthesis in Enterococcus durans is transcriptionally regulated by the extracellular pH and tyrosine concentration. *Microbial Biotechnology*, *2*(6), 625–633. http://doi.org/10.1111/j.1751-7915.2009.00117.x

Liu, S.-Q. (2002). A review: malolactic fermentation in wine -- beyond deacidification. *Journal of Applied Microbiology*, *92*(4), 589–601. Retrieved from http://www.ncbi.nlm.nih.gov/pubmed/11966898

Liu, S. Q. (2003). Practical implications of lactate and pyruvate metabolism by lactic acid bacteria in food and beverage fermentations. *International Journal of Food Microbiology*, *83*(2), 115–131. http://doi.org/10.1016/S0168-1605(02)00366-5

Liu, Y., Tang, H., Lin, Z., & Xu, P. (2015). Mechanisms of acid tolerance in bacteria and prospects in biotechnology and bioremediation. *Biotechnology Advances*, *33*(7), 1484–1492. http://doi.org/10.1016/j.biotechadv.2015.06.001

Lolkema, J. S., Poolman, B., & Konings, W. N. (1995). Role of scalar protons in metabolic energy generation in lactic acid bacteria. *Journal of Bioenergetics and Biomembranes*, *27*(4), 467–473. http://doi.org/10.1007/BF02110009

Lonvaud-Funel, A. (1999). Lactic acid bacteria in the quality improvement and depreciation of wine. *Antonie van Leeuwenhoek*, *76*, 317–331. http://doi.org/10.1023/A

Lucas, P., Landete, J., Coton, M., Coton, E., & Lonvaud-Funel, A. (2003). The tyrosine decarboxylase operon of Lactobacillus brevis IOEB 9809: characterization and conservation in tyramine-producing bacteria. *FEMS Microbiol Lett*, *229*(1), 65–71. http://doi.org/https://doi.org/10.1016/S0378-1097(03)00787-0

Lucas, P., & Lonvaud-Funel, A. (2002). Purification and partial gene sequence of the tyrosine decarboxylase of Lactobacillus brevis IOEB 9809. *FEMS Microbiology Letters*, *211*(1), 85–89. http://doi.org/10.1016/S0378-1097(02)00647-X

Ma, D., Lu, P., Yan, C., Fan, C., Yin, P., Wang, J., & Shi, Y. (2012). Structure and mechanism of a glutamate–GABA antiporter. *Nature*, *483*(7391), 632–636. http://doi.org/10.1038/nature10917

Maicas, S., Ferrer, S., & Pardo, I. (2002). NAD(P)H regeneration is the key for heterolactic fermentation of hexoses in Oenococcus oeni. *Microbiology*, *148*(1), 325–332.

Maicas, S., González-Cabo, P., Ferrer, S., & Pardo, I. (1999). Production of Oenococcus oeni biomass to induce malolactic fermentation in wine by control of pH and substrate addition. *Biotechnology Letters*, *21*(4), 349–353. http://doi.org/10.1023/A:1005498925733

Martín-Galano, J., Ferrándiz, M. ., & G. de la Campa, A. (2001). The promoter of the

operon encoding the F0F1 ATPase of Streptococcus pneumoniae is inducible by pH. *Molecular Microbiology*, *41*(6), 1327–1338.

Marty-Teisset, C., Posthuma, C., Lolkema, J. S., Schmitt, P., Divies, C., & Konings, W. N. (1996). Proton motive force generation by citrolactic fermentation in Leuconostoc mesenteroides. *J. Bacteriol.*, (178), 2178–2185.

Mateo, J. J., Jiménez, M., Pastor, A., & Huerta, T. (2001). Yeast starter cultures affecting wine fermentation and volatiles. *Food Research International*, *34*(4), 307–314. http://doi.org/10.1016/S0963-9969(00)00168-X

McCloskey, D., Palsson, B. Ø., & Feist, A. M. (2013). Basic and applied uses of genome-scale metabolic network reconstructions of Escherichia coli. *Molecular Systems Biology*, *9*(1), 661. http://doi.org/10.1038/msb.2013.18

Mendoza, S. N., Cañón, P. M., Contreras, A., Ribbeck, M., & Agosin, E. (2017). Genome-scale reconstruction of the metabolic network in Oenococcus oeni to assess wine malolactic fermentation. *Frontiers in Microbiology*, *8*, 534. http://doi.org/10.3389/FMICB.2017.00534

Mesas, J. ., Rodríguez, M. C., & Alegre, M. . (2004). Tolerancia de Oenococcus oeni RS1 a las condiciones de estrés del vino. *Ciencia Y Tecnología Alimentaria*, (4), 278–282. Retrieved from http://www.redalyc.org/articulo.oa?id=72440409

Mills, D. A., Rawsthorne, H., Parker, C., Tamir, D., & Makarova, K. (2005). Genomic analysis of Oenococcus oeni PSU-1 and its relevance to winemaking. *FEMS Microbiology Reviews*, *29*(3 SPEC. ISS.), 465–475. http://doi.org/10.1016/j.femsre.2005.04.011

Molenaar, D., Bosscher, J. S., Ten Brink, B., Driessen, A. J. M., & Konings, W. N. (1993). Generation of a proton motive force by histidine decarboxylatioin and electrogenic histidine/histamine antiport in Lactobacllus bucneri. *J. Bacteriol.*, *175*(10), 2864–2870.

Nannen, N. L., & Hutkins, R. W. (1991). Intracellular pH Effects in Lactic Acid Bacteria. *Journal of Dairy Science*, *74*(3), 741–746. http://doi.org/10.3168/jds.S0022-0302(91)78219-2

Nielsen, J. C., Richelieu, M., Nielsen, J. a N. C., S, C. H. a, & Hørsholm, D.-. (1999). Control of Flavor Development in Wine during and after Malolactic Fermentation by Oenococcus oeni Control of Flavor Development in Wine during and after Malolactic Fermentation by Oenococcus oeni, *65*(2), 740–745.

Noens, E. E. E., & Lolkema, J. S. (2017). Convergent evolution of the arginine deiminase pathway: the ArcD and ArcE arginine/ornithine exchangers. *Microbiology Open*, *6*(1), 1–10. http://doi.org/10.1002/mbo3.412

Nomura, M., Fujita, Y., & Kobayashi, M. (1999). Lactococcus lactis contains only one glutamate decarboxylase gene, (145), 1375–1380.

Nomura, M., Kobayashi, M., Ohmomo, S., & Okamoto, T. (2000). Inactivation of the glutamate decarboxylase gene in Lactococcus lactis subsp. cremoris. *Applied and Environmental Microbiology*, *66*(5), 2235–7. Retrieved from http://www.pubmedcentral.nih.gov/articlerender.fcgi?artid=101481&tool=pmcentrez&rendertype=abstract

Novak, L., Lindley, N. ., & Loubiere, P. (1997). Metabolism and Energetics of Lactococcus lactis during Growth in Complex or Synthetic Media. *Applied and Environmental Microbiology*, *63*(7), 2665–2670.

Olguin, N. (2010). *Molecular study of the mechanisms of Oenococcus oeni involved in its adaptation to wine conditions and in the development of malolactic fermentation*. Universitat Rovira i Virgili. Retrieved from http://www.tesisenred.net/handle/10803/8682

Olguín, N., Bordons, A., & Reguant, C. (2009). Influence of ethanol and pH on the gene expression of the citrate pathway in Oenococcus oeni. *Food Microbiology*, *26*(2), 197–203.

http://doi.org/10.1016/j.fm.2008.09.004

Orth, J. D., Thiele, I., & Palsson, B. Ø. (2010). What is flux balance analysis? *Nature Biotechnology*, *28*(3), 245–248. http://doi.org/10.1038/nbt.1614

Park, J. M., Kim, T. Y., & Lee, S. Y. (2011). Genome-scale reconstruction and in silico analysis of the Ralstonia eutropha H16 for polyhydroxyalkanoate synthesis , lithoautotrophic growth , and 2-methyl citric acid production.

Pastink, M. I., Teusink, B., Hols, P., Visser, S., De Vos, W. M., & Hugenholtz, J. (2009). Genome-scale model of Streptococcus thermophilus LMG18311 for metabolic comparison of lactic acid bacteria. *Appl. Environ. Microbiol*, (75), 3627–3633. http://doi.org/10.1128/AEM.00138-09

Pereira, C. I., Matos, D., San Romão, M. V., & Barreto Crespo, M. T. (2009). Dual role for the tyrosine decarboxylation pathway in Enterococcus faecium E17: Response to an acid challenge and generation of a proton motive force. *Applied and Environmental Microbiology*, *75*(2), 345–352. http://doi.org/10.1128/AEM.01958-08

Pereira, R., Nielsen, J., & Rocha, I. (2016). Improving the flux distributions simulated with genome-scale metabolic models of Saccharomyces cerevisiae. *Metab. Eng. Commun*, (3), 153–163. http://doi.org/10.1016/j.meteno.2016.05.002

Poolman, B. (1993). Energy transduction in lactic acid bacteria. *FEMS Microbiology Reviews*, *12*(1–3), 125–147. http://doi.org/10.1016/0168-6445(93)90060-M

Poolman, B., Driessen, A. J. M., & Konings, W. N. (1987). Regulation of arginine-ornithine exchange and the arginine deiminase pathway in Streptococcus lactis. *Journal of Bacteriology*, *169*(12), 5597–5604.

Poolman, B., Molenaar, D., Smid, E. J., Ubbink, T., Abee, T., Renault, P. P., & Konings, W. N. (1991). Malolactic fermentation: electrogenic malate uptake and malate/lactate

antiport generate metabolic energy. *Journal of Bacteriology*, *173*(19), 6030–6037. http://doi.org/0021-9193/91/196030-08$02.00/0

Ramos, A., Lolkema, J. S., Konings, W. N., & Santos, H. (1995). Enzyme basis for pH regulation of citrate and pyruvate metabolism by Leuconostoc oenos. *Applied and Environmental Microbiology*, *61*(4), 1303–1310.

Richter, H., Hamann, I., & Unden, G. (2003). Use of the mannitol pathway in fructose fermentation of Oenococcus oeni due to limiting redox regeneration capacity of the ethanol pathway. *Archives of Microbiology*, *179*(4), 227–233. http://doi.org/10.1007/s00203-003-0519-6

Richter, H., Vlad, D., & Unden, G. (2001). Significance of pantothenate for glucose fermentation by Oenococcus oeni and for suppression of the erythritol and acetate production. *Archives of Microbiology*, *175*(1), 26–31. http://doi.org/10.1007/s002030000233

Romano, A., Trip, H., Lonvaud-Funel, A., Lolkema, J. S., & Lucas, P. M. (2012). Evidence of two functionally distinct ornithine decarboxylation systems in lactic acid bacteria. *Applied and Environmental Microbiology*, *78*(6), 1953–1961. http://doi.org/10.1128/AEM.07161-11

Saguir, F. M., & Manca de Nadra, M. C. (1996). Organic acid metabolism under different glucose concentrations of Leuconostoc oenos from wine. *Journal of Applied Bacteriology*, *81*(4), 393–397.

Salema, M., Lolkema, J. S., & Roma, M. V. S. A. N. (1996). The Proton Motive Force Generated in, *178*(11), 3127–3132.

Salou, P., Leroy, M. J., Goma, G., & Pareilleiux, A. (1991). Influence of pH and malate-glucose ratio on the growth kinetics of Leuconostoc oenos. *Applied Microbiology and Biotechnology*, *36*(1), 87–91.

Shoaie, S., Karlsson, F., Mardinoglu, A., Nookaew, I., Bordel, S., & Nielsen, J. (2013). Understanding the interactions between bacteria in the human gut through metabolic modeling. *Scientific Reports*, *3*(1), 2532. http://doi.org/10.1038/srep02532

Siegumfeldt, H., Björn Rechinger, K., & Jakobsen, M. (2000). Dynamic changes of intracellular pH in individual lactic acid bacterium cells in response to a rapid drop in extracellular pH. *Applied and Environmental Microbiology*, *66*(6), 2330–2335. http://doi.org/10.1128/AEM.66.6.2330-2335.2000

Spry, C., Kirk, K., & Saliba, K. J. (2008). Coenzyme A biosynthesis: An antimicrobial drug target. *FEMS Microbiol Rev*, (32), 56–106. http://doi.org/doi:10.1111/j.1574-6976.2007.00093.x

Sullivan, E. O., & Condon, S. (1999). Relationship between Acid Tolerance , Cytoplasmic pH , and ATP and H + -ATPase Levels in Chemostat Cultures of Lactococcus lactis Relationship between Acid Tolerance , Cytoplasmic pH , and ATP and H 2 -ATPase Levels in Chemostat Cultures of Lactococcus la, *65*(6), 2287–2293.

Teixeira, H., Gonçalves, M. G., Rozès, N., Ramos, A., & San Romão, M. V. (2002). Lactobacillic acid accumulation in the plasma membrane of Oenococcus oeni: A response to ethanol stress? *Microbial Ecology*, (43), 146–153. http://doi.org/10.1007/s00248-001-0036-6

Teixeira, J. S., Seeras, A., Sanchez-maldonado, A. F., Zhang, C., Su, M. S., & Gänzle, M. G. (2014). Glutamine , glutamate , and arginine-based acid resistance in Lactobacillus reuteri, *42*, 172–180.

Terrade, N., & Mira de Orduña, R. (2009). Determination of the essential nutrient requirements of wine-related bacteria from the genera Oenococcus and Lactobacillus. *International Journal of Food Microbiology*, *133*(1–2), 8–13. http://doi.org/10.1016/j.ijfoodmicro.2009.03.020

Teusink, B., Wiersma, A., Molenaar, D., Francke, C., De Vos, W. M., Siezen, R. J., & Smid, E. J. (2006). Analysis of growth of Lactobacillus plantarum WCFS1 on a complex medium using a genome-scale metabolic model. *Journal of Biological Chemistry*, *281*(52), 40041–40048. http://doi.org/10.1074/jbc.M606263200

Toit, M., & Pretorius, I. S. (2000). Microbial Spoilage and Preservation of Wine : Using Weapons from Nature â€TM s Own Arsenal- A Review. *South African Journal of Enology and Viticulture*, *21*, 74–96.

Tonon, T., & Lonvaud-Funel, A. (2000). Metabolism of arginine and its positive effect on growth and revival of Oenococcus oeni. *Journal of Applied Microbiology*, *89*(3), 526–531. http://doi.org/10.1046/j.1365-2672.2000.01142.x

Tourdot-Maréchal, R., Fortier, L. C., Guzzo, J., Lee, B., & Diviès, C. (1999). Acid sensitivity of neomycin-resistant mutants of Oenococcus oeni: A relationship between reduction of ATPase activity and lack of malolactic activity. *FEMS Microbiology Letters*, *178*(2), 319–326. http://doi.org/10.1016/S0378-1097(99)00377-8

Tourdot-Maréchal, R., Gaboriau, D., Beney, L., & Divies, C. (2000). Membrane fliudity of stressed cells of oenococcus oeni, *55*, 269–273.

Tsakalidou, & Papadimitriou. (2011). *Food Microbiology and Food Safety Series*. (M. P. Doyle, Ed.). Springer New York Dordrecht Heidelberg London.

van de Guchte, M., Serror, P., Chervaux, C., Smokvina, T., Ehrlich, S. D., & Maguin, E. (2002). Stress responses in lactic acid bacteria. *Antonie van Leeuwenhoek*, *82*(1–4), 187–216. http://doi.org/10.1023/A:1020631532202

Varela, C., Agosin, E., Baez, M. E., Klapa, M., & Stephanopoulos, G. (2003). Metabolic flux redistribution in Corynebcterium glutamicum in response to osmotic stress. *Appl. Microbiol. Biotechnol.*, (60), 547–55. http://doi.org/10.1007/s00253-002-1120-7

Veiga-Da-Cunha, M., Santos, H., & Van Schaftingen, E. (1993). Pathway and regulation of erythritol formation in Leuconostoc oenos. *Journal of Bacteriology*, *175*(13), 3941–3948. http://doi.org/10.1128/JB.175.13.3941-3948.1993

Vermeulen, N., Gänzle, M. G., & Vogel, R. F. (2007). Glutamine deamidation by cereal-associated lactic acid bacteria. *Journal of Applied Microbiology*, *103*, 1197–1205. http://doi.org/10.1111/j.1365-2672.2007.03333.x

Versari, A., Parpinello, G. P., & Cattaneo, M. (1999). Leuconostoc oenos and malolactic fermentation in wine: a review. *Journal of Industrial Microbiology & Biotechnology*, *23*(May), 447–455. http://doi.org/10.1038/sj.jim.2900733

Vrancken, G., Rimaux, T., Weckx, S., De Vuyst, L., & Leroy, F. (2009). Environmental pH determines citrulline and ornithine release through the arginine deiminase pathway in Lactobacillus fermentum IMDO 130101. *International Journal of Food Microbiology*, *135*(3), 216–222. http://doi.org/10.1016/j.ijfoodmicro.2009.07.035

Wagner, N., Tran, Q. H., Richter, H., Paul, M., Unden, G., & Selzer, P. M. (2005). Pyruvate Fermentation by Oenococcus oeni and Leuconostoc mesenteroides and Role of Pyruvate Dehydrogenase in Anaerobic Fermentation Pyruvate Fermentation by Oenococcus oeni and Leuconostoc mesenteroides and Role of Pyruvate Dehydrogenase in Anaerobic Ferm, *71*(9), 4966–4971. http://doi.org/10.1128/AEM.71.9.4966

Wisselink, H. W., Weusthuis, R. A., Eggink, G., Hugenholtz, J., & Grobben, G. J. (2002). Mannitol production by lactic acid bacteria : A review. *International Dairy Journal*, 151–161. http://doi.org/10.1016/S0958-6946(01)00153-4

Wolken, W. A. M., Lucas, P. M., Lonvaud-Funel, A., & Lolkema, J. S. (2006). The mechanism of the tyrosine transporter TyrP supports a proton motive tyrosine decarboxylation pathway in Lactobacillus brevis. *Journal of Bacteriology*, *188*(6), 2198–2206. http://doi.org/10.1128/JB.188.6.2198-2206.2006

Wu, C., Huang, J., & Zhou, R. (2014). Progress in engineering acid stress resistance of lactic acid bacteria. *Applied Microbiology and Biotechnology*, *98*(3), 1055–1063. http://doi.org/10.1007/s00253-013-5435-3

Zamora, F. (2008). *Wine Chemistry and Biochemistry*. (V. Moreno-Arrivas & C. Polo, Eds.). Springer. Retrieved from https://books.google.cl/books?id=q_AkYRM-RR8C&pg=PA4&dq=alcoholic+fermentation+wine&hl=en&sa=X&redir_esc=y#v=onepage&q=alcoholic fermentation wine&f=false

Zaunmüller, T., Eichert, M., Richter, H., & Unden, G. (2006). Variations in the energy metabolism of biotechnologically relevant heterofermentative lactic acid bacteria during growth on sugars and organic acids. *Applied Microbiology and Biotechnology*, *72*(3), 421–429. http://doi.org/10.1007/s00253-006-0514-3

Zhang, D. S., & Lovitt, R. W. (2005). Studies on growth and metabolism of Oenococcus oeni on sugars and sugar mixtures. *Journal of Applied Microbiology*, *99*(3), 565–572. http://doi.org/10.1111/j.1365-2672.2005.02628.x

Zuljan, F. a, Repizo, G. D., Alarcon, S. H., & Magni, C. (2014). International Journal of Food Microbiology α -Acetolactate synthase of Lactococcus lactis contributes to pH homeostasis in acid stress conditions Pals Pcit als als. *International Journal of Food Microbiology*, *188*, 99–107. http://doi.org/10.1016/j.ijfoodmicro.2014.07.017

A P P E N D I X

APPENDIX A: FIRST SIMULATIONS WITH ISM454

Experimental data was obtained from the master thesis of Gutiérrez (2015). Table A-1 shows the consumption and production fluxes of compounds measured experimentally on a wine-like defined medium, at two different external pH conditions (4.8 and 3.5), and two or four different ethanol concentrations (0,3,9,12% v/v). Specific growth rate of each case is presented too.

Table A-1: Experimental data provided by Gutiérrez (2015)

pH	Ethanol (v/v)	Glucose (mmol/ gDCW h)	Fructose (mmol/ gDCW h)	Lactic acid (mmol/ gDCW h)	Citric acid (mmol/ gDCW h)	Malic acid (mmol/ gDCW h)	Acetic acid (mmol/ gDCW h)	Erithritol (mmol/ gDCW h)	Specific growth rate (1/h)
4.8	0%	-1.9089	-1.9469	3.0327	-0.1957	-0.6937	1.4298	0.0712	0.0263
4.8	3%	-1.3254	-1.6008	2.7435	-0.1638	-0.6354	1.5076	0.0332	0.0241
4.8	9%	-0.6273	-1.1631	1.9395	-0.1287	-0.7738	0.9707	0.0070	0.0176
4.8	12%	-0.4232	-1.0579	1.8553	-0.1253	-0.8609	0.9507	0.0172	0.0166
3.5	0%	-1.2765	-1.6121	2.3338	-0.3502	-0.9187	1.3736	0.0060	0.0150
3.5	12%	-0.5050	-0.6512	1.7643	-0.1740	-0.8494	0.7216	0.0159	0.0134

Average fluxes from two biological replicates.

APPENDIX B: METABOLITE-SPECIFIC TABLES CONSTRUCTED

As the tables generated have 536 rows, an extract of both tables is given as an example of the work carried out in Table B-1 and Table B-2.

Table B-1: Table of metabolite-specific pKas (extract)

Metabolites	**pKa**				
3,5-dimethoxytoluene [e]	non ionizable				
fucose [e]	11.3	12.72	13.66		
fucose [c]	11.3	12.72	13.66		
cyanate [e]	non ionizable				
cyanate [c]	non ionizable				
4-aminobutanoate [e]	4.53	10.22			
4-aminobutanoate [c]	4.53	10.22			
xanthine [e]	7.95	10.77	16.61		
xanthine [c]	7.95	10.77	16.61		
Cd2+ [e]	non ionizable				
Cd2+ [c]	non ionizable				
L-ascorbate [e]	5.88	8.27	11.18	12.99	15.49
L-ascorbate [c]	5.88	8.27	11.18	12.99	15.49
K+ [e]	non ionizable				
K+ [c]	non ionizable				
(R)-pantothenate [e]	15.05	12.69	15.92		4.36
(R)-pantothenate [c]	15.05	12.69	15.92		4.36
riboflavin [c]	6.97	12.85	13.96	15.84	14.94
cytosine [e]	2.35	9.98			

Table B-2**:** Table of metabolite information

Metabolites	**Formula**	**charge**	**CHEBI ID**	**SMILES**	**InCHI**	**Kegg ID**
3,5-dimethoxytoluene [e]	$C_9H_{12}O_2$	0		CC1(=CC(=CC(=C1)OC)OC)	1S/C9H12O2/c1-7-4-8(10-2)6-9(5-7)11-3/h4-6H,1-3H3	
fucose [c]	$C_6H_{12}O_5$	0	2181	C[C@@H]1OC(O)[C@@H](O)[C@H](O)[C@@H]1O	1S/C6H12O5/c1-2-3(7)4(8)5(9)6(10)11-2/h2-10H,1H3/t2-,3+,4+,5-,6?/m0/s1	C01019
cyanate [c]	$C_1N_1O_1$	-1	29195	[O-]C#N	1S/CHNO/c2-1-3/h3H/p-1	C01417
4-aminobutanoate [c]	$C_4H_9NO_2$	0	59888	C(C[N+])CC([O-])=O	1S/C4H9NO2/c5-3-1-2-4(6)7/h1-3,5H2,(H,6,7)	C00334
xanthine [c]	$C_5H_4N_4O_2$	0	15318	C12(NC(=O)NC(C=1N=CN2)=O)	1S/C5H4N4O2/c10-4-2-3(7-1-6-2)8-5(11)9-4/h1H,(H3,6,7,8,9,10,11)	C00385
Cd2+ [c]	Cd_1	2	22977	[Cd]	1S/Cd	C01413

APPENDIX C: CURATION OF ISM454 MODEL

C.1 Reactions

a) Manually curated reactions

23 reactions were manually curated due to major mass imbalance. Table C-1 lists the name of 18 of these reactions, the reaction as it is present in iSM454, and the modifications done in model iMR453.

Table C-1: Modifications carried out during manual curation

Reaction name	Reaction in iSM454	Reaction in iMR453
3.2.1.10-RXN	1 isomaltose [c] + 1 H2O [c] -> 1 alpha-D-glucose [c]	1 isomaltose [c] + 1 H2O [c] -> **2** alpha-D-glucose [c]
FERRIC-CHELATE-REDUCTASE-RXN	1 Fe2+ [c] + 1 NAD+ [c] + 1 H+ [c] <-> 1 Fe3+ [c] + 1 NADH [c]	**2** Fe2+ [c] + 1 NAD+ [c] + 1 H+ [c] <-> **2** Fe3+ [c] + 1 NADH [c]
6.3.4.16-RXN	1 NH4+ [c] + 1 CO2 [c] + 1 ATP [c] + 1 H2O [c] -> 1 carbamoyl-P [c] + + 1 ADP [c] + 1 P [c] + 1 H+ [c]	1 NH4+ [c] + 1 CO2 [c] + **2** ATP [c] + 1 H2O [c] -> 1 carbamoyl-P [c] + **2** ADP [c] + 1 P [c] + **3** H+ [c]
AMACETOXID-RXN	1 aminoacetone [c] + 1 O2 [c] + 1 H2O [c] -> 1 methylglyoxal [c] + 1 NH4+ [c] + 1 H+ [c]	1 aminoacetone [c] + 1 O2 [c] + 1 H2O [c] -> 1 methylglyoxal [c] + 1 NH4+ [c] + **1 H2O2 [c]**
RXN-12541	1 Fe2+ [c] + 1 O2 [c] -> 1 Fe3+ [c]	**4** Fe2+ [c] + 1 O2 [c] + **4 H+ [c]** -> **4** Fe3+ [c] + **2 H2O [c]**

RXNK9E-138	1 NO3 [e] + 1 ATP [c] -> 1 NO3 [c] + 1 ADP [c] + 1 P [c]	1 NO3 [e] + 1 ATP [c] + **1 H2O [c]** -> 1 NO3 [c] + 1 ADP [c] + 1 P [c] + **1 H+ [c]**
TRANS-RXNK9E-432	1 D-mannose [e] + 1 phospho-enolpyruvate [c] -> 1 D-mannose [c] + 1 pyruvate [c]	1 D-mannose [e] + 1 phospho-enolpyruvate [c] -> **1 D-mannose-6P[c]** + 1 pyruvate [c]
CARBPSYN-RXN	1 L-Gln [c] + 1 HCO3 [c] + 1 ATP [c] + 1 H2O [c] -> 1 carbamoyl-P [c] + 1 L-Glu [c] + 1 ADP [c] + 1 P [c] + 1 H+ [c]	1 L-Gln [c] + 1 HCO3 [c] + **2** ATP [c] + 1 H2O [c] -> 1 carbamoyl-P [c] + 1 L-Glu [c] + **2** ADP [c] + 1 P [c] + **2** H+ [c]
RXN-12352	2 ubiquinol-8 [c] + 1 O2 [c] -> 2 ubiquinone-8 [c] + 6 H+ [c] + 2 H2O[c]	2 ubiquinol-8 [c] + 1 O2 [c] + **6 H+ [e]** -> 2 ubiquinone-8 [c] + 6 H+ [c] + 2 H2O [c]
TRANS-RXNK9E-524*	1 (R)-lactate [c] + 2 H+ [c] -> 1 (R)-lactate [e] + 2 H+ [e]	1 (R)-lactate [c] + **1** H+ [c] -> 1 (R)-lactate [e] + **1** H+ [e]
GLUTSEMIALDEHYDROG-RXN	1 L-glutamate-5-phosphate [c] + 1 NADPH [c] + 1 H+ [c] -> 1 L-glutamate gamma-semialdehyde [c] + 1 NADP+ [c]	1 L-glutamate-5-phosphate [c] + 1 NADPH [c] + 1 H+ [c] -> 1 L-glutamate gamma-semialdehyde [c] + **1 P [c]** + 1 NADP+ [c]
FORMATETHFLIG-RXN	1 formate [c] + 1 ATP [c] + 1 tetrahydrofolate-Glu [c] <-> 1 10-CHO-THF [c] + 1 ADP [c] + 1 P [c]	1 formate [c] + 1 **tetrahydrofolate [c]** + 1 ATP [c] <-> 1 10-CHO-THF [c] + 1 ADP [c] + 1 P [c]
ERITHRITIOL-RXN	1 D-erythrose-4P [c] + 1 NADPH [c] + 1 H+ [c] -> 1 P [c] + 1 NADP+ [c] + 1 D-erythritol [c]	1 D-erythrose-4P [c] + 1 NADPH [c] + 1 H+ [c] + **1 H2O [c]** -> 1 P [c] + 1 NADP+ [c] + 1 D-erythritol [c]
TRANS_RXNK9E_539	1 acetate [c] + 1 H+ [c] <-> 1 acetate [e]	1 acetate [c] <-> 1 acetate [e]

TRANSRXNK9E525*	1 (S)-lactate [c] + 2 H+ [c] -> 1 (S)-lactate [e] + 2 H+ [e]	1 (S)-lactate [c] + **1** H+ [c] -> 1 (S)-lactate [e] + **1** H+ [e]
PHOSPHATIDATE-PHOSPHATASE-RXN	1 1,2-diacyl-sn-glycerol-3P [c] + 1 H2O [c] <-> 1 1,2-diacylglycerol [c] + 1 P [c]	1 1,2-diacyl-sn-glycerol-3P [c] + 1 H2O [c] <-> 1 1,2-diacylglycerol [c] + 1 P [c] + **1 H+ [c]**
METHYLENETHFDEHYDROG-NADP-RXN	1 5,10-CH2-THF [c] + 1 NADP+ [c] <-> 1 5,10-CH=THF [c] + 1 NADPH [c] + 1 H+ [c]	1 5,10-CH2-THF [c] + 1 NADP+ [c] <-> 1 5,10-CH=THF [c] + 1 NADPH [c]
RXNK9E-175	1 folate [c] + 1 NADP+ [c] -> 1 7,8-dihydrofolate [c] + 1 NADPH [c] + 1 H+ [c]	1 folate [c] + 1 **NADPH [c]** + **1 H+ [c]** -> 1 7,8-dihydrofolate [c] + 1 **NADP+ [c]**

Changes are highlighted in bold. Reactions marked with an asterisk (*) were modified in order to adjust to transport characterization carried out by Salema (1996).

Also, reactions 'ACETATEKIN_RXN' and 'RIBOKIN_RXN' were made irreversible, and reactions 'PHOSACETYLTRANS_RXN' and 'ACETALD_DEHYDROG_RXN' were turned into reversible reactions.

b) Automatically curated reactions

134 reactions had mass imbalance only in protons, with charge imbalance coherent with this number. Consequently, the curation could be done automatically using our algorithm. These 134 reactions are:

TRANS_RXNK9E_538,TRANS_RXNK9E_537, TRANS_RXNK9E_475, RXNK9E_220, ASPARAGHYD_RXN,

UDPNACETYLGLUCOSAMENOLPYRTRANS_RXN, LCYSDESULF_RXN, _3_2_1_10_RXN, HOMOSERDEAM_RXN, GALPMUT_RXN, UDP_NACMURALGLDAPAALIG_RXN, DURIDKI_RXN, URACIL_PRIBOSYLTRANS_RXN, ADENINE_DEAMINASE_RXN, GUANYL_KIN_RXN, TRANS_RXNK9E_474, , AIRS_RXN, ADENYLOSUCCINATE_SYNTHASE_RXN, AMPSYN_RXN, HYPOXANPRIBOSYLTRAN_RXN, GUANPRIBOSYLTRAN_RXN, ARGININE_DEIMINASE_RXN, IPHOSPHOMEVALONTE_DECARBOXYLASE_RXN, ADENPRIBOSYLTRAN_RXN, DIACYLGLYKIN_RXN, PYRROLINECARBREDUCT_RXN, ARGSUCCINSYN_RXN, P_PANTOCYSLIG_RXN, NICOTINATEPRIBOSYLTRANS_RXN, TRANS_RXNK9E_479, CYSTATHIONINE_BETA_LYASE_RXN, DSERDEAM_RXN, _2_4_1_157_RXN, ADENYL_KIN_RXN, GLUC1PURIDYLTRANS_RXN, OROPRIBTRANS_RXN, _6_PHOSPHO_BETA_GLUCOSIDASE_RXN, NAD_SYNTH_NH3_RXN, FARNESYLTRANSTRANSFERASE_RXN, UGD_RXN, TRANS_RXNK9E_471, TRANS_RXNK9E_480, RXNN_404, NICOTINAMID_RXN, RXN_7904, RXN_9623, RXN_10715, RXN66_3, TRANS_RXNK9E_466, RXN0_1441, RXN_9591, _2_7_4_22_RXN, GLUCOSAMINE_6_P_DEAMIN_RXN, TRANS_RXNK9E_478, FERRIC_CHELATE_REDUCTASE_RXN, PHOSPHATIDATE_PHOSPHATASE_RXN, RXN0_1603, _6_3_4_16_RXN, ACYLPHOSPHATASE_RXN, PRPPSYN_RXN, DGDPKIN_RXN, DUDPKIN_RXN, DCTP_DEAM_RXN, DCDPKIN_RXN, NAG1P_URIDYLTRANS_RXN, RXN_12195, RXN_12196, RXN_12197, RXN_12200, CDPKIN_RXN, UDPKIN_RXN, RXN_7605, URA_PHOSPH_RXN, RXN0_5405, AKBLIG_RXN, AMACETOXID_RXN, THREOSPON_RXN, TRANS_RXNK9E_448, TRANS_RXNK9E_532, RXNK9E_143, RXN0_742, RXNK9E_222, TRANS_RXNK9E_473, TRANS_RXNK9E_477, RXN_8992,

RXNK9E_197, RXNK9E_153, TRANS_RXNK9E_468, TRANS_RXNK9E_470, TRANS_RXNK9E_484, RXN_12541, TRANS_RXNK9E_467, RXNK9E_223, TRANS_RXNK9E_531, TRANS_RXNK9E_476, TRANS_RXNK9E_472, TRANS_RXNK9E_447, RXNK9E_157, TRANS_RXNK9E_530, _2_5_1_32_RXN, TRANS_RXNK9E_483, TRANS_RXNK9E_482, RXNK9E_224, TRANS_RXNK9E_481, RXNK9E_169, RXNK9E_214, RXNARA_8002, TRANS_RXNK9E_458, METHYL_GLYOXAL_DEHYDROG_RXN, _325_BISPHOSPHATE_NUCLEOTIDASE_RXN, _2_4_2_12_RXN, RXNK9E_221, RXN_9590, RXNK9E_133, RXNK9E_134, RXNK9E_116, RXNK9E_136, RXNK9E_137, RXNK9E_138, RXNK9E_101, RXNK9E_103, TRANS_RXNK9E_311, TRANS_RXNK9E_432, CARBPSYN_RXN, RXN_12352, TRANS_RXNK9E_539, TRANS_RXNK9E_524, TRANSRXNK9E525, GLUTSEMIALDEHYDROG_RXN, RXNK9E_175, METHYLENETHFDEHYDROG_NADP_RXN, GMP_REDCT_RXN, FORMATETHFLIG_RXN, ERITHRITIOL_RXN.

c) Added reactions

Reaction ‘Phosphomannose-isomerase' was added as indicated by Cibrario et al (2016) and gene identification OEOE_0249 (gene id: 4415535).

d) Removed reactions

Reactions 'FOLYLPOLYGLUTAMATESYNTH_RXN' and 'METHIONYL_TRNA_FORMYLTRANSFERASE_RXN' where retired from the model as they participate in the generation of glutamate transference RNA, which is not required for modelling purposes. Reaction '_1_11_1_12_RXN' that participates in lipid salvage, was discarded due to the same reason. Because of these, genes OEOE_1391 and OEOE_0787 were removed.

'RXN_11811', which correspond to the equilibrium between NH3 and $NH4^+$, was discarded to avoid metabolite redundancy.

Reactions 'putrescine_ex_' and 'spermidine_ex_' were discarded as they were the only references to the metabolites 'spermidine[e]' and 'putrescine[e]'.

C.2 Metabolites

The metabolites vector in iMR453 differs with model iSM454 in nine metabolites, which are detailed below.

a) New metabolites

The metabolite 537 D-mannose-6P [c] was included to balance reaction ‘TRANS-RXNK9E-432’, PTS transport of D-mannose.

b) Removed metabolites

Due to elimination of reactions that included these compounds, the following metabolites were removed from the model: Mannose [c], NH3 [c], THF-Glu [c], lipid_hydroperoxide[c], lipid[c], 'spermidine[e]' and 'putrescine[e]'.

c) Name modifications

The name of three metabolites was modified to facilitate its use. Metabolite 180 was changed from 'N-acetyl-L,L-2,6-diaminopimelate__Cytosol_ [c]' to 'N-acetyl-L,L-2,6-diaminopimelate [c]'. Metabolite 275 from '2-acetamido-6-oxoheptanedioate__Cytosol_ [c]' to '2-acetamido-6-oxoheptanedioate [c]'; and Metabolite 251, '6P-beta-D-glucosyl-(1,4)-D-glucose', was modified to 'cellobiose-6P [c]'.

C.3 Subsystems

89 subsystems were added to the model. These correspond to: 4-aminobutyrate degradation, Acetylglucosamine degradation, Adenine and adenosine salvage, Alanine biosynthesis, Anaerobic respiration, Arginine biosynthesis, Asparagine degradation, asparragine biosynthesis, Aspartate biosynthesis, Beta-oxidation, Biomass assembly, Carbon dioxyde fixation, Cardiolipin biosynthesis, CDP-diacylglycerol biosynthesis, Cis-vaccenate biosynthesis, Citrate degradation, Cyclopropane Fatty acid biosynthesis, D-gluconate degradation, Diglucosyl diacylglycerol biosynthesis, Disaccharides degradation, D-serine degradation, dTDP-L-rhamnose biosynthesis, Erythritol biosynthesis, Exchange, Exopolysaccharide biosynthesis, Fatty acid biosynthesis, Flavin salvage and biosynthesis, Folate salvage pathway, Galactose degradation, Gluconeogenesis, Glucose degradation, Glutamine biosynthesis, Glutathione redox reactions, Glycerol degradation, Glycine biosynthesis, Guanine and guanosine salvage, H2O2 degradation, Heterolactic fermentation, Homocysteine degradation, Homoserine biosynthesis, Inorganic metabolism, L-arabinose degradation, L-cysteine biosynthesis, Leucine biosynthesis, Lipoate salvage, Lysine biosynthesis, Lysophosphatidylglycerol biosynthesis, Macromolecules assembly, Malolactic fermentation, Malonyl-CoA biosynthesis, Mannitol biosynthesis, Menaquinol metabolism, Methionine biosynthesis, Mevalonate pathway, NAD salvage and biosynthesis pathway, Non Growth-associated ATP maintenance, Palmitoleate biosynthesis, Pantothenate salvage and CoA biosynthesis, Pentose phosphate pathway, Peptidoglycan biosynthesis I, Proline biosynthesis, Purines biosynthesis, Pyridoxine salvage and biosynthesis pathway, Pyrimidine nucleotides salvage, Pyrimidines biosynthesis, Ribose degradation, S-adenosyl-L-methionine cycle, Serine biosynthesis, Sulfate reduction, Terpenes biosynthesis, Tetrahydrofolate salvage and metabolism, Thiamin salvage pathway,

Threonine biosynthesis, Threonine degradation, Transport of alcohols, Transport of amino acids, Transport of carbohydrates, Transport of gases, Transport of ions, Transport of metabolism products, Transport of nucleotides, Transport of organic acids, Transport of other molecules, Transport of vitamins, Tyrosine degradation, Ubiquinol-8 metabolism, UDP-N-acetyl-D-glucosamine biosynthesis, UDP-N-acetylmuramoyl-pentapeptide biosynthesis III and Valine degradation.

APPENDIX D: TIME COURSE PRODUCTION AND CONSUMPTION OF COMPOUNDS DURING GROWTH OF *O. OENI* PSU-1 AT 0, 3, 6, 9, AND 12% V/V ETHANOL CONCENTRATION, AND FLUX DISTRIBUTION

The following figures are part of the supplementary information present in the paper "Nutritional and energetic requirements of *Oenococcus oeni* grown in a defined wine like culture medium at different ethanol levels". These correspond to the consumption and production time courses of the compounds present in the MaxOeno medium during growth at different ethanol concentrations (Figure D-1 and Figure D-2), the specific consumption rate of the other amino acids that didn't shown a clear tendency with ethanol concentration (Figure D-3), and the flux distribution of phases II and III predicted by the model (Figure D-4 and Figure D-5).

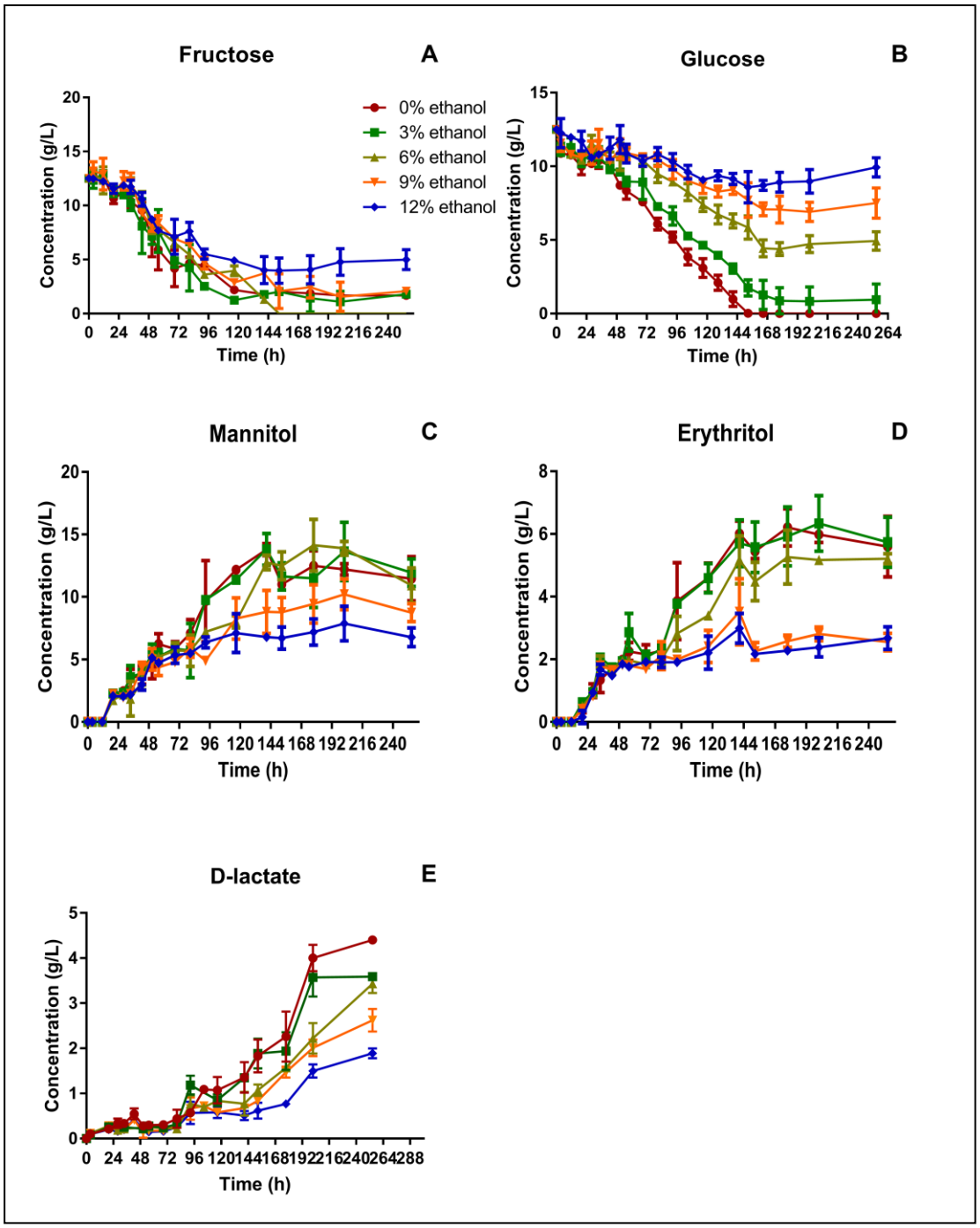

Figure D-1: Time course of fructose consumption and metabolite production by *O. oeni* PSU-1, cultured at different ethanol concentrations.

A) fructose consumption B) glucose consumption C) mannitol production and D) erythritol production E) D-lactate production.

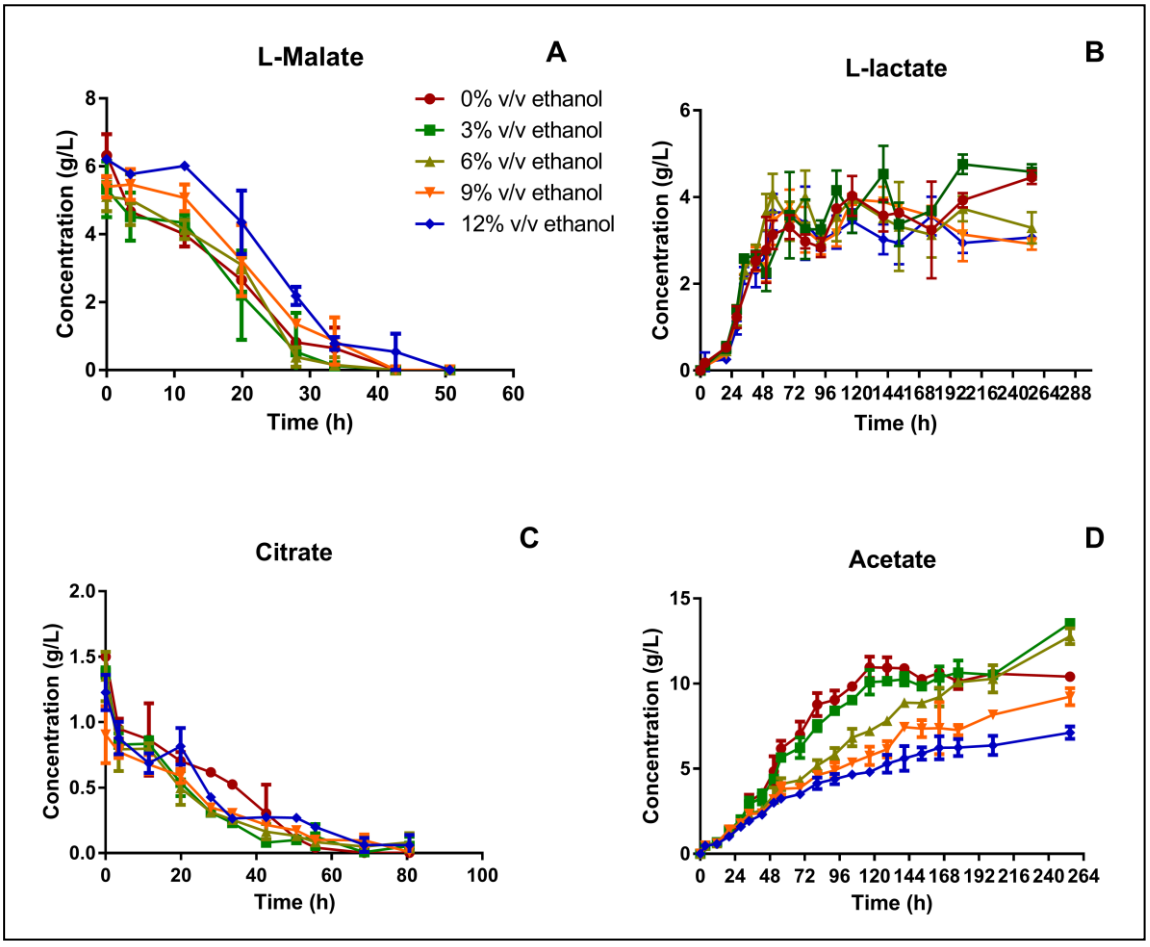

Figure D-2: Time course of some of substrates and metabolites produced mainly by *O. oeni* PSU-1, cultured at different ethanol concentrations

A) Malate consumption, B) L-lactate production, C) citrate consumption, D) acetate production.

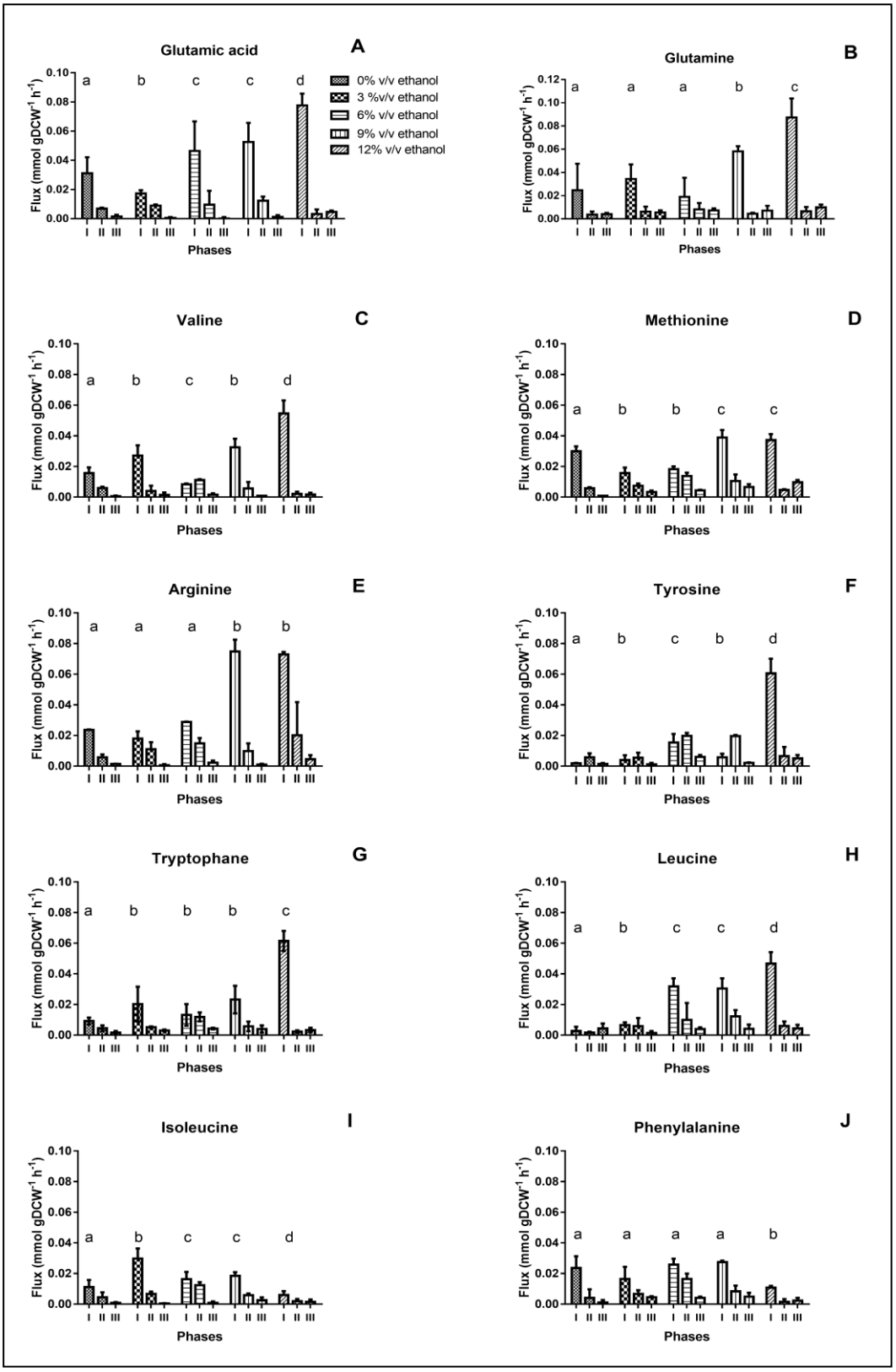
A
Glutamic acid
0% v/v ethanol
3 %v/v ethanol
6% v/v ethanol
9% v/v ethanol
12% v/v ethanol
Flux (mmol gDCW-1 h-1)
Phases
B
Glutamine
C
Valine
D
Methionine
E
Arginine
F
Tyrosine
G
Tryptophane
H
Leucine
I
Isoleucine
J
Phenylalanine

Figure D-3: Specific amino acids consumption rate by *O. oeni* PSU-1, during cultivation under increasing ethanol contents.

A) Glutamic acid. B) Glutamine. C) Valine. D) Methionine. E) Arginine. F) Tyrosine. G) Tryptophan. H) Leucine. I) Isoleucine. J) Phenylalanine. The growth phases I, II and III are represented as 1, 2 and 3, respectively. Statistical analysis only was performed in phase I and shared letters indicate no significant difference (Mood test, $p < 0.05$).

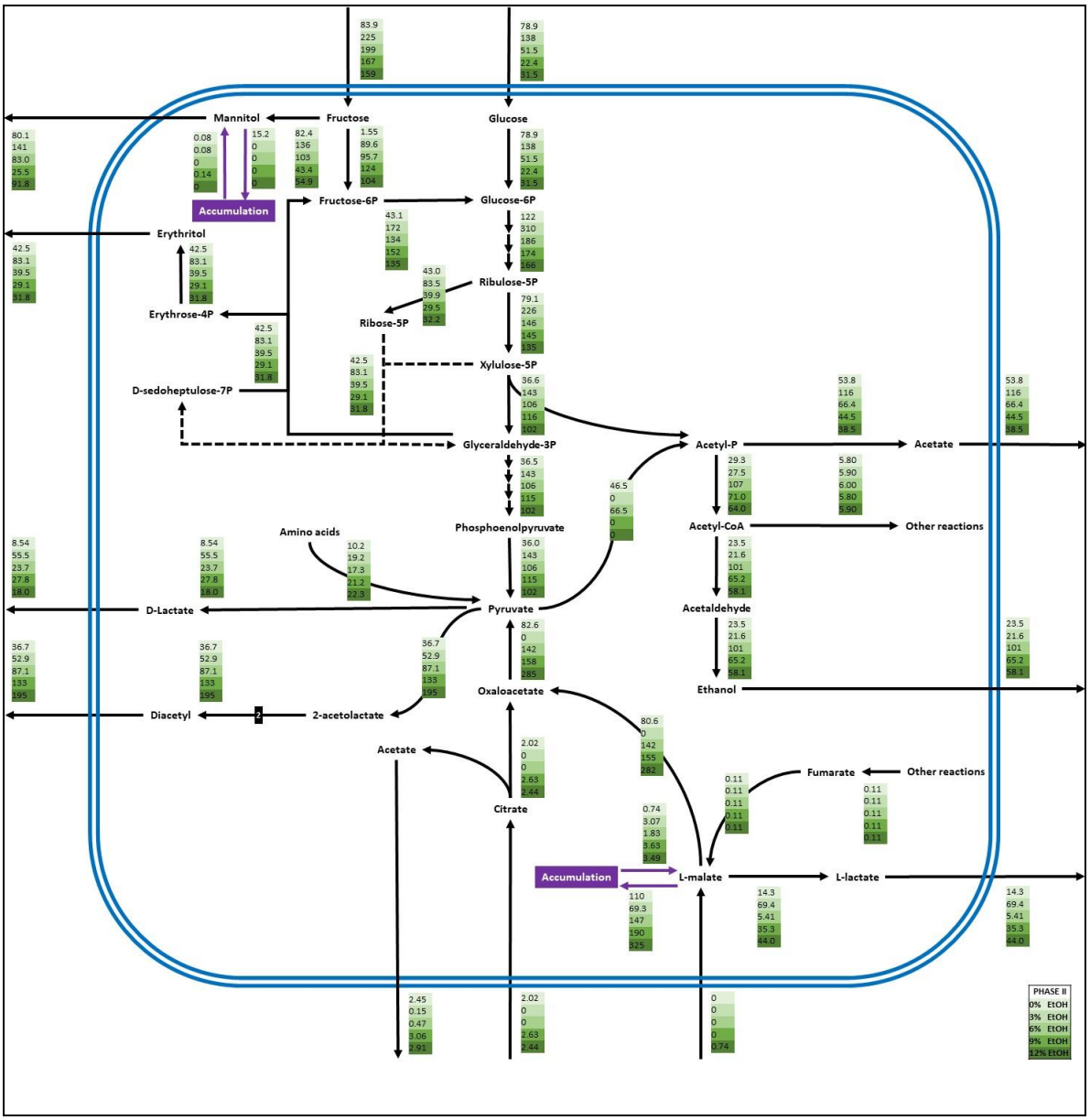

Figure D-4: Metabolic flux redistribution of the central carbon metabolic pathways of *O. oeni* PSU-1 upon cultivation in a culture medium without and with 3, 6, 9 and 12% (green boxes, from top to bottom) ethanol concentration, during growth phase II.

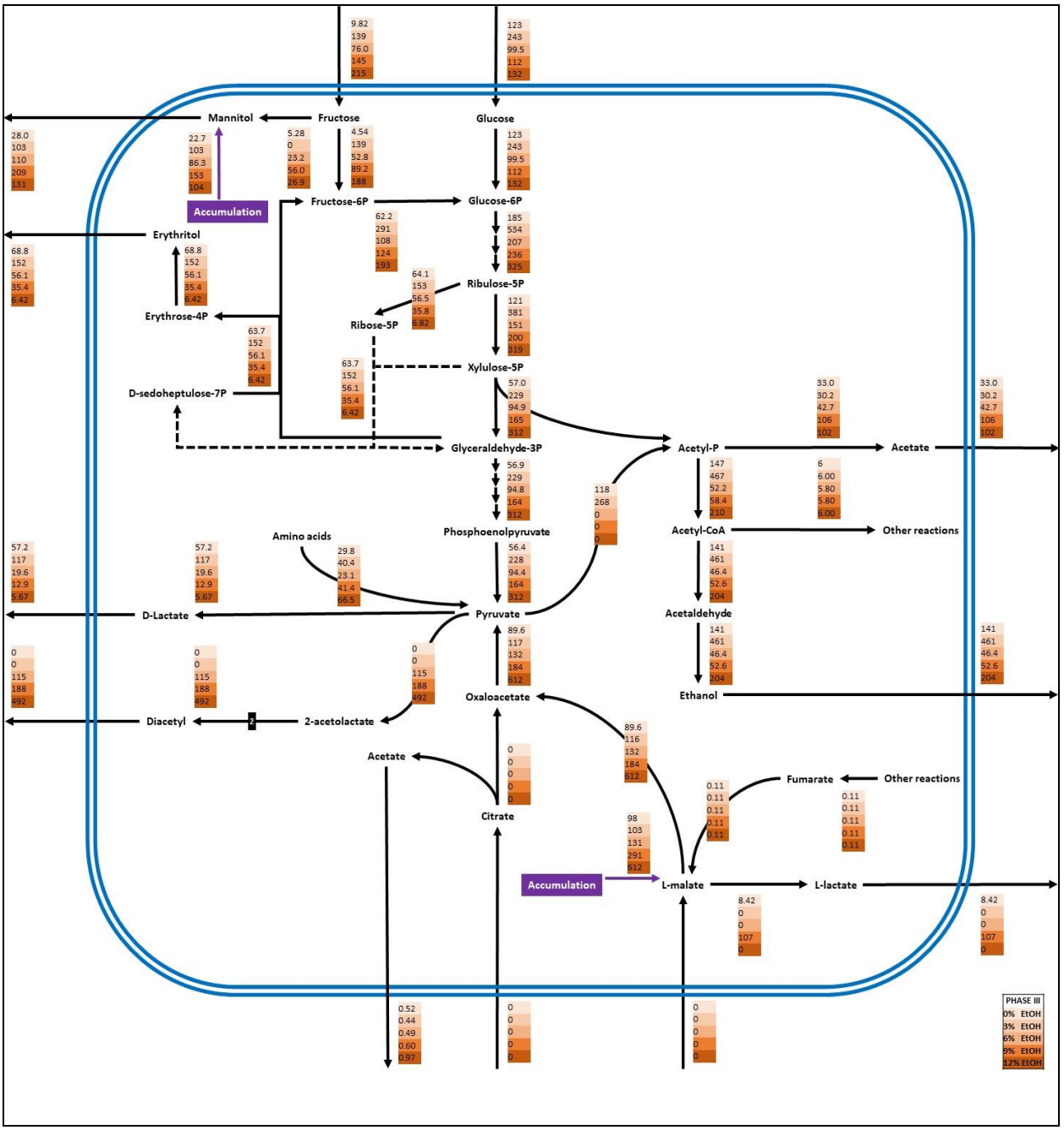

Figure D-5: Metabolic flux redistribution of the central carbon metabolic pathways of *O. oeni* PSU-1 upon cultivation in a culture medium without and with 3, 6, 9 and 12% (orange boxes, from top to bottom) ethanol concentration, during growth phase III.

APPENDIX E: TIME COURSE PRODUCTION AND CONSUMPTION OF COMPOUNDS DURING GROWTH OF *O. OENI* PSU-1 AT PH 4.0, 3.5 AND 3.2, AND FLUX DISTRIBUTION

The following figures show the consumption and production time courses of the compounds present in the MaxOeno medium during growth at acidic conditions (Figure E-1 and Figure 0-2), and the flux distribution of phases II and III predicted by the model iMR453 (Figure E-3 and Figure).

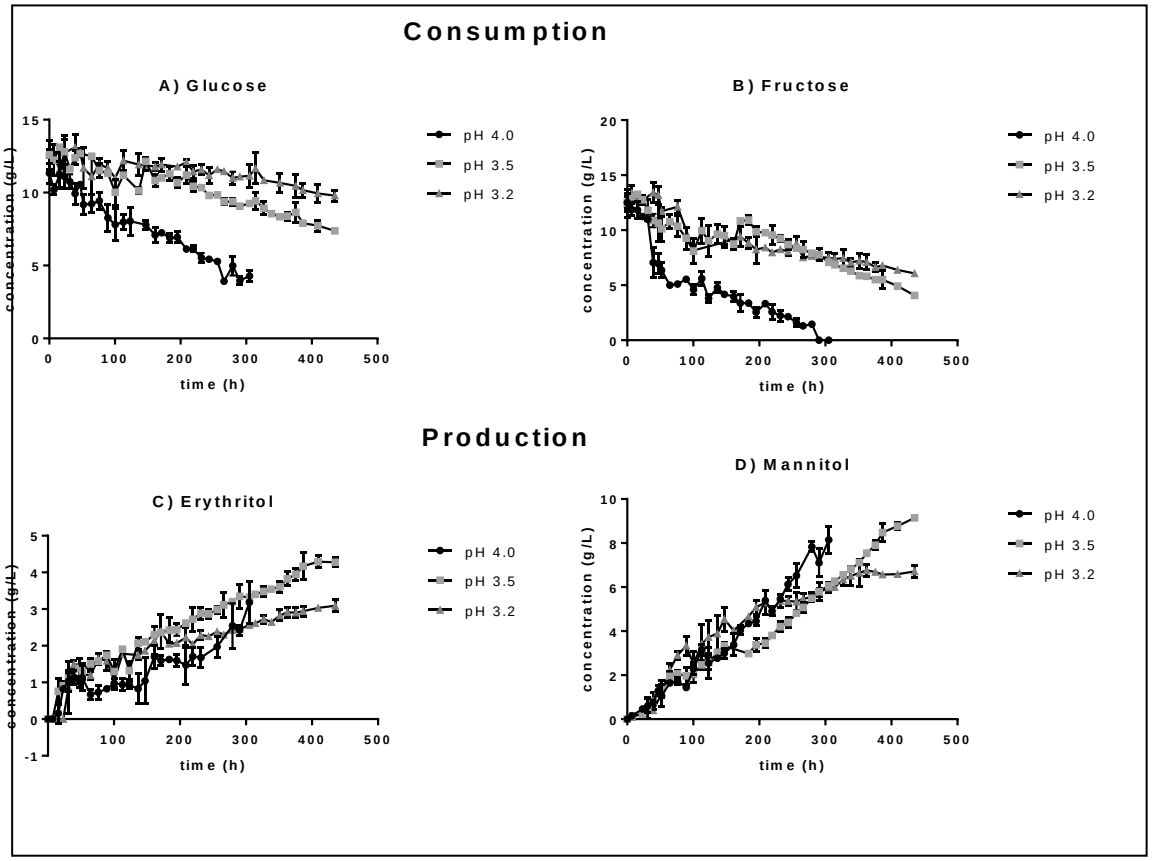

Figure E-1: Evolution of sugars (glucose and fructose) consumption and polyols (mannitol and erythritol) production during growth of *O. oeni* PSU-1 at pH 4.0, 3.5 and 3.2

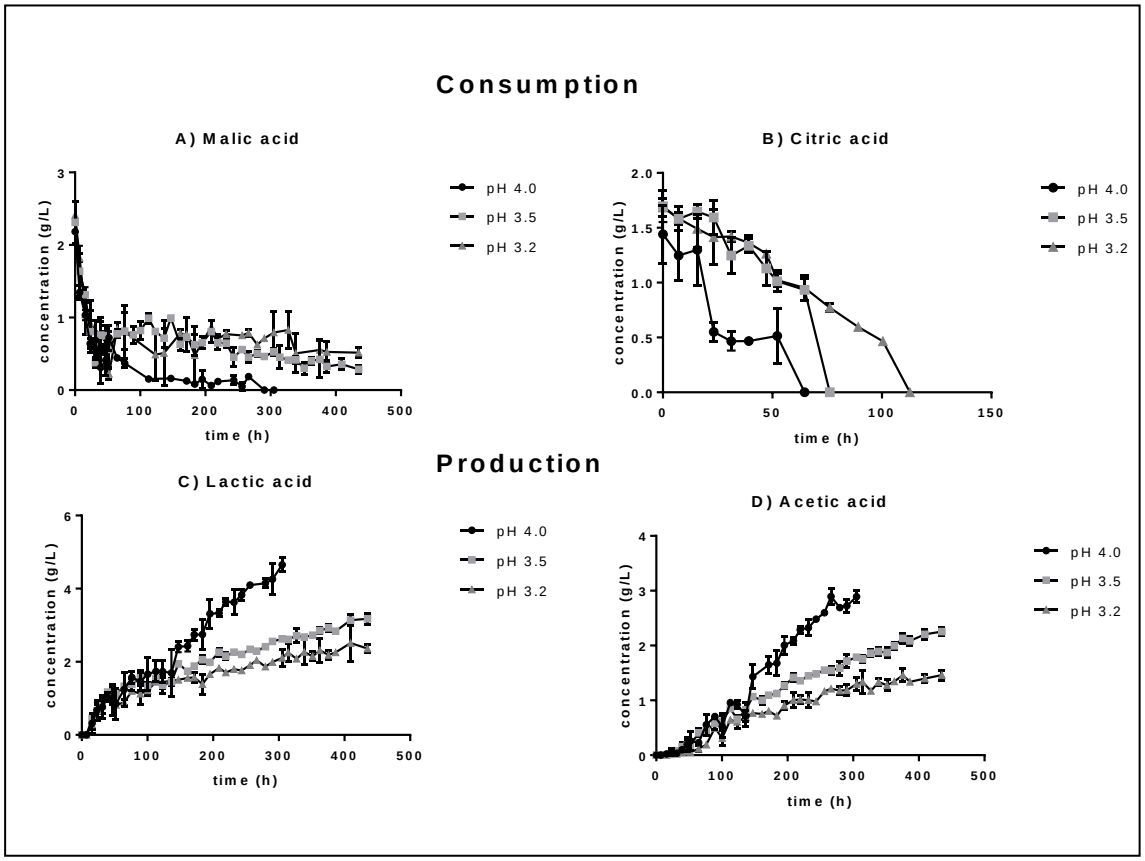

Figure 0-2: Evolution of organic acid consumption and production during growth of *O. oeni* PSU-1 at pH 4.0, 3.5 and 3.2

Malic and citric acids uptake, as well as lactic and acetic acid production were measured.

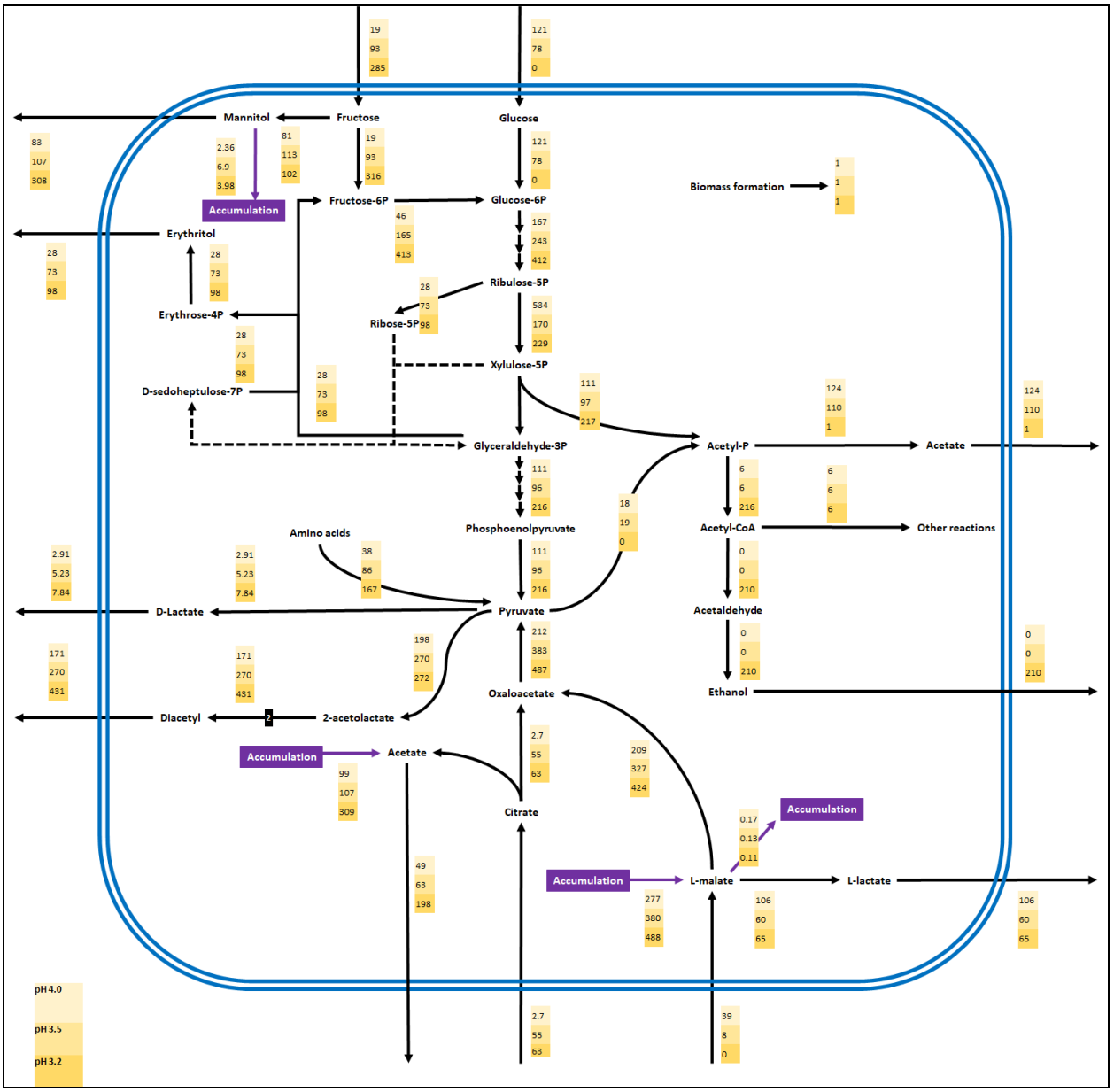

Figure E-3: Metabolic flux redistribution of the central carbon metabolic pathways of *O. oeni* PSU-1 upon cultivation in a culture medium at pH 4.0, 3.5 and 3.2 (from top to bottom), during growth phase II.

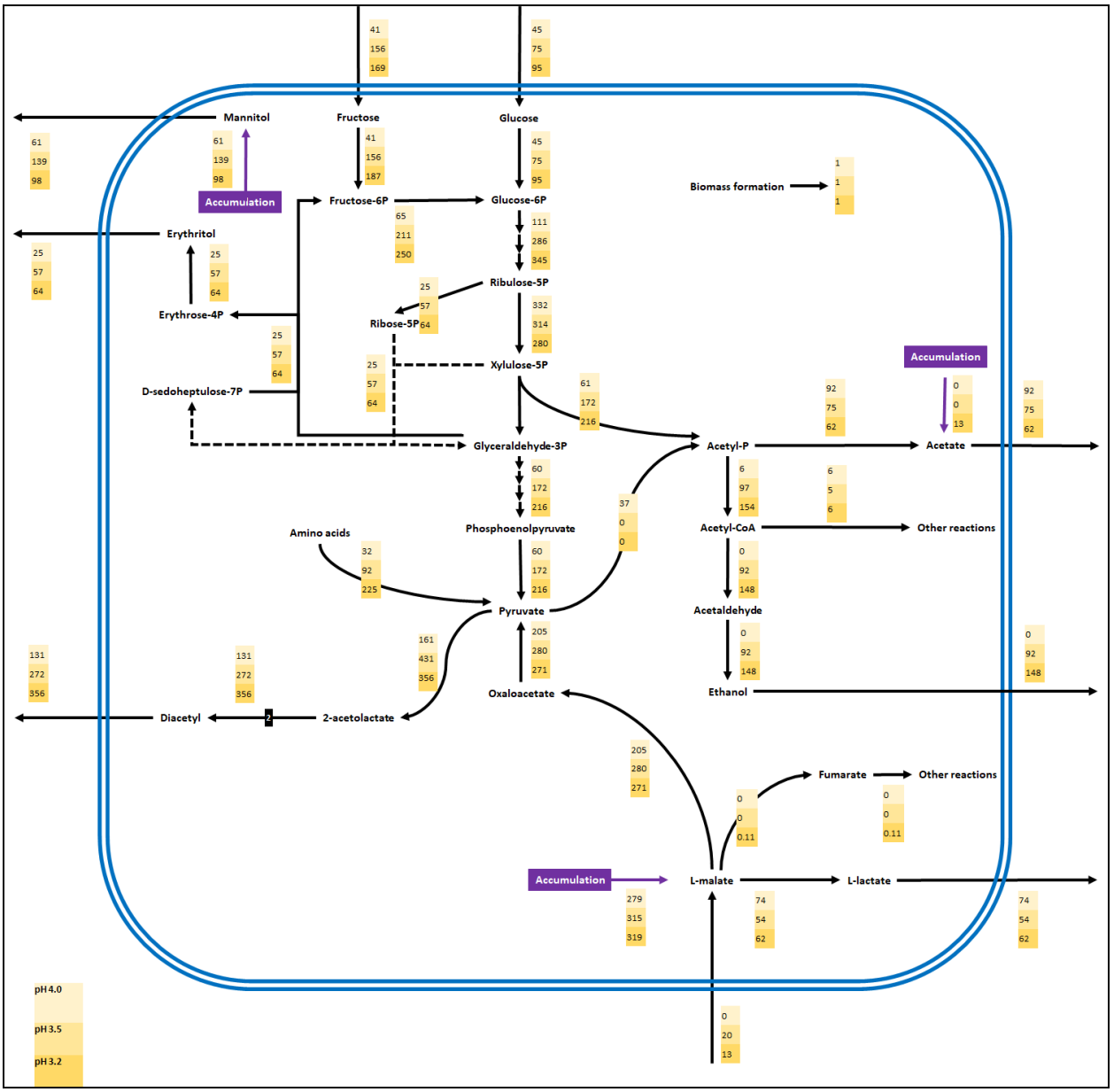

Figure E-4: Metabolic flux redistribution of the central carbon metabolic pathways of *O. oeni* PSU-1 upon cultivation in a culture medium at pH 4.0, 3.5 and 3.2 (from top to bottom), during growth phase III.

APPENDIX F: FORM ABREVIATIONS

ADI = Arginine DeIminase Pathway

AF = Alcoholic Fermentation

FBA = Flux Balance Analysis

FVA = Flux Variability Analysis

ChEBI = Chemical Entities of Biological Interest

CPPE = Cumulative Percentage Prediction Error

GABA = γ-aminobutyrate

GSMM = Genome-Scale Metabolic Model

HLF = HeteroLactic Fermentation

InChI = IUPAC International Chemical Identifier

KEGG = Kyoto Encyclopedia of Genes and Genomes

LAB = Lactic Acid Bacteria

MLF = MaloLactic Fermentation

MRS = De Man, Rogosa & Sharpe Medium

NGAM = non-growth associated ATP

pH_{in} = internal (cytoplasmatic) pH

pH_{set} = pH fixed as objective

pH_{out} = external (medium) pH

PMF = Proton Motive Force

SMILES = Simplified Molecular-Input Line-Entry System

TYE = Tryptone Yeast Extract

ΔpH = gradient of internal and external pH

$\Delta \Psi$ = transmembrane potential

μ = specific growth rate

μ_{max} = maximum specific growth rate

APPENDIX G: EXTRACT OF NGAM SENSITIVITY TABLE

The following table shows an extract of the NGAM sensitivity analysis done to acknowledge the variation range on NGAM estimation due to changes of 1% on the fixed exchange reactions.

Table G-1: NGAM sensitivity analysis, extract

			_S__malate_ex_	citrate_ex_	a_D_glucose_ex_	D_mannitol_ex_
Ethanol 0%	**phase 1**	**1%**	0.115	0.09	0.132	0.015
		-1%	0.079	0.104	0.062	0.179
	phase 2	**1%**	0.157	0.157	0.167	0.143
		-1%	0.157	0.157	0.148	0.172
	phase 3	**1%**	0.328	0.328	0.338	0.325
		-1%	0.328	0.328	0.318	0.331
Ethanol 3%	**phase 1**	**1%**	0.329	0.301	0.341	0.21
		-1%	0.286	0.314	0.274	0.406
	phase 2	**1%**	0.961	0.961	0.977	0.936
		-1%	0.961	0.961	0.945	0.986
	phase 3	**1%**	0.983	0.983	0.996	0.983
		-1%	0.983	0.983	0.97	0.983
Ethanol 6%	**phase 1**	**1%**	0.269	0.238	0.284	0.159
		-1%	0.221	0.253	0.206	0.331
	phase 2	**1%**	0.579	0.579	0.584	0.568
		-1%	0.579	0.579	0.574	0.59
	phase 3	**1%**	0.705	0.705	0.711	0.693
		-1%	0.705	0.705	0.698	0.716
Ethanol 9%	**phase 1**	**1%**	0.963	0.931	0.973	0.825

		-1%	0.91	0.942	0.9	1.048
	phase 2	**1%**	1.333	1.333	1.335	1.329
		-1%	1.333	1.333	1.331	1.337
	phase 3	**1%**	1.888	1.888	1.894	1.869
		-1%	1.888	1.888	1.881	1.907
Ethanol 12%	**phase 1**	**1%**	1.683	1.647	1.691	1.562
		-1%	1.628	1.664	1.62	1.749
	phase 2	**1%**	1.271	1.271	1.27	1.271
		-1%	1.271	1.271	1.272	1.271
	phase 3	**1%**	1.292	1.292	10	1.32
		-1%	1.292	1.292	1.316	10